R-08-85

Explorative analysis of microbes, colloids and gases

SDM-Site Forsmark

Lotta Hallbeck, Karsten Pedersen
Microbial Analytics Sweden AB

August 2008

Svensk Kärnbränslehantering AB
Swedish Nuclear Fuel
and Waste Management Co
Box 250, SE-101 24 Stockholm
Tel +46 8 459 84 00

ISSN 1402-3091
SKB Rapport R-08-85

Explorative analysis of microbes, colloids and gases

SDM-Site Forsmark

Lotta Hallbeck, Karsten Pedersen
Microbial Analytics Sweden AB

August 2008

Preface

The overall objectives of the hydrogeochemical description for Forsmark are to establish a detailed understanding of the hydrogeochemical conditions at the site and to develop models that fulfil the needs identified by the safety assessment groups during the site investigation phase. Issues of concern to safety assessment are radionuclide transport and technical barrier behaviour, both of which are dependent on the chemistry of groundwater and pore water and their evolution with time.

The work has involved the development of descriptive and mathematical models for groundwaters in relation to rock domains, fracture domains and deformation zones. Past climate changes are the major driving force for hydrogeochemical changes and therefore of fundamental importance for understanding the palaeohydrogeological, palaeohydrogeochemical and present evolution of groundwater in the crystalline bedrock of the Fennoscandian Shield.

Understanding current undisturbed hydrochemical conditions at the proposed repository site is important when predicting future changes in groundwater chemistry. The causes behind of copper corrosion and/or bentonite degradation are of particular interest as they may jeopardise the long-term integrity of the planned SKB repository system. Thus, the following variables are considered for the hydrogeochemical site descriptive modelling: pH, E_h, sulphur species, iron, manganese, carbonate, phosphate, nitrogen species, total dissolved solids (TDS), isotopes, colloids, fulvic and humic acids and microorganisms. In addition, dissolved gases (e.g. carbon dioxide, methane and hydrogen) are of interest because of their likely participation in microbial reactions.

In this report, part of the final hydrogeochemical evaluation work of the site investigation at the Forsmark site, is presented. The work was conducted by SKB's hydrogeochemical project group, ChemNet, which consists of independent consultants and university researchers with expertise in geochemistry, hydrochemistry, hydrogeochemistry, microbiology, geomicrobiology, analytical chemistry etc. The resulting site descriptive model version, mainly based on 2.2 data and complementary 2.3 data, was carried out during September 2006 to December 2007. Several groups within ChemNet were involved and the evaluation was conducted independently using different approaches ranging from expert knowledge to geochemical and mathematical modelling including transport modelling. During regular project meetings the results have been presented and discussed.

The original works by the ChemNet modellers are presented in five level III reports containing complementary information for the bedrock hydrogeochemistry Forsmark Site Descriptive Model (SDM-Site Forsmark, R-08-47) level II report.

There is also an additional level III report: Fracture mineralogy of the Forsmark area by Sandström et al. R-08-102.

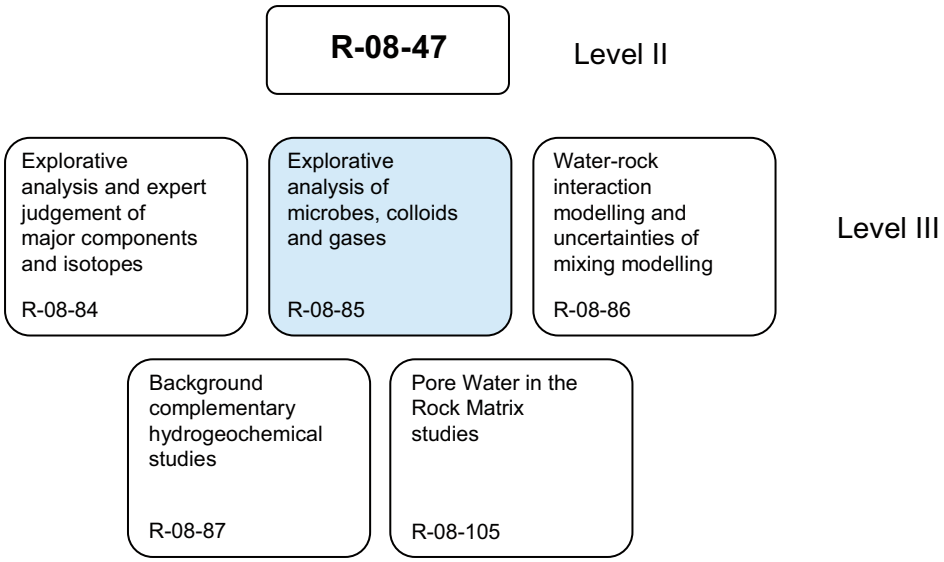

This report focuses on microbiology, colloids and gases

– *Microbes (Chapter 1):* Several methods must be used to characterize active microbial communities in groundwater. Microbial parameters of interest are the total number of cells (TNC) and the presence of various metabolic groups of microorganisms. Different microbial groups influence the environment in different ways, depending on what metabolic group is dominant. Typically, the following redox couples are utilized by bacteria in granitic groundwater: H_2O/O_2, NO_3^-/N_2, $Mn^{2+}/Mn(IV)$, $Fe^{2+}/Fe(III)$, S^{2-}/SO_4^{2-}, CH_4/CO_2, CH_3COOH/CO_2, and H_2/H^+. The data will indicate the activity of specific microbial populations at particular sites and how they may affect the geochemistry.

– *Colloids (Chapter 2):* Particles in the size range from 1 to 1×10^{-3} μm are regarded as colloids. Their small size prohibits them from settling, which gives them the potential to transport radionuclides in groundwater. The aim of the study of colloids in the Forsmark 2.3 site investigation was to quantify and determine the composition of colloids in groundwater samples from the boreholes. There are both inorganic and organic colloids, and the site investigation measured both types.

– *Gases (Chapter 3):* Dissolved gases in groundwater contribute to the mass of dissolved species. The distribution and composition of dissolved gases in deep groundwater are important to understand in the safety assessment of a deep geological nuclear waste repository: Micro bubbles of gas may potentially transport radionuclides from the repository to the surface. Oxygen, hydrogen sulphide and carbon dioxide are parts of fundamental redox couples that participate in several solid-aqueous phase transformations such as the precipitation of ferric iron oxides, iron sulphide and calcite. Methane and hydrogen, may serve as sources of energy to various microbiological processes.

Contents

1 Microbiology and microbial model 7
1.1 Introduction 7
1.2 Characterizing the influence of different metabolic groups of microorganisms 8
1.3 Available data 10
1.4 Quality controls for the most probable number analysis 10
1.4.1 Tests for reproducibility of the pressure vessel method 10
1.4.2 Detection limits and uncertainties in the microbiological methods used 10
1.5 Evaluation of the microbial biomass data 13
1.5.1 Analysis of microbial biomass 13
1.5.2 Dissolved organic carbon and total number of cells 14
1.5.3 Relations between microbiology and organic material 16
1.6 Cultivable heterotrophic aerobic bacteria 17
1.7 Nitrate-reducing bacteria 17
1.8 Iron-reducing bacteria and Fe^{2+} 19
1.9 Manganese-reducing bacteria and manganese 21
1.10 Sulphate-reducing bacteria, sulphate, and sulphide 23
1.11 Methanogens 25
1.12 Acetogens 25
1.13 Total number of cells versus MPN 27
1.14 Correlations between variables deemed important for microbiological concenptual models 28
1.15 Discussion – The microbial model 39
1.15.1 A theoretical model of microbial reactions in a granitic groundwater environment 39
1.15.2 The microbial model in Forsmark 39
1.15.3 Limitations of microbial processes 43
1.16 Conclusions 44

2 Colloids 45
2.1 Introduction 45
2.2 Methods 45
2.3 Databases 46
2.4 Evaluation of colloid data from the filtration method 46
2.4.1 Colloids versus depth 46
2.6 Colloids and iron 49
2.7 Composition of colloids – size distribution 51
2.8 Inorganic colloids – fractionation 51
2.9 Laser-induced breakdown colloid detection 52
2.10 Colloid analyses by means of micro-filtration plus scanning electron microscopy and energy-dispersive spectroscopy 53
2.11 Microbes and viruses as possible colloids 53
2.12 Conclusions 56

3 Gases 57
3.1 Introduction 57
3.1.1 Observations of gas in Fennoscandian shield groundwater 57
3.1.2 Microbubbles of gas 57
3.1.3 Biochemically active gases 58
3.1.4 Origin of gases, tracer properties 59

3.2 Available Forsmark 2.3 gas data 59
3.3 Data quality 59
3.4 Total gas volumes 61
3.5 Gas composition 62
3.5.1 Nitrogen 62
3.5.2 Helium 63
3.5.3 Carbon dioxide 64
3.5.4 Methane and higher hydrocarbons 64
3.5.5 Argon 66
3.5.6 Hydrogen 67
3.6 Ratios 68
3.6.1 Nitrogen over argon 68
3.7 Nitrogen over helium 69
3.8 Methane over helium 70
3.9 Conclusions 71

4 References 73

Microbial abbreviations:

TNC = total number of cells
ATP = adenosine-tri-phosphate
CHAB = cultivable heterotrophic aerobic bacteria
IRB = iron-reducing bacteria
NRB = nitrate-reducing bacteria
MRB = manganese-reducing bacteria
SRB = sulphate-reducing bacteria
AA = autotrophic acetogens
HA = heterotrophic acetogens
AM = autotrophic methanogens
HM = heterotrophic methanogens
MOB = methane-oxidizing bacteria

1 Microbiology and microbial model

1.1 Introduction

Microbial metabolic activities greatly influence groundwater chemistry. To understand current undisturbed conditions at the proposed repository site, the following parameters are of interest for hydrogeochemical site description modelling: pH, E_h, sulphide, sulphur, sulphate, iron(II), manganese(II), carbonate, phosphate, nitrogen species, total dissolved solids (TDS), colloids, fulvic and humic acids, dissolved organic carbon (DOC), and microorganisms. As well, the dissolved gases carbon dioxide, methane and hydrogen may participate in microbial reactions. Furthermore, a full understanding entails being able to predict how conditions will change during the repository construction and during the following phases of the storage of spent nuclear waste. This part of the report will deal with the microbial data from the site investigation of the Forsmark area.

Several methods must be used to characterize active microbial communities in groundwater. Microbial parameters of interest are the total number of cells (TNC) and the presence of various metabolic groups of microorganisms /Pedersen 2001/. The groups cultured for the microbial part of the site investigation were cultivable heterotrophic aerobic bacteria (CHAB), nitrate-reducing bacteria (NRB), iron-reducing bacteria (IRB), manganese-reducing bacteria (MRB), sulphate-reducing bacteria (SRB), auto- and heterotrophic methanogens (AM and HM), and auto- and heterotrophic acetogens (AA and HA). These groups utilize the following redox couples commonly observed in granitic groundwater: H_2O/O_2, NO_3^-/N_2, $Mn^{2+}/Mn(IV)$, $Fe^{2+}/Fe(III)$, S^{2-}/SO_4^{2-}, CH_4/CO_2, CH_3COOH/CO_2, and H_2/H^+ (Figure 1-1). The data will indicate the activity of specific

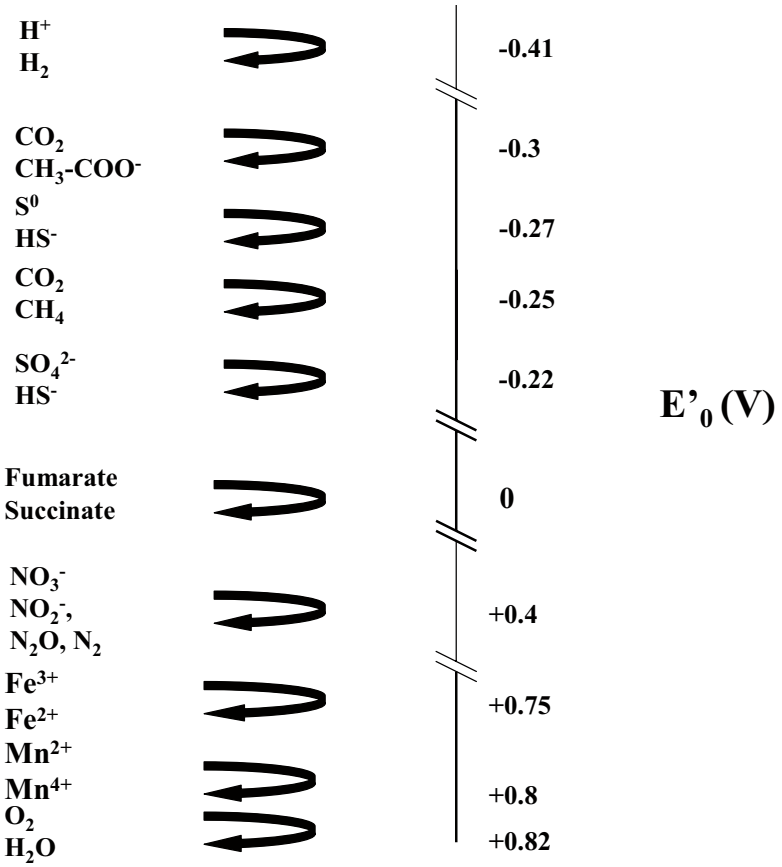

Figure 1-1. *Redox couples found in deep groundwater and the various groups of microorganisms involved in their metabolism.*

microbial populations at particular sites and how they may affect the geochemistry. Counting the different metabolic groups was done using the most probable number of cells (MPN) method, a statistical cultivation method for counting the most probable number of cells of different cultivable metabolic groups of microorganisms /Greenberg et al. 1992, Hallbeck and Pedersen 2008/.

1.2 Characterizing the influence of different metabolic groups of microorganisms

Microbial decomposition and the production of organic material depend on the energy sources and electron acceptors present /Madigan and Martinko 2006/. Organic carbon and methane and reduced inorganic molecules, including hydrogen, are possible energy sources in the subterranean environment. During the microbial oxidation of these energy sources, microbes preferentially use electron acceptors in a particular order (Figure 1-2): first oxygen, and thereafter nitrate, manganese(IV), iron(III), sulphate, sulphur, and carbon dioxide are utilized. Simultaneously, fermentative processes supply the metabolizing microorganisms with, for example, hydrogen and short-chain organic acids. As the solubility in water is low, and because oxygen is the preferred electron acceptor of many bacteria that utilize organic compounds in shallow groundwater, anaerobic environments and processes usually dominate at depth in the subterranean environment.

Different microbial groups influence the environment in different ways, depending on what metabolic group is dominant. Table 1-1 lists the activities of these groups and their possible effects on their environment. These microbial processes generally lower the redox potential, E_h. Most of the microbially mediated reactions will not occur in a lifeless groundwater environment without the presence of the catalyzing enzymes of the microorganisms. However, the concentrations of reduced electron acceptors alone will not reveal when, where, or the rate at which the individual microbial processes occur. The microbial methods applied, TNC and MPN, will be used to estimate the total number of cells and their diversity, which in turn indicate what microbial processes dominate in a particular groundwater.

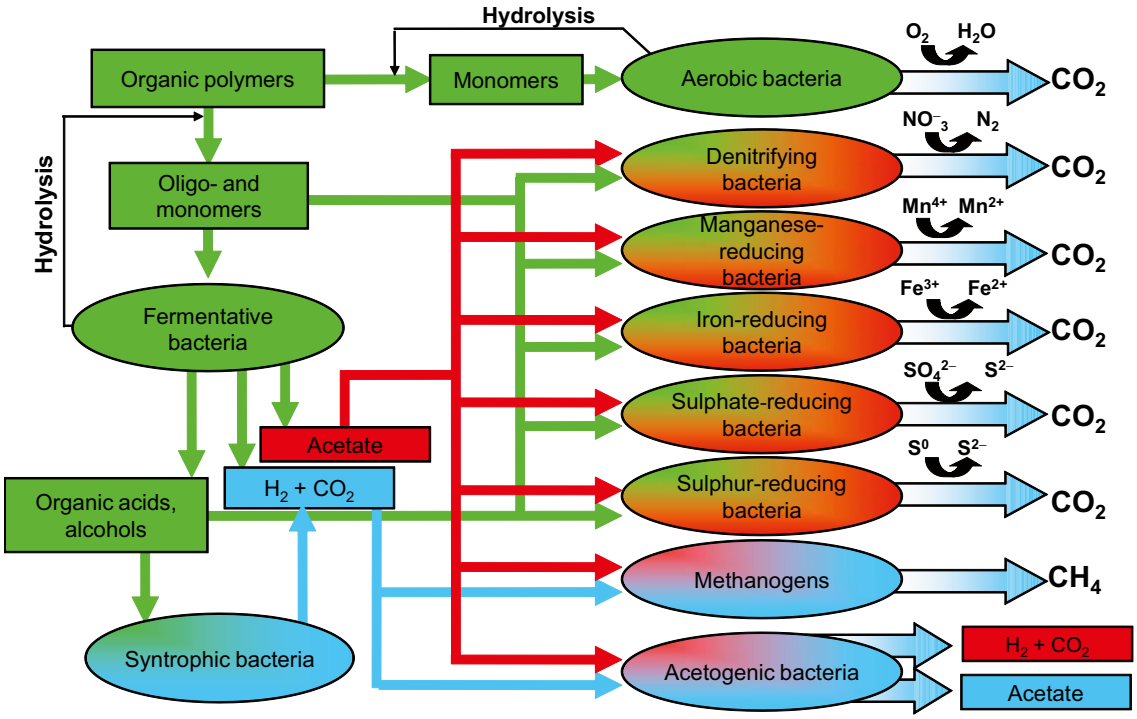

Figure 1-2. *Possible pathways for the flow of carbon in the subterranean environment. Organic carbon is respired with oxygen, if present, or else fermentation and anaerobic respiration occur with an array of different electron acceptors.*

Table 1-1. Activities and effects of the different physiological groups of microorganisms found in deep groundwater.

Metabolic groups of microorganisms	Activity	Effect on the environment
Aerobes	Oxidation of organic material by oxygen reduction	Depletion of oxygen and organic material; Increase in alkalinity; Lowering of redox potential
Anaerobes	Oxidation of organic material along with the reduction of compounds other than oxygen	See below for each specific group of bacteria
Iron-reducing bacteria	Oxidation of organic material along with ferric iron reduction	Depletion of organic material and ferric iron; Increase in ferrous iron concentration and alkalinity; Lowering of redox potential
Manganese-reducing bacteria	Oxidation of organic material along with manganese(IV) ion reduction	Depletion of organic matter and manganese(IV); Increase in manganese(II) concentration and alkalinity; Lowering of redox potential
Sulphate-reducing bacteria	Oxidation of organic material along with sulphate reduction	Depletion of organic matter and sulphate; Increase in sulphide concentration and alkalinity; Lowering of redox potential
Methanogenesis		
Heterotrophic methanogens	Convert short-chained organic material to methane and carbon dioxide	Depletion of organic material; Increase in methane gas and carbon dioxide (alkalinity) concentrations; Redox not influenced
Autotrophic methanogens	Oxidation of hydrogen gas and reduction of carbon dioxide to methane gas	Depletion of hydrogen gas and alkalinity; Increase in methane gas concentration; Redox lowered
Acetogenesis		
Heterotrophic acetogens	Convert organic material to acetate	Depletion of organic material other than acetate; Increase in acetate concentration; Redox not influenced
Autotrophic acetogens	Oxidation of hydrogen gas along with reduction of carbon dioxide to acetate	Depletion of hydrogen gas and alkalinity; Increase in acetate concentration Redox lowered

1.3 Available data

This report uses data from the extended December 2007 data freeze 2.3 in Forsmark. Microbiological data were available from 18 sections of the following ten boreholes: KFM01A, KFM01D, KFM02A, KFM03A, KFM06A, KFM07A, KFM08A, KFM08D, KFM10A, and KFM11A. Information regarding the extent of MPN culturing of samples from the various boreholes can be found in Table 1-2. The use of culturing methods was expanded over the site investigation period, so results for some of the metabolic groups are missing from samples taken early on. All the different MPN media were used for samples from borehole KFM07A to KFM11A (Table 1-2). In this report, microbial data are analysed in relation to the chemistry and gas data important for the various microbial processes.

1.4 Quality controls for the most probable number analysis

The reproducibility of the sampling and analysis procedures was tested with the PVB pressure vessel. The 353.5–360.0-m section of the Forsmark site investigation borehole KFM06A was sampled on 14 March 2005 using two PVB samplers installed at the same time. It was also deemed important to test reproducibility over time in borehole sections that were expected to harbour stable and reproducible populations. This was done in two boreholes at the MICROBE site /Pedersen 2005a/ in the Äspö HRL tunnel, denoted KJ0052F01 and KJ0052F03. Groundwater from the borehole sections was sampled using PVB samplers on two occasions, 26 October 2004 and 9 February 2005. The PVB samplers were attached to the flows from each borehole section, and groundwater was circulated overnight under in situ pressure, temperature, and chemistry conditions. Early in the morning, the samplers were closed, detached, and transported to the laboratory in Göteborg; analysis started the same afternoon, before 14.00. All parts of this procedure resembled the sampling of sections in the Forsmark deep boreholes, except that in this case the samplers were not operated remotely from the ground surface; instead, personnel standing next to the PVB samplers in the tunnel manually operated the samplers using adjustable spanners.

1.4.1 Tests for reproducibility of the pressure vessel method

The results of the MPN analyses of groundwater samples taken simultaneously in the Forsmark section in borehole KFM06A at a depth of 357 m were very reproducible (Table 1-3). The lower and upper 95% confidence intervals for the MPN method applied to five parallel tubes equalled approximately 1/3 and 3 times the obtained values, respectively /Greenberg et al. 1992/. There was a small bias towards higher numbers in the PVB sampler denoted 1. The maximum discrepancy between the samples was observed for SRB and equalled a factor of two, well within the 95% confidence intervals of the MPN analysis. The TNC determinations and ATP analysis also displayed good reproducibility; this included the sampling procedure, transportation logistics, and MPN inoculation, cultivation, and analysis for each physiological group of microorganisms, i.e. TNC, CHAB, and ATP. The second test explored the reproducibility of two different analytical rounds on groundwater from two different borehole sections and of repeated sampling over time. This test also included the effects of different personnel involved and different preparations of chemicals and media. In general, groundwater from the two borehole sections had very different result profiles that reproduced well (Table 1-4). The MPNs of MRB, SRB and AM differed most between the sampling times, while the MPNs of AA and HM indicated high reproducibility.

1.4.2 Detection limits and uncertainties in the microbiological methods used

The detection limit of the MPN method is 0.2 cells mL^{-1}. The lower and upper 95% confidence intervals of the MPN method applied to five parallel tubes equalled approximately 1/3 and 3 times the obtained value, respectively /Greenberg et al. 1992/. The detection limit of the TNC method is 1×10^3 mL^{-1}. The results are normally distributed and the uncertainty is 10% if enough cells are counted.

Table 1-2. The MPN of different metabolic groups tested for in groundwater from six depths in the boreholes in Forsmark.

Metabolic group	KFM01A, 112 m	KFM01A, 176 m	KFM01D, 341 m	KFM01D, 445 m	KFM02A, 503 m	KFM03A, 439 m	KFM03A, 632 m	KFM03A, 930 m	KFM03A, 978 m	KFM06A, 302 m	KFM06A, 645 m	KFM07A–KFM11A
Nitrate-reducing bacteria	–	–	–	–	–	–	–	–	–	–	–	X
Iron-reducing bacteria	X	X	X	X	X	X	X	X	X	X	X	X
Manganese-reducing bacteria	X	X	X	X	X	X	X	X	X	X	X	X
Sulphate-reducing bacteria	X	X	X	X	X	X	X	X	X	X	X	X
Autotrophic methanogens	–	–	X	X	X	X	X	X	X	X	X	X
Heterotrophic methanogens	X	X	X	X	X	X	X	X	X	X	X	X
Autotrophic acetogens	–	–	X	X	X	X	X	X	X	X	X	X
Heterotrophic acetogens	X	X	X	X	X	X	X	X	X	X	X	X

Table 1-3. The total numbers of cells, ATP, and most probable numbers of various physiological groups of microorganisms in groundwater sampled using two different PVB samplers, taken simultaneously on 14 March 2005 at the same location in borehole KFM06A, section 353.5–360.0 m.

Analysis[a] and physiological group	Sample		
	KFM06A:1	KFM06A:2	KFM06A:1 / KFM06A:2
TNC × 10^4 (cells mL^{-1})	7.2 (1.7)[b]	5.2 (1.7)	1.4
ATP × 10^4 (amol mL^{-1})	1.51 (0.07)	0.95 (0.05)	1.6
IRB (cells mL^{-1})	30 (10–120)[c]	23 (9–86)	1.3
MRB (cells mL^{-1})	13 (5–39)	30 (10–130)	0.44
SRB (cells mL^{-1})	0.8 (0.3–2.4)	0.4 (0.1–1.7)	2.0
AA (cells mL^{-1})	30 (10–130)	24 (10–94)	1.3
HA (cells mL^{-1})	24 (10–94)	24 (10–94)	1.0
AM (cells mL^{-1})	<0.2	0.2 (0.1–1.1)	<1.0
HM (cells mL^{-1})	0.2 (0.1–1.1)	0.4 (0.1–1.7)	0.5

[a] TNC = total number of cells, ATP = adenosine-tri-phosphate, CHAB = cultivable heterotrophic aerobic bacteria, IRB = iron-reducing bacteria, MRB = manganese-reducing bacteria, SRB = sulphate-reducing bacteria, AA = autotrophic acetogens, HA = heterotrophic acetogens, AM = autotrophic methanogens, HM = heterotrophic methanogens, and MOB = methane-oxidizing bacteria. [b] Standard deviation, $n = 6$. [c] Lower and upper 95% confidence limits.

Table 1-4. The most probable numbers of various physiological groups of microorganisms in two different boreholes sampled on 14 October 2004 and 9 February 2005.

Physiological group[a]	KJ0052F01:1	KJ0052F01:2	KJ0052F01:1 / KJ0052F01:2
IRB (cells mL^{-1})	<0.2	<0.2	1
MRB (cells mL^{-1})	<0.2	<0.2	1
SRB (cells mL^{-1})	300 (100–1,300)[b]	1,600 (600–5,300)	0.19
AA (cells mL^{-1})	1,600 (600–5,300)	1,600 (600–5,300)	1
HA (cells mL^{-1})	1,600 (600–5,300)	1,600 (600–5,300)	1
AM (cells mL^{-1})	17 (7–48)	5 (2–17)	3.4
HM (cells mL^{-1})	2.3 (0.9–8.6)	2.3 (0.9–8.6)	1
	KJ0052F03:1	**KJ0052F03:2**	**KJ0052F03:1 / KJ0052F03:2**
IRB (cells mL^{-1})	<0.2	0.8 (0.3–2.4)	<1
MRB (cells mL^{-1})	5.0 (2–17)	1.1 (0.4–2.9)	4.6
SRB (cells mL^{-1})	2.3 (0.9–8.6)	5 (2–17)	0.46
AA (cells mL^{-1})	5 (2–17)	17 (7–48)	0.30
HA (cells mL^{-1})	8 (3–25)	11 (4–30)	0.73
AM (cells mL^{-1})	2.3 (0.9–8.6)	0.4 (0.1–1.5)	8.0
HM (cells mL^{-1})	1.3 (0.5–3.8)	<0.2	>1

[a] TNC = total number of cells, ATP = adenosine-tri-phosphate, CHAB = cultivable heterotrophic aerobic bacteria, IRB = iron-reducing bacteria, MRB = manganese-reducing bacteria, SRB = sulphate-reducing bacteria, AA = autotrophic acetogens, HA = heterotrophic acetogens, AM = autotrophic methanogens, HM = heterotrophic methanogens. [b] Lower and upper 95% confidence limits.

1.5 Evaluation of the microbial biomass data

1.5.1 Analysis of microbial biomass

The microbial biomass in granitic rock aquifers of the Fennoscandian Shield has been analysed in terms of total and viable numbers for almost two decades /Pedersen 2001, 2002/; total number estimates have ranged from 10^3 to 10^6 cells mL^{-1}, while viable number estimates have ranged from 10^0 to 10^5 cells mL^{-1}. Between 0.00084 and 14.8% of the total numbers have been cultivated and detected using most probable number (MPN) methods /Haveman and Pedersen 2002a/. Although low viable numbers have been detected relative to the total numbers observed, in vitro radiographic and radiotracer estimates have suggested that the absolute majority of the total cells observed using microscopy was viable /Pedersen and Ekendahl 1990, 1992ab/. Consequently, there was a significant gap between estimates of potentially viable total numbers and evidently viable cultivable numbers. Hence, a method for estimating the total amount of viable biomass in groundwater was sought. A recent investigation found that analysing the ATP concentration in shallow and deep Fennoscandian groundwater (including Forsmark groundwater) using a commercial assay supplied needed information about the metabolic state and biovolume of the bacteria present /Eydal and Pedersen 2007/. The assay appeared robust and reliable and had a detection range that took in all samples analysed. The analysed ATP concentrations were found to correlate both with the microscopic counts and with the volume and metabolic status of the investigated pure culture and groundwater cells. The results suggested that bacterial populations in deep groundwater vary significantly in size, and that metabolic activity is a function of prevailing environmental conditions.

ATP was first analysed in Forsmark groundwater in spring 2004. When ATP was analysed concomitantly with TNC, a good correlation was obtained (Figure 1-3). As ATP is an energy transport compound present in all living cells, measuring its concentration indicates the biovolume and metabolic state of the biomass in any system. A groundwater containing many active cells should thus have a higher ATP concentration than one containing few such cells.

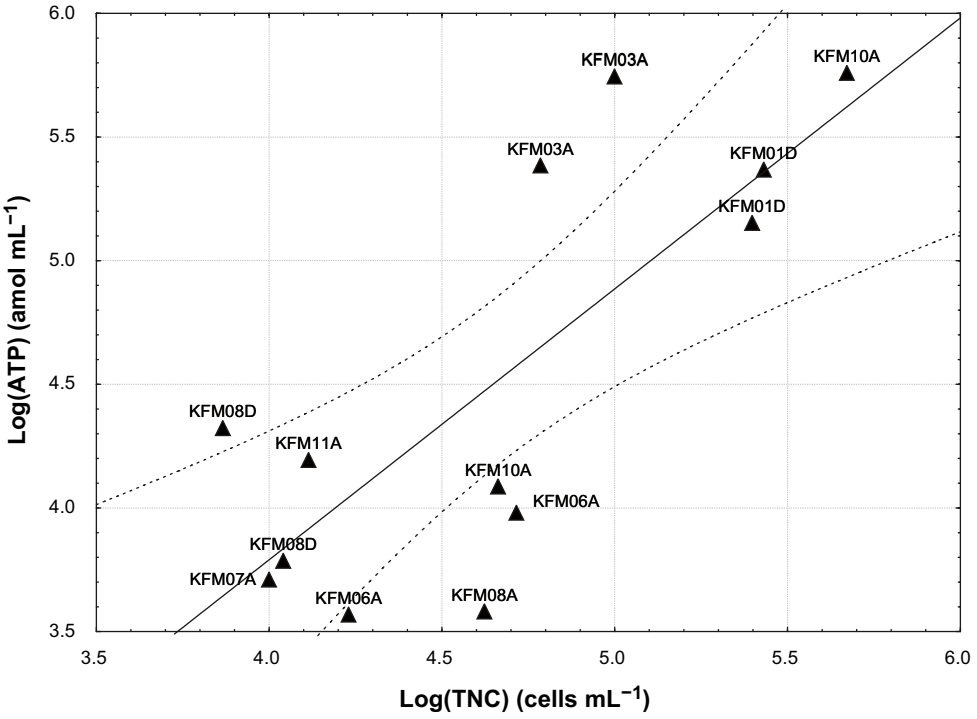

Figure 1-3. *The relationship between the total number of cells (TNC) and the concentration of ATP in Forsmark groundwater. Statistics:* $^{10}Log(ATP)=0.59 +1.10 \times {}^{10}Log(TNC)$, *r=–0.77, significant at p=0.002, n=13. Dashed lines denote the 95% confidence interval. Symbols at –1 denote data below the detection limit of 0.2 cells* mL^{-1}. *Data from extended freeze 2.3 (December 2007) in Forsmark.*

If the cells are large, this will increase the content of ATP per cell. It has been demonstrated that the ATP/TNC ratio is a good indicator of the metabolic activity of cells in groundwater /Eydal and Pedersen 2007/. The average ATP/TNC ratio for 13 Forsmark groundwater determinations was 1.30, and for 166 deep Fennoscandian shield groundwater determinations it was 0.43. However, the two high KFM03A values were unusually high (Figure 1-4). If they are excluded, the average becomes 0.63, which still suggests that the microbial populations analysed in Forsmark were somewhat more active than average. Hence, the average microbial population of Forsmark was more active than the average Fennoscandian shield population.

A special case is the possible occurrence of microbes that grow attached to aquifer surfaces, a phenomenon repeatedly observed in groundwater from deep hard rock aquifers /Ekendahl and Pedersen 1994/. Such biofilms will increase their cell numbers until they reach steady state. A comparison of the hypothetical cell numbers and activities of attached versus unattached bacteria in a 0.1-mm wide fracture was previously done (see Table 4.5 in /Pedersen 2001/) and was reported in Appendix 2 in the Hydrogeochemical evaluation for the Laxemar subarea – version 1.2 /SKB 2006/. It demonstrated the potential importance of attached versus unattached microorganisms in underground environments. The studied microorganisms attached to artificial surfaces generally exhibited greater activity per cell than did the unattached microorganisms. Taken together with the cell numbers, there was up to five orders of magnitude more activity on the surfaces than in the groundwater. It is still an open question whether attached bacteria are common and active on aquifer rock surfaces under pristine conditions.

1.5.2 Dissolved organic carbon and total number of cells

Dissolved organic carbon (DOC) and the total number of cells are parameters that in most cases display parallel trends. DOC provides a basis for microbial populations, at least in ecosystems fed by photosynthetically produced carbon compounds, i.e. systems in contact with the ground surface. In deeper groundwater containing chemolithotrophic microorganisms, the connection between DOC and TNC is not necessarily so strong.

In all sampled sections, except in boreholes KFM01D and KFM10A at a depth of 441 and 328 m respectively, the dissolved organic carbon was less than 4 mg L^{-1} (Figure 1-5). Figure 1-6 shows that the TNCs in the boreholes were all below 10^5 mL^{-1}, except the two levels in boreholes

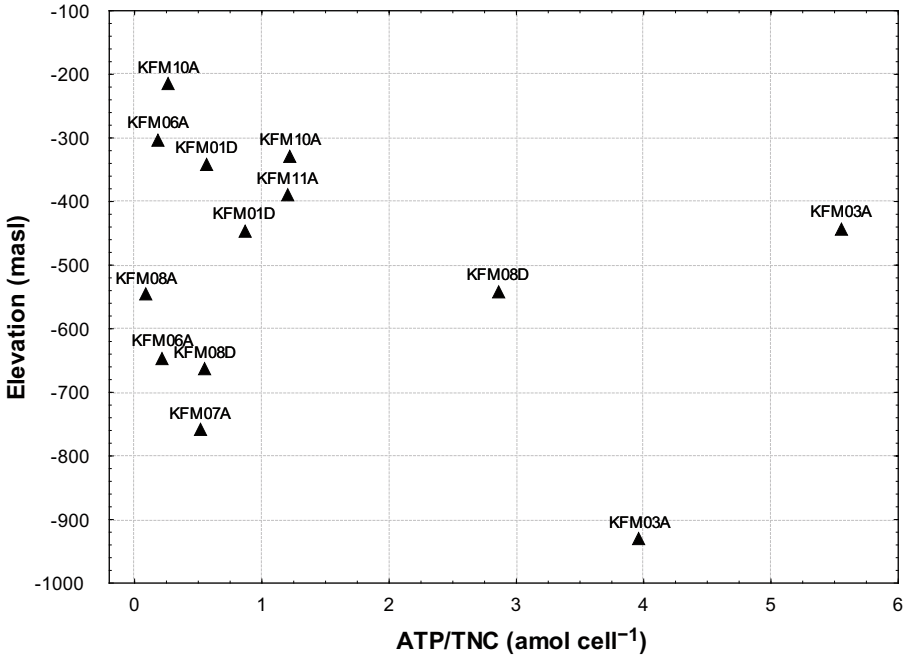

Figure 1-4. *The concentrations of ATP per total number cell (TNC) distributed over depth in Forsmark groundwater.*

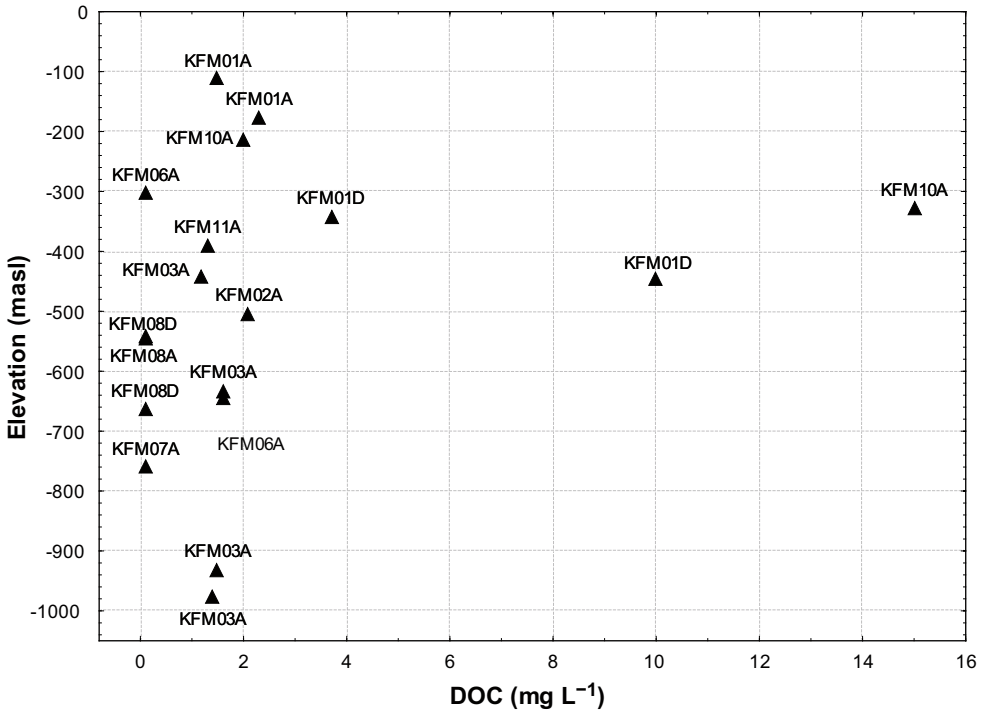

Figure 1-5. *Dissolved organic carbon (DOC) versus depth. Symbols for DOC at 0.1 denote data below the detection limit of 1 mg DOC L^{-1}. Data from extended freeze 2.3 (December 2007) in Forsmark.*

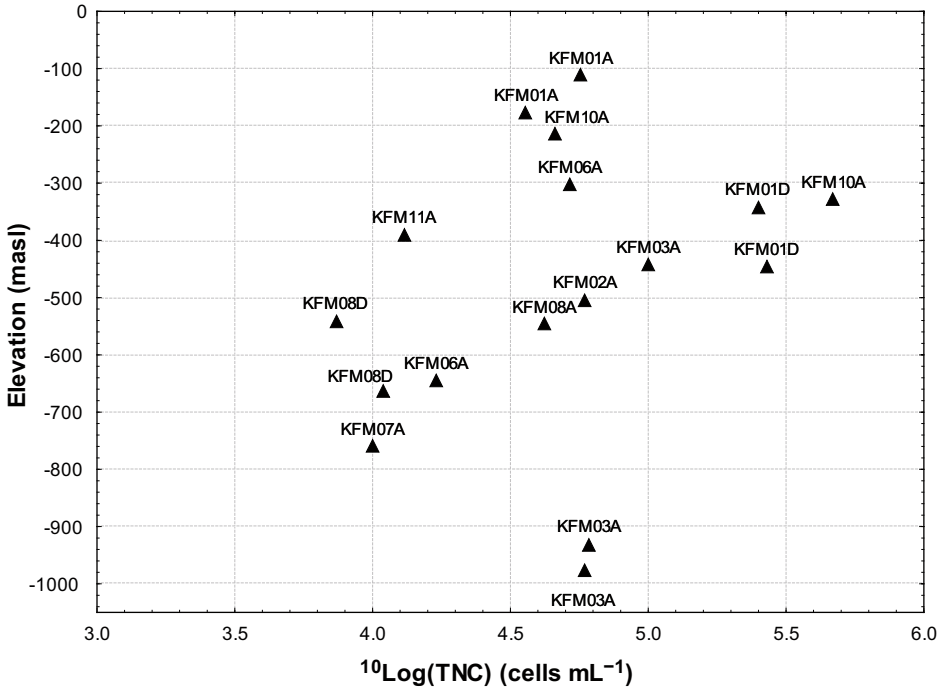

Figure 1-6. *Total number of cells (TNC) versus depth. Data from extended freeze 2.3 (December 2007) in Forsmark.*

KFM01D and level 328 m in KFM10A. The lowest numbers, at about 1×10^4 mL^{-1}, were found at 760 m in KFM07A and in KFM08D. These data are in the range of the cell numbers earlier found in boreholes in the Fennoscandian Shield /Pedersen 2001/. The DOC values follow a decreasing trend with depth, in agreement with the results of earlier studies /Pedersen 2001/. There was also a significant ($p<0.05$) correlation between DOC and TOC (Figure 1-7).

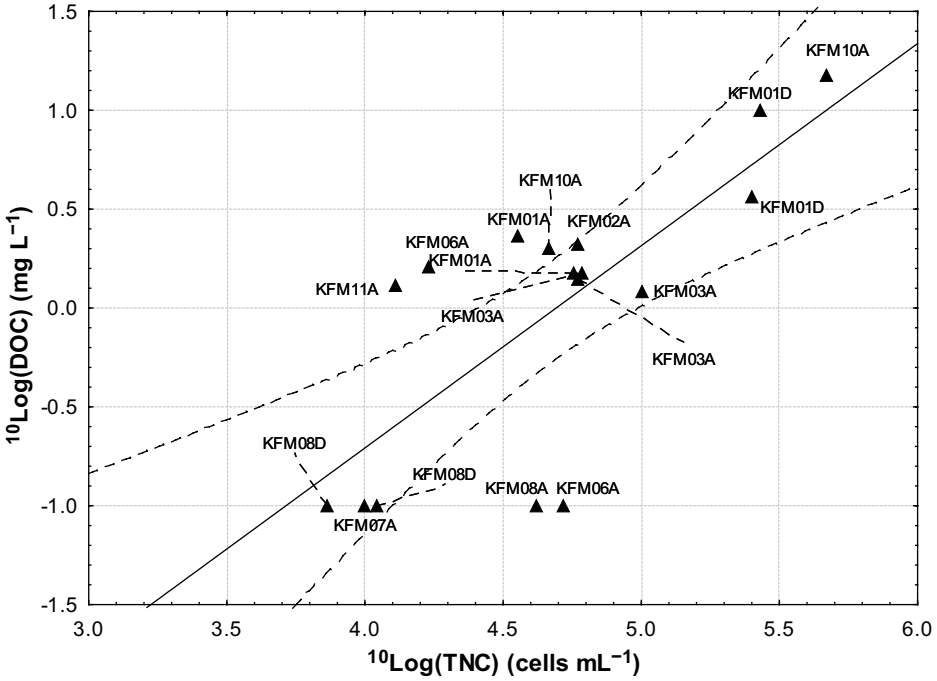

Figure 1-7. *The relation between total number of cells (TNC) and dissolved organic carbon (DOC). Symbols for DOC at –1 denote data below the detection limit of 1 mg DOC L^{-1}. Statistics: $^{10}Log(DOC)=–4.80+1.02 \times {}^{10}Log(TNC)$, r=0.74, significant at p=0.0007, n=17. Dashed lines denote the 95% confidence interval. Data from extended freeze 2.3 (December 2007) in Forsmark.*

DOC and TNC from one sections each of the boreholes KFM01D and KFM10A, at a depth of 441 and 328 m, respectively, showed higher numbers than have generally been found in this site investigation and also higher than what have usually been observed in Fennoscandian Shield groundwater /Pedersen 2001/. The lowest values of both parameters were found in the boreholes KFM07A and KFM08D.

1.5.3 Relations between microbiology and organic material

To understand the size distribution of the organic material in groundwater, samples from several sections of seven boreholes were subjected to fractionation filtration (see Table 1-5). Defined cut-off filters of 1,000 and 5,000 Dalton (D) were used; one Dalton is equivalent to the mass of one hydrogen atom, i.e. 1.67×10^{-24} g. Fulvic acids are smaller than humic acids and have molecular weights below 1,000 D. Humic acids, on the other hand, have molecular weights up to several hundred thousand D. The 1,000–5,000 D fraction is considered to represent colloidal organic material. The results of the filtration indicated that most of the organic material was smaller than 1,000 D in size but that some was in the >5000 D fraction. Organic material in the 1,000–5,000 D fraction was found in five sections. DOC data for borehole KFM08A from two different sampling occasions display very different values, i.e. 2.6 and <0.1 mg L^{-1}; the sample with the higher value was taken at the same time as was the sample of organic colloids.

Most of the other DOC data for this borehole have values >0.1 mg L^{-1}, which agrees with the TNC data. The presence of organic colloids was not correlated with high MPNs for the different physiological groups of microorganisms (not shown). As well, it must be considered that molecules with a molecular weight of 1,000 D are relatively large. These molecules could easily contain 20 or more carbons. For example, complex binding molecules produced by microorganisms have approximately 40 carbons together with nitrogen, oxygen, and hydrogen atoms /Johnsson et al. 2006/. When compared to the number of colloids, TNC showed an inverse relationship (Figure 2-6) but the correlation was not significant (p> 0.05). More data are needed before conclusions can be drawn.

Table 1-5. Organic material (mg L^{-1}) in groundwater sampled from boreholes in the Forsmark area, measured for three fractions using fractionation filtration and DOC measurements.

Borehole section	<1,000 D (mg L^{-1})	1,000–5,000 D (mg L^{-1})	>5,000 D (mg L^{-1})	DOC (mg L^{-1})
KFM01A, 112 m	3.80±0.5	0	0	1.5
KFM01A, 176 m	2.90±0.30	0	0.3±0.1	2.3
KFM01D, 341 m	2.30±0.60	0	0	2.3
KFM01D, 445 m	7.50±1.0	0	0	10
KFM02A, 109 m	4.60±0.50	1.50±0.4	3.70±0.7	11
KFM02A, 415 m	1.20±0.20	0	0.11±0.04	d.m.
KFM02A, 418 m	1.00±0.10	0.20±0.05	d.m.	d.m.
KFM02A, 503 m	1.70±0.20	0.50±0.10	0	2.1
KFM03A, 441 m	1.10±0.10	0	0	1.2
KFM03A, 379 m	1.20±0.10	0	0	1.3
KFM03A, 442 m	1.30±0.10	0.29±0.07	0	d.m.
KFM03A, 631 m	1.40±0.20	d.m.	d.m.	1.6
KFM03A, 632 m	1.20±0.10	0	0	1.2
KFM03A, 978 m	1.40±±0.20	0	0	1.1
KFM06A, 302 m	1.20±0.20	0	0	1.1
KFM06A, 645 m	1.50±0.20	0	0	1.5
KFM07A, 760 m	0	0	0	0
KFM08A, 546 m	2.60±0.30	0.30±0.10	0	2.6 (<0.1)

[1] n.d. = not detected; [2] d.m. = data missing; /Wacker et al. 2003, 2004ab/.

1.6 Cultivable heterotrophic aerobic bacteria

The analysis of CHAB showed no correlation with depth (see Figure 1-8). This analysis started with borehole KFM08A (Table 1-4), so there are no CHAB data for the boreholes sampled earlier. It should be noted that the numbers of CHAB were very high, i.e. above 10,000 mL^{-1}, in KFM01D, 445 m and KFM10A, 215 m. In both these sections, high MPNs were found for most of the different groups of microorganisms (Figure 1-28). Some of these bacteria are facultative anaerobes which means that they can live without oxygen and instead use nitrate as the electron acceptor. The weak decreasing trend of CHAB with depth was not statistically significant ($p>0.05$) (Table 1-1).

1.7 Nitrate-reducing bacteria

Analysis of NRB was introduced in the MPN analyses starting from borehole KFM07A (Table 1-4); the results of this analysis are shown in Figure 1-9. NRB numbers displayed a decreasing trend with depth; the highest value was found in borehole KFM01D at a depth of 445 m. The weak decreasing trend of NRB with depth was, however, not statistically significant ($p>0.05$) (Table 1-1). Nitrate reducers reduce nitrate with organic material to nitrogen gas or, in some species, to nitrite. The nitrate concentrations in groundwater in Forsmark were generally very low. Several genera and species that are nitrate reducers can also use other electron acceptors, such as oxygen, ferric iron and manganese(IV); one such genus is *Shewanella* /Meyers and Nealson 1990/. Therefore, the presence of nitrate reducers in a sampled section does not necessarily indicate that nitrate reduction is occurring.

The CHAB were analysed under aerobic conditions, unlike all other cultivation methods used here, which were performed under anaerobic conditions. As said above, many bacteria are known to be facultative anaerobes, i.e. they can switch from aerobic respiration using oxygen to anaerobic respiration using nitrate and often also ferric iron and manganese(IV) as alternative electron acceptors /Madigan and Martinko 2006/. Microorganisms in groundwater must be adapted to anoxic conditions but, if oxygen should appear, it is advantageous for the microbe

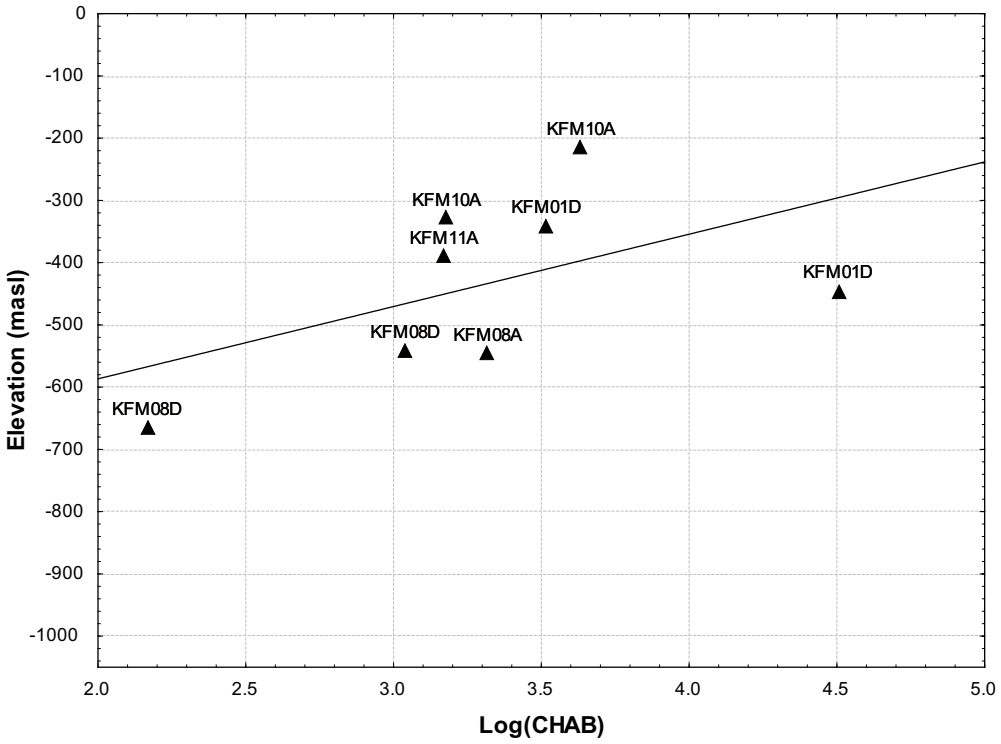

Figure 1-8. *The relation between cultivable bacteria (CHAB) and depth. r=0.54, not significant at p=0.18, n=8. Data from extended freeze 2.3 (December 2007) in Forsmark.*

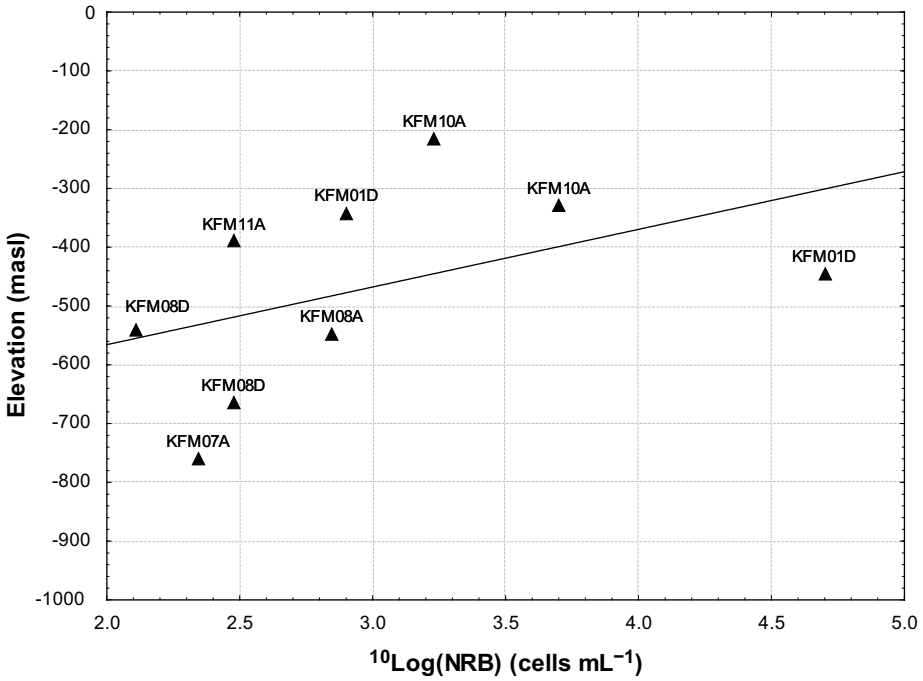

Figure 1-9. *The relation between nitrate reducing bacteria (NRB) and depth. r=0.46, not significant at p=0.21, n=9. Data from extended freeze 2.3 (December 2007) in Forsmark.*

to be able to switch to oxygen respiration. Indigenous groundwater microorganisms should consequently be detectable as both CHAB and NRB, while contaminants from the surface should have a smaller tendency to do so. Comparing the CHAB data to the NRB data indicated a reasonably good correlation (Figure 1-10), suggesting that the microorganisms analysed as CHAB were generally indigenous.

1.8 Iron-reducing bacteria and Fe^{2+}

The highest number of IRB, i.e. 4×10^3 per mL, was found at a depth of 112 m in borehole KFM01A (see Figure 1-11), and numbers above 10^3 mL^{-1} were also found in boreholes KFM10A−328 m and in KFM08D−664 m. In general, there was a significant trend towards decreasing numbers of iron reducers with depth (Table 1-6), with exception for KFM08D-664 m and KFM01A−176 m. The concentrations of ferrous iron decreased exponentially with depth in Forsmark (see Figure 1-12). There were two exceptional values, 15.4 mg L^{-1} at an elevation of −328 m in borehole KFM10A and 0.004 mg L^{-1} in KFM08D at −540 m elevation (not shown in Figure 1-12). Iron in the groundwater occurred mainly in a ferrous state and, if sulphide was present, ferrous iron may have precipitated as ferrous sulphide and become adsorbed to surfaces in fractures. This could explain why the correlation between the concentration of Fe^{2+} and IRB was weak for some samples (Figure 1-13). A model of the influence of microorganisms on groundwater geochemistry must consider ferrous iron and sulphide production simultaneously. These two components will interact depending on pH and E_h. Ferric-state iron will probably mostly be found mineralized on fracture surfaces.

The relatively high numbers of IRB imply that they are important for the geochemistry in the Forsmark area. Since most IRB use partially oxidized organic matter, such as short-chain organic acids, as their sources of energy, electron, and carbon, they participate in the degradation of organic matter originating from the ground surface. The origin of organic material found at the different depths is unclear. A source alternate to ground surface processes could be autotrophic acetate produced by acetogens at depth.

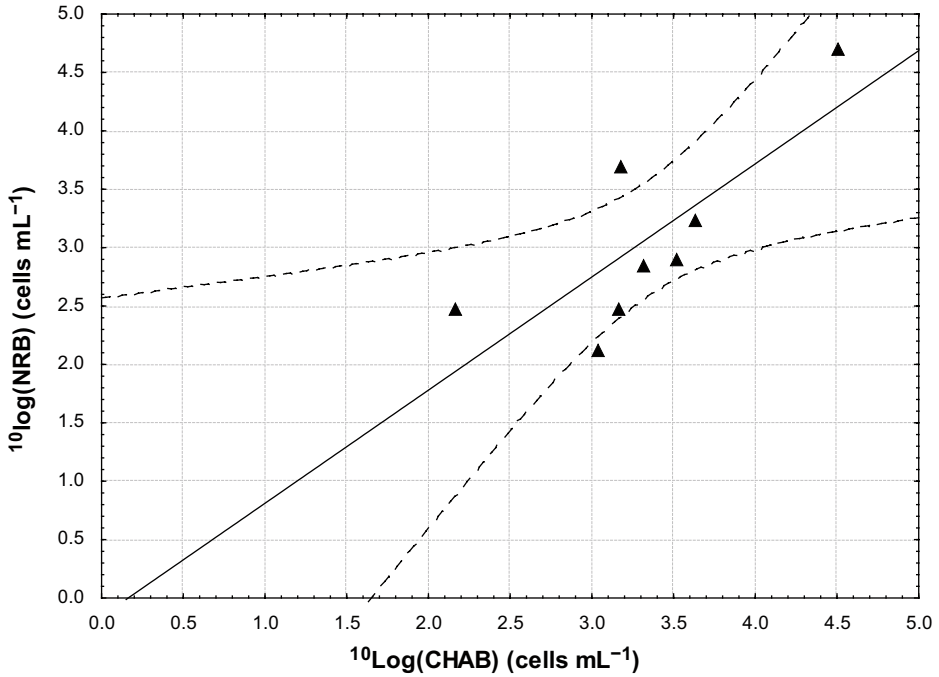

Figure 1-10. *The relation between the number of nitrate reducing bacteria (NRB) and the number of cultivable bacteria (CHAB). Statistics: $^{10}Log(NRB)=-0.157 + 0.97 \times {}^{10}Log(CHAB)$, r=–0.76, significant at p=0.026, n=8. Dashed lines denote the 95% confidence interval. Data from extended freeze 2.3 (December 2007) in Forsmark.*

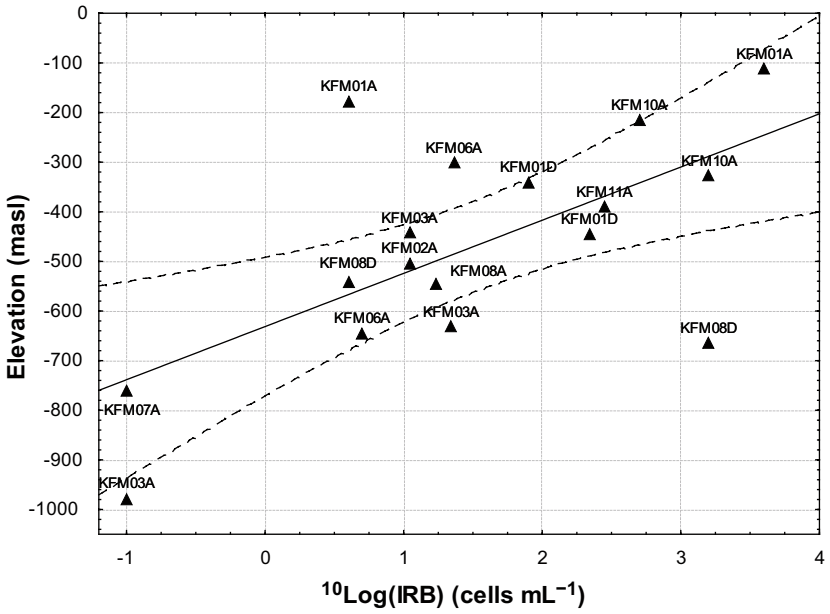

Figure 1-11. *The relation between the number of iron reducing bacteria (IRB) and elevation. Statistics: Elevation=–631+107 × ^{10}Log(IRB), r=–0.64, significant at p=0.0055, n=17. Symbols for IRB at –1 denote data below the detection limit of 0.2 cells mL^{-1}. Dashed lines denote the 95% confidence interval. Data from extended freeze 2.3 (December 2007) in Forsmark.*

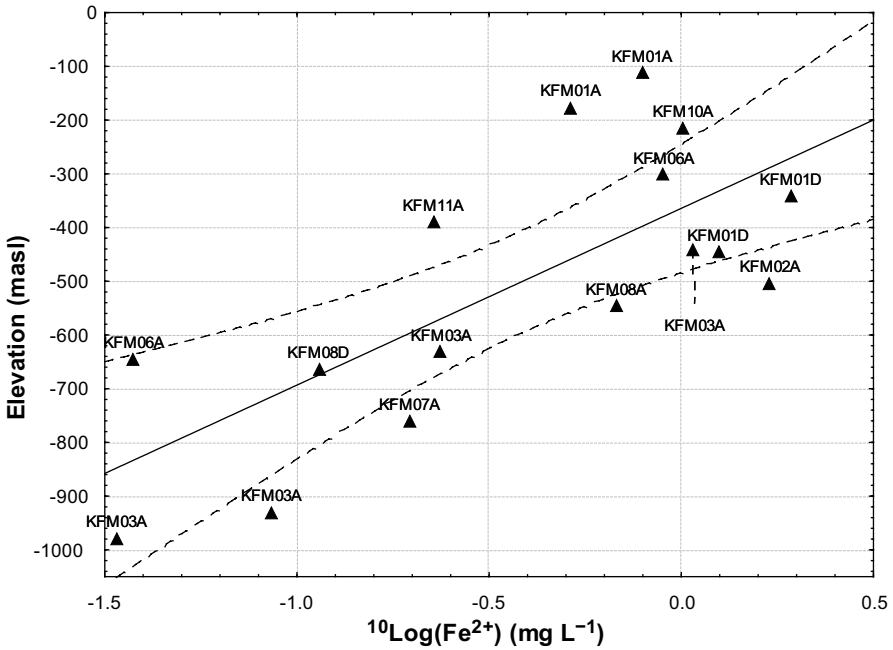

Figure 1-12. *The relation between the concentration of Fe^{2+} and elevation. Statistics: Elevation=–364+328 × ^{10}Log(Fe^{2+}), r=–0.74, significant at p=0.0011, n=16. Data for KFM10A-328 m and KFM08D-540 m were excluded from the calculation. Dashed lines denote the 95% confidence interval. Data from extended freeze 2.3 (December 2007) in Forsmark.*

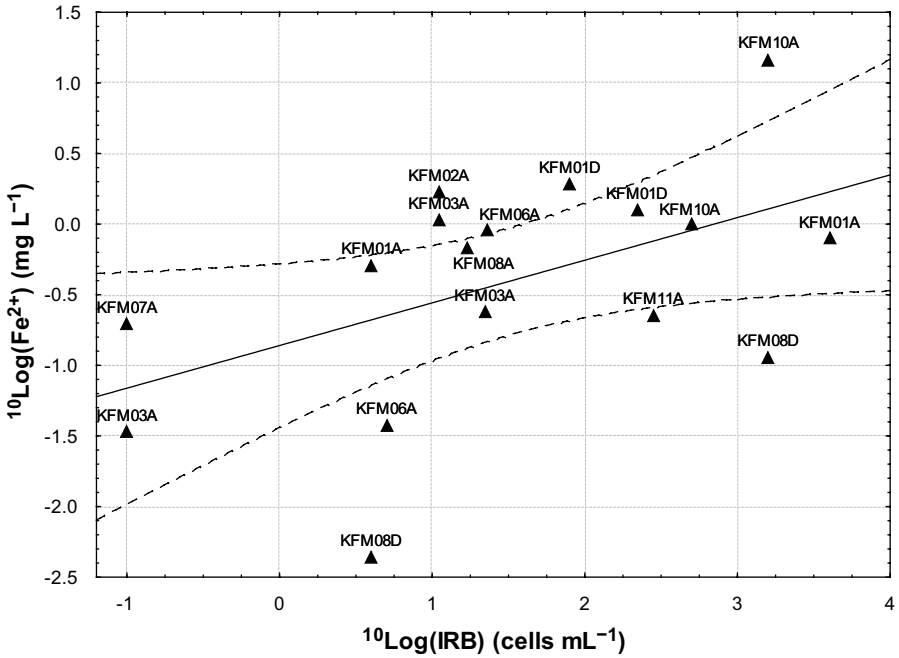

Figure 1-13. *The relation between the Log concentration of Fe^{2+} and log iron reducing bacteria. Statistics: $^{10}Log(Fe^{2+})=-0.86+0.30 \times {}^{10}Log(IRB)$, r=–0.49, significant at p=0.044, n=17, all available data were included. Symbols for IRB at –1 denote data below the detection limit of 0.2 cells mL^{-1}. Dashed lines denote the 95% confidence interval. Data from extended freeze 2.3 (December 2007) in Forsmark.*

1.9 Manganese-reducing bacteria and manganese

In natural water in the pH 5–8 range, Mn(IV) occurs mostly in precipitates as insoluble MnO_2; manganese found in solution in such environments therefore consists of Mn^{2+} ions. The concentration of manganese decreased significantly with depth in Forsmark (see Figure 1-14). As discussed for IRB above, MRB are part of the groundwater community that degrade organic matter from the surface or utilize acetic acid produced by acetogens; MRB are therefore an important part of the process that lowers the redox potential in groundwater by oxidizing organic matter with oxidized manganese compounds.

The highest numbers of MRB were found in borehole KFM01A at a depth of 112 m (Figure 1-15). The numbers of MRB decreased exponentially with depth scattered along a line of correlation that was significant at p=0.004 (Table 1-6). When MRB was compared to the concentration of Mn^{2+} a correlation could not be demonstrated (Table 1-6) which reflect a fairly large scatter among the observations at the analysed elevations.

Many of the MRB can also reduce ferric iron. Therefore, an excellent correlation was found between IRB and MRB (Figure 1-16). These organisms can toggle between the electron acceptors ferric iron and manganese(IV) depending on availability. This correlation also attests the stability and reproducibility between the different physiological MPN groups applied.

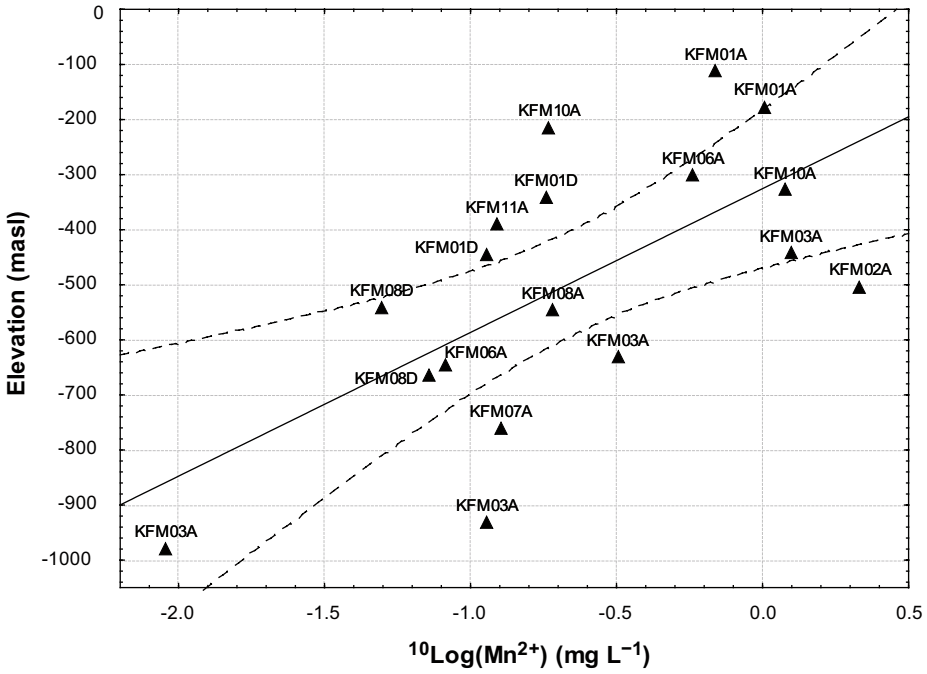

Figure 1-14. *The relation between the concentration of Mn^{2+} and elevation. Statistics: Elevation=–325 +261 × ^{10}Log(Mn^{2+}), r=–0.64, significant at p=0.0041, n=18. Dashed lines denote the 95% confidence interval. Data from extended freeze 2.3 (December 2007) in Forsmark.*

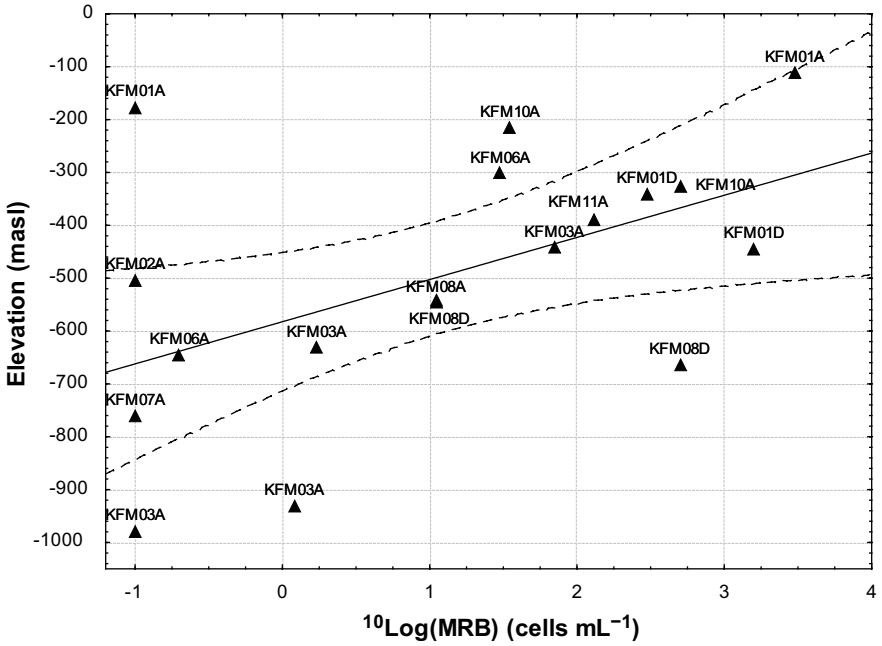

Figure 1-15. *The relation between the number of manganese reducing bacteria (MRB) and elevation. Statistics: Elevation=–582+80 × ^{10}Log(MRB), r=–0.51, significant at p=0.029, n=18. Symbols for MRB at –1 denote data below the detection limit of 0.2 cells mL^{-1}. Dashed lines denote the 95% confidence interval. Data from extended freeze 2.3 (December 2007) in Forsmark.*

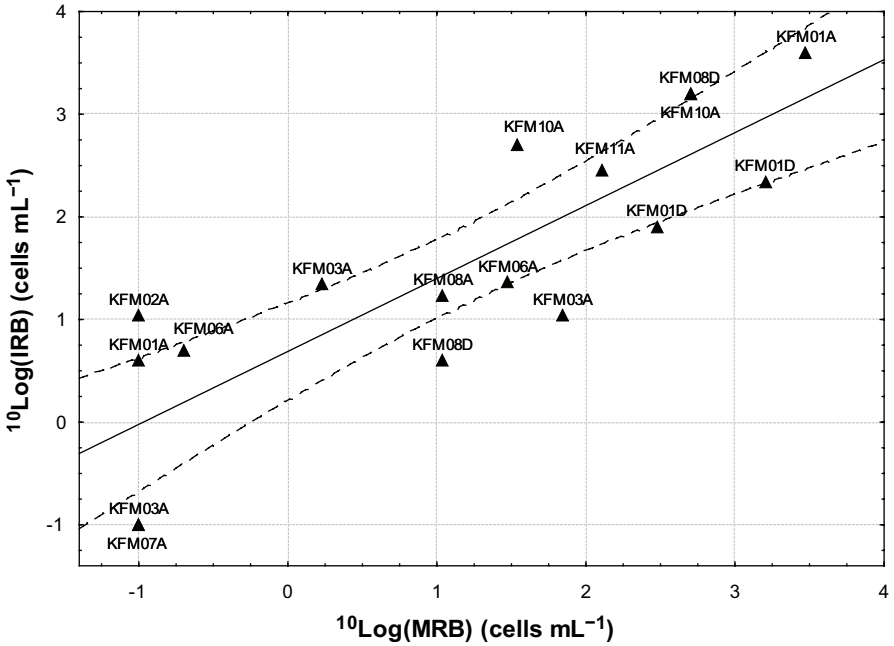

Figure 1-16. *The relation between the number of manganese reducing bacteria (MRB) and the number of iron reducing bacteria (IRB). Statistics:* $^{10}Log(IRB)=0.69+0.71 \times {}^{10}Log(MRB)$, *r=–0.84, significant at p=0.00002, n=17. Symbols at –1 denote data below the detection limit of 0.2 cells* mL^{-1}. *Dashed lines denote the 95% confidence interval. Data from extended freeze 2.3 (December 2007) in Forsmark.*

1.10 Sulphate-reducing bacteria, sulphate, and sulphide

The number of SRB was highest at a depth of 445 m in KFM01D at 1.3×10^4 mL^{-1} (see Figure 1-17). Thus, the number of SRB peaks at a depth of 300 to 400 m; this peak coincides with the highest amounts of DOC and TNC (Figure 1-5 and Figure 1-6). A significant relation between elevation and the numbers of SRB could not be established (Figure 1-17). The SRB data were totally scattered over the sampled elevation range.

The presence of SRB in groundwater in Forsmark was accompanied by very low sulphide values, close to the detection limit of about 0.002 mg L^{-1} as shown in Figure 1-18. One explanation of this could be the formation and precipitation of amorphous iron sulphides in fractures if the groundwater is rich in ferrous iron. The highest sulphide values were found in groundwater below 700 m. The ferrous iron concentration is low in the deep groundwater in Forsmark. Sulphate was present throughout the sampled elevation, although it decreased significantly in concentration below about 600 m elevation (Figure 1-19). The boreholes were pumped with a pump rate of about 200 mL min^{-1} before sampling for analysis of SRB and sulphide. Prolonged pumping may introduce a disturbance that influences the numbers of SRB and that washed out sulphide from the groundwater system. This effect has been documented at the MICROBE site in the Äspö hard rock laboratory /Pedersen 2005b/. Pumping may also trigger FeS precipitation as a consequence of ferrous iron production by IRB which may be stimulated by an increased flow in the sampled fractures. The values for SRB and sulphide are, because of the large risk for such disturbances, unfortunately not reliable for predictive modelling of microbial processes.

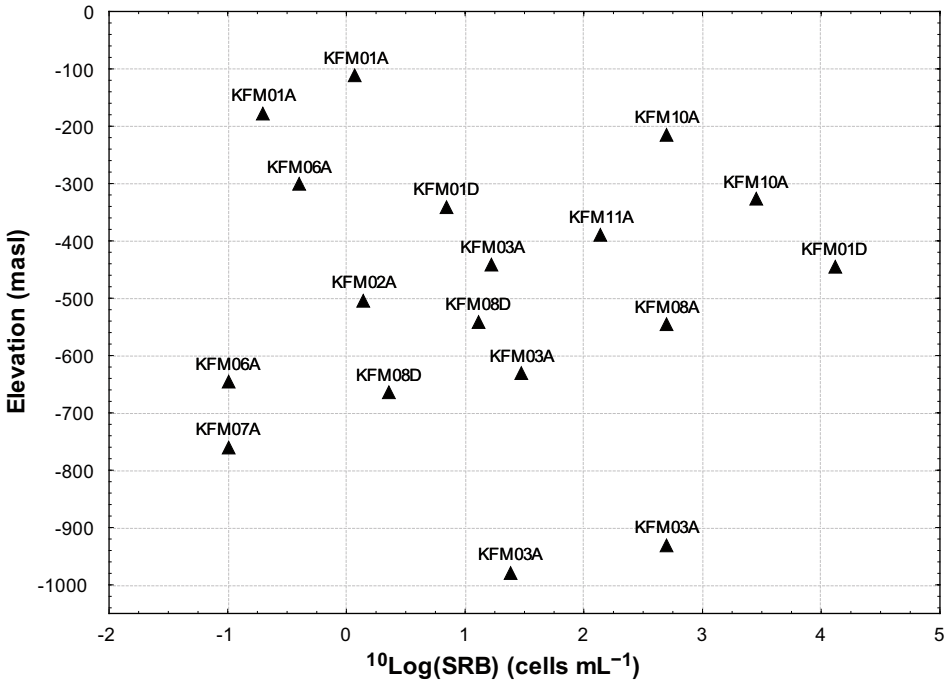

Figure 1-17. *Most probable number of cells (MPN) for sulphate-reducing bacteria (SRB) versus elevation in the Forsmark area. Symbols for SRB at –1 denote data below the detection limit of 0.2 cells mL^{-1}. Data from extended freeze 2.3 (December 2007) in Forsmark.*

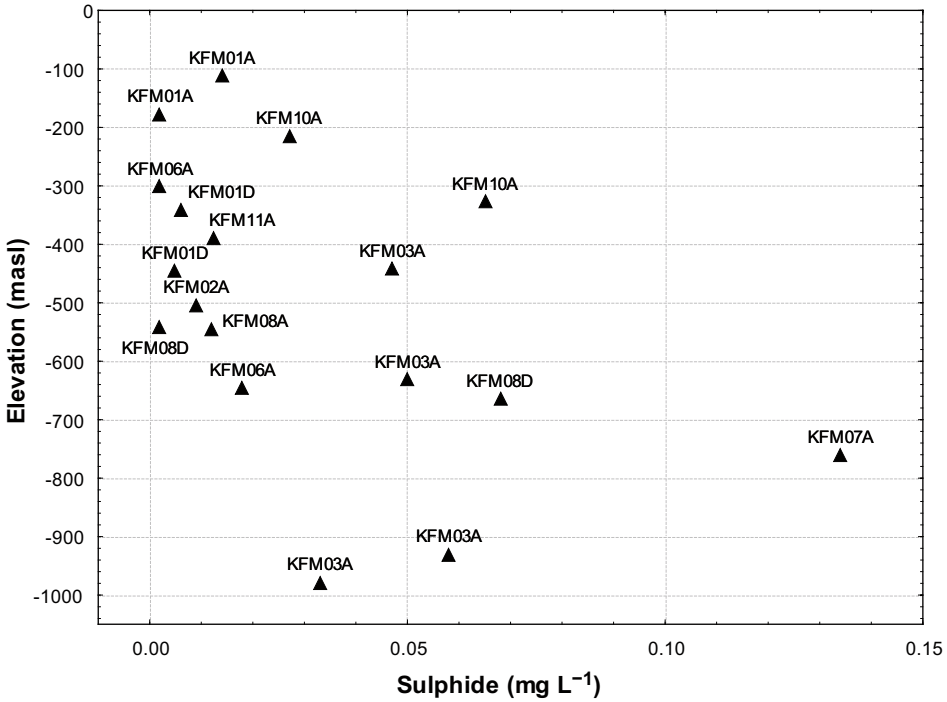

Figure 1-18. *Sulphide concentration versus elevation in the Forsmark area. Symbols for sulphide at 0.001 denote data below the detection limit of 0.002 mg L^{-1}. Data from extended freeze 2.3 (December 2007) in Forsmark.*

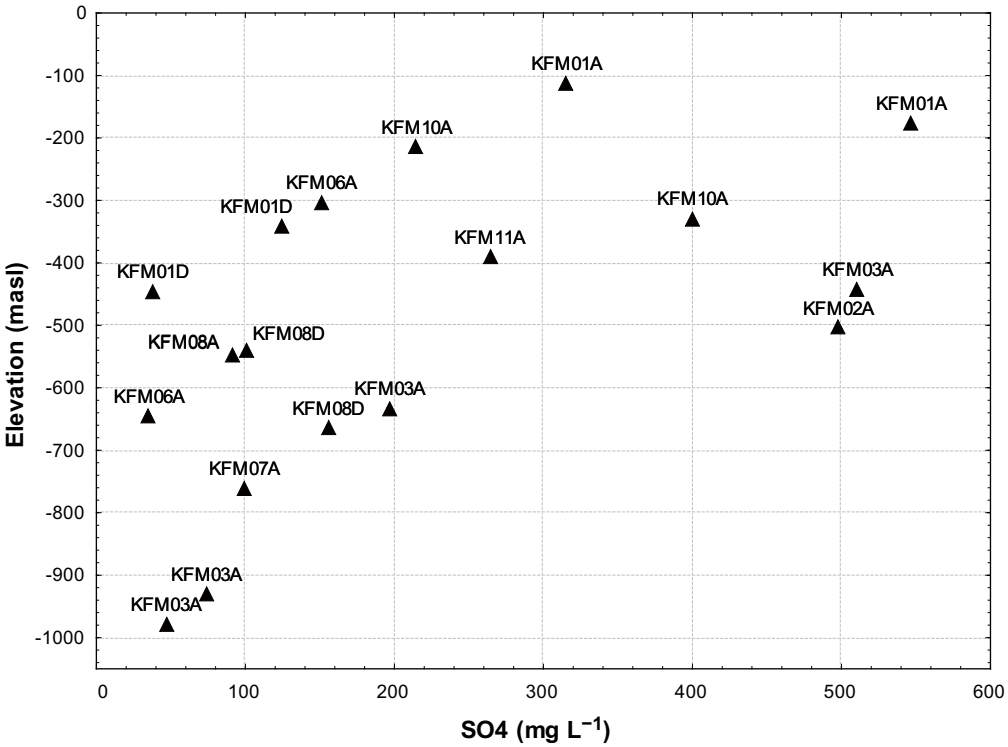

Figure 1-19. *Sulphate concentration versus elevation in the Forsmark area. Data from extended freeze 2.3 (December 2007) in Forsmark.*

1.11 Methanogens

Figure 1-20 presents the MPN numbers of the two different types of methanogens, autotrophic (AM) and heterotrophic (HM), plotted against depth. Unfortunately, no data are available for autotrophic methanogens from the two depths in borehole KFM01A. The highest amount of methane in this investigation was found in KFM01D at a depth of 445 m (Figure 3-6). MPN culturing of methanogens produced no growth at this depth. The highest number of methanogens observed was 7 mL^{-1} for HM at a depth of 439 m in KFM03A; the amount of methane here was 0.04 mL L^{-1}, corresponding to 2 µM. Autotrophic methanogens were present, but only in trace amounts, here and at 642.5 m in KFM03A.

No isotopic data are available for the measured methane so it is difficult to determine its origin; however, the C1/(C2 + C3) ratio (see section3.5.4, "Methane and higher hydrocarbons") implies that the methane is a mixture of biogenic and abiogenic methane. The only section that displayed more biotic methane was KFM01D, 445 m.

1.12 Acetogens

Acetogenic activity results in acetate production. Acetogens were the dominant microorganisms in the sections studied; there were often one or two orders of magnitude more acetogens than the second most common organism type. Many acetogens are both heterotrophic and autotrophic. The highest numbers were found in borehole KFM10A at a depth of 328 m and in KFM01D at 445 m (see Figure 1-21). There was no significant relationship between the numbers of acetogens and depth (Table 1-6). Some of the metabolic groups analysed using MPN may overlap in numbers. At the onset of this investigation it was unclear whether AA and HA would differ in numbers.

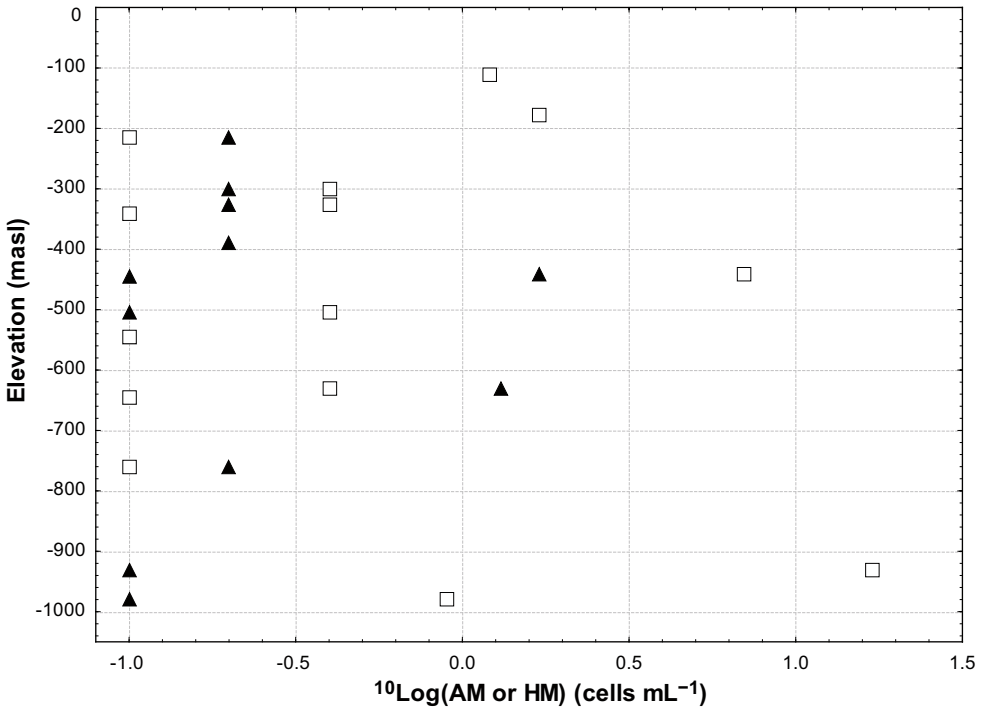

Figure 1-20. *Most probable numbers of cells (MPN) for auto- and heterotrophic methanogens (AM and HM) versus depth in boreholes in the Forsmark area. Solid triangles = autotrophic methanogens, open squares = heterotrophic methanogens. Symbols at –1 denote data below the detection limit of 0.2 cells mL^{-1}. Data from extended freeze 2.3 (December 2007) in Forsmark.*

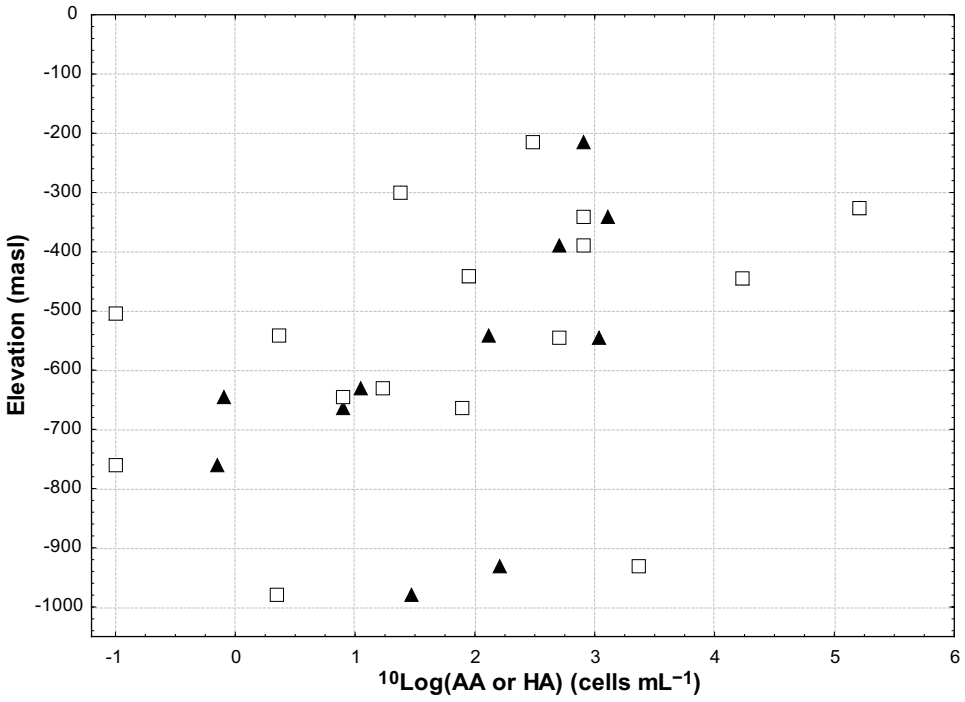

Figure 1-21. *Most probable numbers of cells (MPN) for auto- and heterotrophic acetogens (AM and HM) versus depth at six depths in boreholes in the Forsmark area. Solid symbols = heterotrophic acetogens, open symbols = autotrophic acetogens. . Symbols at –1 denote data below the detection limit of 0.2 cells mL^{-1}. Data from extended freeze 2.3 (December 2007) in Forsmark.*

The acetogens are known to be a diverse group of organisms that may switch between different metabolic states /Drake et al. 2002/. Comparing the MPN numbers of AA and HA indicates that they correlated very well (Figure 1-22). So far, acetate data have not been available, though acetate could well be an important parameter to measure. One problem is that, because acetate is one of the most microbially utilized organic molecules, its concentration in groundwater is probably below the detection limits of available analyses.

1.13 Total number of cells versus MPN

The MPN methods for enumerating microorganisms in deep groundwater were first used for analysing methanogens and acetogens in Äspö HRL groundwater /Kotelnikova and Pedersen 1998/. Later, the methods were further developed, and they have been used to analyse more types of microorganisms in deep groundwater samples from Finland /Haveman et al. 1999, Haveman and Pedersen 2002a/, including from Olkiluoto, and from the natural nuclear reactors in Bangombé, Gabon, Africa /Haveman and Pedersen 2002b/. The methods have been modified and changed over time. As the numbers of samples and types of organisms analysed have increased, the manual preparation of single tubes, as used for analysing methanogens and acetogens in Äspö HRL groundwater /Kotelnikova and Pedersen 1998/, has had to give way to methods that could handle the approximately three hundred MPN tubes needed during each of the Forsmark field samples.

The expression "the great plate count anomaly" was coined by /Staley and Konopka 1985/ to describe the difference in orders of magnitude between the numbers of cells from natural environments that form colonies on agar media (CHAB) and the numbers countable by means of microscopic examination (TNC). In general, only 0.01–0.1% of bacterial cells sampled from various environmental aquatic systems produce colonies when using standard plating techniques so, as expected from the relevant literature results, there were no correlations between TNC and CHAB data for Forsmark groundwater (Table 1-6). The anaerobic cultivation methods presented

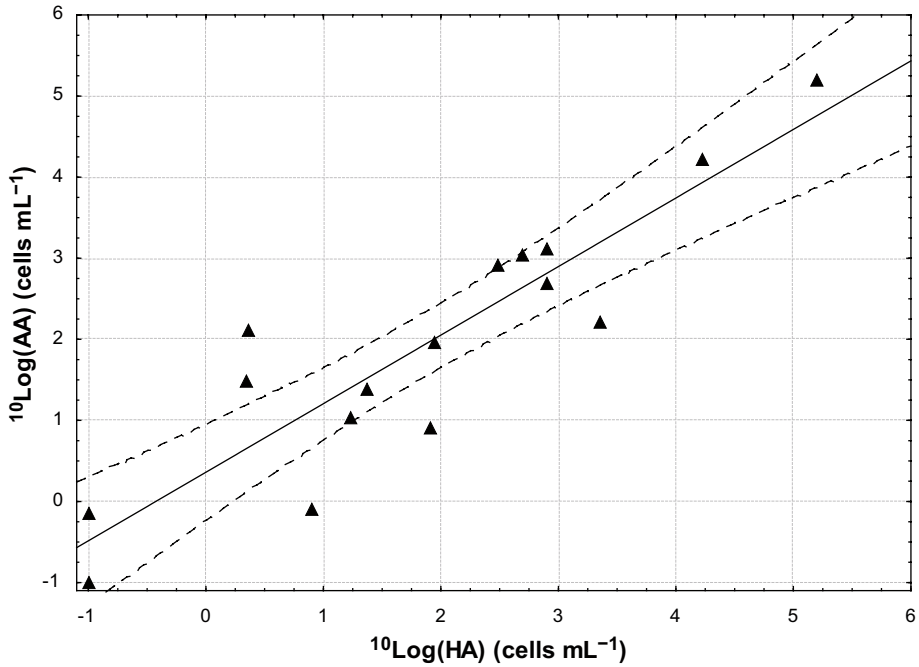

Figure 1-22. *The relationship between autotrophic (AA) and heterotrophic (HA) acetogens. Statistics: $^{10}Log(AA)=0.36+0.85\times{}^{10}Log(HA)$, r=–0.89, significant at p=0.0001, n=16. Dashed lines denote the 95% confidence interval. Symbols at –1 denote data below the detection limit of 0.2 cells mL^{-1}. Data from extended freeze 2.3 (December 2007) in Forsmark.*

here represent the culmination of almost 10 years of development, testing, and adaptation for deep groundwater. The success and usefulness of these methods are reflected in the maximum MPN cultivability of 70% of the TNC in the sample from the borehole KFM10A in the 328 m section and the 0.02–70% MPN cultivability range in all groundwater samples (Figure 1-23). The use of multiple, liquid anaerobic media) has obviously overcome much of the discrepancy found between TNC and cultivations that use agar media only. However, it should be understood that there may still be microorganisms in the groundwater not cultivable using the applied methods. One example is that of anaerobic methane-oxidizing bacteria (ANME), which as of the time of writing have escaped successful cultivation by the world microbiology community. ANME have been observed in environmental samples but their successful cultivation in the laboratory has yet not been described in the literature.

1.14 Correlations between variables deemed important for microbiological concenptual models

The dataset from Forsmark 2.3 includes a large range of variables with many cases. Here, a correlation matrix was constructed for the variables judged important for understanding microbial processes (Table 1-6). As shown previously, there were generally good crosswise correlations between the different cultivation and biomass results. Many of these parameters also showed good correlations with TOC and DOC. The drill water residual (DWR) was not found to correlate with any of the included variables. Several of the chemical variables such as log ferrous iron and manganese and sulphate showed good correlation with depth as expected because the amount of dissolved species generally decreases with depth in Fennoscandian groundwater. This is an example of nested variables, implying that some caution should be taken when evaluating multiple correlation matrices before conclusions are drawn about how different variables have effect on other variables. The correlation matrix in Table 1-6 should be regarded as a guide to possible relations that can be further evaluated as done next.

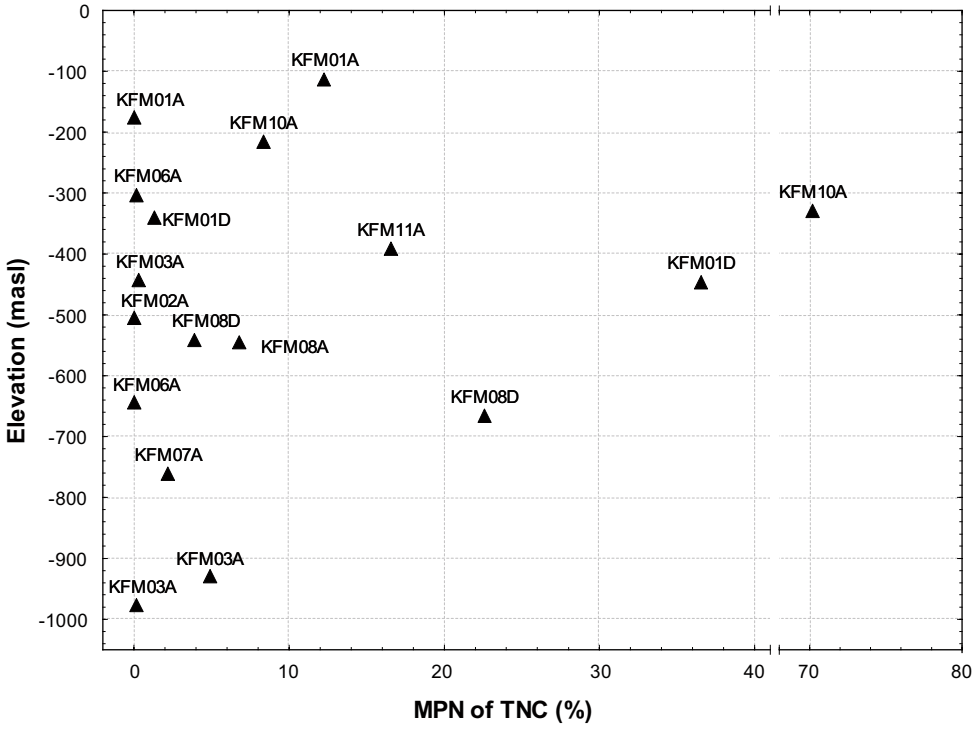

Figure 1-23. *Percentages of the total number of cells cultured using MPN in the analysed sections in boreholes in the Forsmark area. Nitrate reducing bacteria were included in analyses of KFM07A, KFM08A, KFM08D, KFM01D, KFM10A and KFM11A. Data from extended freeze 2.3 (December 2007) in Forsmark.*

Table 1-6. Correlation matrix of analysed variables that were related to microbial processes and, therefore, potentially correlated. For each pair of correlation, the correlation coefficient, r, is given followed by the number of observations and the significans level, p, for the correlation. Pairwise missing data deletion was applied. Correlations marked with red are significant at p<0.0500. Data from extended freeze 2.3 (December 2007) in Forsmark.

Variable	Variable (m)	Log(TNC)	Log(ATP)	Log(CHAB)	Log(NRB)	Log(IRB)	Log(MRB)	Log(SRB)
Elevation (m)		.2779	.1408	.5242	.4561	.6418	.5150	–.0227
		N=17	N=14	N=8	N=9	N=17	N=18	N=18
		p=.280	p=.631	p=.182	p=.217	p=.005	p=.029	p=.929
Log(TNC)	.2779		.7726	.6037	.8180	.3277	.3816	.5173
	N=17		N=13	N=8	N=9	N=16	N=17	N=17
	p=.280		p=.002	p=.113	p=.007	p=.215	p=.131	p=.033
Log(ATP)	.1408	.7726		.4881	.6916	.3342	.4467	.5573
	N=14	N=13		N=8	N=9	N=13	N=14	N=14
	p=.631	p=.002		p=.220	p=.039	p=.264	p=.109	p=.038
Log(CHAB)	.5242	.6037	.4881		.7673	–.1479	.1960	.7324
	N=8	N=8	N=8		N=8	N=8	N=8	N=8
	p=.182	p=.113	p=.220		p=.026	p=.727	p=.642	p=.039
Log(NRB)	.4561	.8180	.6916	.7673		.4544	.5878	.7880
	N=9	N=9	N=9	N=8		N=9	N=9	N=9
	p=.217	p=.007	p=.039	p=.026		p=.219	p=.096	p=.012
Log(IRB)	.6418	.3277	.3342	–.1479	.4544		.8451	.4203
	N=17	N=16	N=13	N=8	N=9		N=17	N=17
	p=.005	p=.215	p=.264	p=.727	p=.219		p=.000	p=.093
Log(MRB)	.5150	.3816	.4467	.1960	.5878	.8451		.4589
	N=18	N=17	N=14	N=8	N=9	N=17		N=18
	p=.029	p=.131	p=.109	p=.642	p=.096	p=.000		p=.055
Log(SRB)	–.0227	.5173	.5573	.7324	.7880	.4203	.4589	
	N=18	N=17	N=14	N=8	N=9	N=17	N=18	
	p=.929	p=.033	p=.038	p=.039	p=.012	p=.093	p=.055	
Log(AA)	.4329	.6120	.6132	.6517	.7352	.5646	.7524	.8429
	N=16	N=15	N=14	N=8	N=9	N=15	N=16	N=16
	p=.094	p=.015	p=.020	p=.080	p=.024	p=.028	p=.001	p=.000
Log(HA)	.3785	.6222	.6265	.4486	.7501	.7641	.7722	.7903
	N=16	N=15	N=14	N=8	N=9	N=15	N=16	N=16
	p=.148	p=.013	p=.017	p=.265	p=.020	p=.001	p=.000	p=.000
Log(AM)	.1647	.0204	.2782	–.4951	–.3585	.0431	.1282	–.0467
	N=14	N=13	N=12	N=6	N=7	N=13	N=14	N=14
	p=.574	p=.947	p=.381	p=.318	p=.430	p=.889	p=.662	p=.874
Log(HM)	–.1641	.1928	.6797	–.7664	.7741	.0111	.0081	.1553
	N=14	N=13	N=10	N=4	N=5	N=13	N=14	N=14
	p=.575	p=.528	p=.031	p=.234	p=.124	p=.971	p=.978	p=.596
MPN/TNC	.1993	.4797	.4433	.0684	.6239	.5904	.5640	.5985
	N=17	N=17	N=13	N=8	N=9	N=16	N=17	N=17
	p=.443	p=.051	p=.129	p=.872	p=.073	p=.016	p=.018	p=.011
Log(SO_4^{2-})	.6034	.1293	.3354	–.5124	–.2636	.3345	.1351	–.1314
	N=18	N=17	N=14	N=8	N=9	N=17	N=18	N=18
	p=.008	p=.621	p=.241	p=.194	p=.493	p=.189	p=.593	p=.603
Fe (mg L^{-1})	.2639	.6045	.4976	.0003	.4101	.3747	.3118	.3815

Variable	Variable (m)	Log(TNC)	Log(ATP)	Log(CHAB)	Log(NRB)	Log(IRB)	Log(MRB)	Log(SRB)
	N=18	N=17	N=14	N=8	N=9	N=17	N=18	N=18
	p=.290	p=.010	p=.070	p=.999	p=.273	p=.138	p=.208	p=.118
Log(Fe^{2+})	.5765	.7593	.4940	.3910	.6776	.5280	.4171	.3063
	N=18	N=17	N=14	N=8	N=9	N=17	N=18	N=18
	p=.012	p=.000	p=.073	p=.338	p=.045	p=.029	p=.085	p=.216
Fe^{2+} (mg L^{-1})	.2730	.6059	.4934	.0017	.4102	.3850	.3162	.3847
	N=18	N=17	N=14	N=8	N=9	N=17	N=18	N=18
	p=.273	p=.010	p=.073	p=.997	p=.273	p=.127	p=.201	p=.115
Mn^{2+} (mg L^{-1})	.3729	.3498	.5913	–.0281	.3655	.0853	–.1122	–.1566
	N=18	N=17	N=14	N=8	N=9	N=17	N=18	N=18
	p=.128	p=.169	p=.026	p=.947	p=.333	p=.745	p=.658	p=.535
Log(Mn^{2+})	.6417	.3810	.5173	.1510	.4416	.3359	.1380	–.1168
	N=18	N=17	N=14	N=8	N=9	N=17	N=18	N=18
	p=.004	p=.131	p=.058	p=.721	p=.234	p=.188	p=.585	p=.644
S^{2-} (mg L^{-1})	–.4775	–.1694	–.0037	–.5989	–.2319	–.2160	–.1828	–.0878
	N=18	N=17	N=14	N=8	N=9	N=17	N=18	N=18
	p=.045	p=.516	p=.990	p=.117	p=.548	p=.405	p=.468	p=.729
Log(S^{2-})	–.4972	–.0100	.1043	–.4666	–.0995	.0016	–.0672	.1365
	N=18	N=17	N=14	N=8	N=9	N=17	N=18	N=18
	p=.036	p=.970	p=.723	p=.244	p=.799	p=.995	p=.791	p=.589
TOC (mg L^{-1})	.3909	.8226	.9115	.4238	.8007	.5492	.7615	.6073
	N=8	N=8	N=8	N=8	N=8	N=8	N=8	N=8
	p=.338	p=.012	p=.002	p=.295	p=.017	p=.159	p=.028	p=.110
Log(DOC)	.2603	.7396	.7101	.6343	.7890	.3225	.1763	.4292
	N=18	N=17	N=14	N=8	N=9	N=17	N=18	N=18
	p=.297	p=.001	p=.004	p=.091	p=.011	p=.207	p=.484	p=.076
E_h SO_4^{2-}/FeS	.3897	.3004	.4379	–.1770	.0826	.2332	–.0122	–.0916
	N=18	N=17	N=14	N=8	N=9	N=17	N=18	N=18
	p=.110	p=.241	p=.117	p=.675	p=.833	p=.368	p=.962	p=.718
E_h Chemmac	.0852	–.2115	–.1673	–.3169	–.3226	–.3885	–.4076	–.6929
	N=13	N=12	N=10	N=6	N=6	N=12	N=13	N=13
	p=.782	p=.509	p=.644	p=.541	p=.533	p=.212	p=.167	p=.009
DWR (%)	–.0862	–.0264	–.0344	–.5100	–.4284	.0498	–.1613	.1005
(Drilling water	N=18	N=17	N=14	N=8	N=9	N=17	N=18	N=18
residual)	p=.734	p=.920	p=.907	p=.197	p=.250	p=.850	p=.523	p=.692
Log Fe^{2+}/S^{2-}	.7940	.5789	.2479	.8682	.6715	.3468	.3529	.0716
	N=16	N=15	N=12	N=6	N=7	N=15	N=16	N=16
	p=.000	p=.024	p=.437	p=.025	p=.099	p=.205	p=.180	p=.792

Variable	**Variable**							
	Log(AA)	**Log(HA)**	**Log(AM)**	**Log(HM)**	**MPN/TNC**	**Log(SO_4^{2-})**	**Fe (mg L^{-1})**	**Log(Fe^{2+})**
Elevation (m)	.4329	.3785	.1647	–.1641	.1993	.6034	.2639	.5765
	N=16	N=16	N=14	N=14	N=17	N=18	N=18	N=18
	p=.094	p=.148	p=.574	p=.575	p=.443	p=.008	p=.290	p=.012
Log(TNC)	.6120	.6222	.0204	.1928	.4797	.1293	.6045	.7593
	N=15	N=15	N=13	N=13	N=17	N=17	N=17	N=17
	p=.015	p=.013	p=.947	p=.528	p=.051	p=.621	p=.010	p=.000
Log(ATP)	.6132	.6265	.2782	.6797	.4433	.3354	.4976	.4940
	N=14	N=14	N=12	N=10	N=13	N=14	N=14	N=14
	p=.020	p=.017	p=.381	p=.031	p=.129	p=.241	p=.070	p=.073
Log(CHAB)	.6517	.4486	–.4951	–.7664	.0684	–.5124	.0003	.3910
	N=8	N=8	N=6	N=4	N=8	N=8	N=8	N=8
	p=.080	p=.265	p=.318	p=.234	p=.872	p=.194	p=.999	p=.338
Log(NRB)	.7352	.7501	–.3585	.7741	.6239	–.2636	.4101	.6776
	N=9	N=9	N=7	N=5	N=9	N=9	N=9	N=9
	p=.024	p=.020	p=.430	p=.124	p=.073	p=.493	p=.273	p=.045
Log(IRB)	.5646	.7641	.0431	.0111	.5904	.3345	.3747	.5280
	N=15	N=15	N=13	N=13	N=16	N=17	N=17	N=17
	p=.028	p=.001	p=.889	p=.971	p=.016	p=.189	p=.138	p=.029
Log(MRB)	.7524	.7722	.1282	.0081	.5640	.1351	.3118	.4171
	N=16	N=16	N=14	N=14	N=17	N=18	N=18	N=18
	p=.001	p=.000	p=.662	p=.978	p=.018	p=.593	p=.208	p=.085
Log(SRB)	.8429	.7903	–.0467	.1553	.5985	–.1314	.3815	.3063
	N=16	N=16	N=14	N=14	N=17	N=18	N=18	N=18
	p=.000	p=.000	p=.874	p=.596	p=.011	p=.603	p=.118	p=.216
Log(AA)		.8981	–.0562	.0612	.6811	.0181	.5593	.4349
		N=16	N=14	N=12	N=15	N=16	N=16	N=16
		p=.000	p=.849	p=.850	p=.005	p=.947	p=.024	p=.092
Log(HA)	.8981		–.0535	.1934	.7048	.0288	.5354	.5321
	N=16		N=14	N=12	N=15	N=16	N=16	N=16
	p=.000		p=.856	p=.547	p=.003	p=.916	p=.033	p=.034
Log(AM)	–.0562	–.0535		.3101	–.0161	.5414	.0047	.0910
	N=14	N=14		N=12	N=13	N=14	N=14	N=14
	p=.849	p=.856		p=.327	p=.958	p=.046	p=.987	p=.757
Log(HM)	.0612	.1934	.3101		–.0462	.2725	–.0678	–.0671
	N=12	N=12	N=12		N=13	N=14	N=14	N=14
	p=.850	p=.547	p=.327		p=.881	p=.346	p=.818	p=.820
MPN/TNC	.6811	.7048	–.0161	–.0462		.1110	.8265	.4657
	N=15	N=15	N=13	N=13		N=17	N=17	N=17
	p=.005	p=.003	p=.958	p=.881		p=.671	p=.000	p=.060
Log(SO_4^{2-})	.0181	.0288	.5414	.2725	.1110		.3235	.5072
	N=16	N=16	N=14	N=14	N=17		N=18	N=18
	p=.947	p=.916	p=.046	p=.346	p=.671		p=.190	p=.032
Fe (mg L^{-1})	.5593	.5354	.0047	–.0678	.8265	.3235		.6042
	N=16	N=16	N=14	N=14	N=17	N=18		N=18
	p=.024	p=.033	p=.987	p=.818	p=.000	p=.190		p=.008
Log(Fe^{2+})	.4349	.5321	.0910	–.0671	.4657	.5072	.6042	
	N=16	N=16	N=14	N=14	N=17	N=18	N=18	
	p=.092	p=.034	p=.757	p=.820	p=.060	p=.032	p=.008	

Variable	**Variable**							
	Log(AA)	**Log(HA)**	**Log(AM)**	**Log(HM)**	**MPN/TNC**	**Log(SO_4^{2-})**	**Fe (mg L^{-1})**	**Log(Fe^{2+})**
Fe^{2+} (mg L^{-1})	.5609	.5375	.0024	–.0708	.8228	.3278	.9996	.6116
	N=16	N=16	N=14	N=14	N=17	N=18	N=18	N=18
	p=.024	p=.032	p=.993	p=.810	p=.000	p=.184	p=0.00	p=.007
Mn^{2+} (mg L^{-1})	–.1750	–.1344	.2219	.2571	.0870	.7525	.3914	.5506
	N=16	N=16	N=14	N=14	N=17	N=18	N=18	N=18
	p=.517	p=.620	p=.446	p=.375	p=.740	p=.000	p=.108	p=.018
Log(Mn^{2+})	.0241	.1285	.4077	.1758	.1578	.8063	.3969	.7353
	N=16	N=16	N=14	N=14	N=17	N=18	N=18	N=18
	p=.930	p=.635	p=.148	p=.548	p=.545	p=.000	p=.103	p=.001
S^{2-} (mg L^{-1})	–.2081	–.1589	.2887	.0268	.1903	–.0266	.1758	–.0316
	N=16	N=16	N=14	N=14	N=17	N=18	N=18	N=18
	p=.439	p=.557	p=.317	p=.928	p=.464	p=.916	p=.485	p=.901
Log(S^{2-})	–.1263	.0168	.3666	.1020	.2512	–.0237	.2043	.0580
	N=16	N=16	N=14	N=14	N=17	N=18	N=18	N=18
	p=.641	p=.951	p=.197	p=.729	p=.331	p=.926	p=.416	p=.819
TOC (mg L^{-1})	.8079	.8571	.1239	.9275	.8699	.1005	.7711	.6829
	N=8	N=8	N=6	N=4	N=8	N=8	N=8	N=8
	p=.015	p=.007	p=.815	p=.072	p=.005	p=.813	p=.025	p=.062
Log(DOC)	.4495	.5258	–.0429	.2116	.4596	.1611	.4863	.5168
	N=16	N=16	N=14	N=14	N=17	N=18	N=18	N=18
	p=.081	p=.036	p=.884	p=.468	p=.063	p=.523	p=.041	p=.028
E_h SO_4^{2-}/FeS	–.0933	.0509	.4477	.4653	.0408	.8227	.2767	.6171
	N=16	N=16	N=14	N=14	N=17	N=18	N=18	N=18
	p=.731	p=.852	p=.108	p=.094	p=.876	p=.000	p=.266	p=.006
E_h Chemmac	–.7532	–.6060	.3384	.2558	–.4145	.5521	–.2525	.0793
	N=11	N=11	N=10	N=10	N=12	N=13	N=13	N=13
	p=.007	p=.048	p=.339	p=.476	p=.180	p=.050	p=.405	p=.797
DWR (%)	.0084	.0675	–.3157	.1324	–.1891	.0782	–.0486	–.0075
(Drilling water	N=16	N=16	N=14	N=14	N=17	N=18	N=18	N=18
residual)	p=.975	p=.804	p=.271	p=.652	p=.467	p=.758	p=.848	p=.976
Log Fe^{2+}/S^{2-}	.3837	.2855	–.1113	–.1458	.0666	.3987	.8073	.8567
	N=14	N=14	N=13	N=13	N=15	N=16	N=16	N=16
	p=.176	p=.322	p=.717	p=.634	p=.814	p=.126	p=.000	p=.000

Variable	**Variable**						
	Fe^{2+} (mg L^{-1})	**Mn^{2+} (mg L^{-1})**	**Log(Mn^{2+})**	**S^{2-} (mg L^{-1})**	**Log(S^{2-})**	**TOC**	**Log(DOC)**
Elevation (m)	.2730	.3729	.6417	–.4775	–.4972	.3909	.2603
	N=18	N=18	N=18	N=18	N=18	N=8	N=18
	p=.273	p=.128	p=.004	p=.045	p=.036	p=.338	p=.297
Log(TNC)	.6059	.3498	.3810	–.1694	–.0100	.8226	.7396
	N=17	N=17	N=17	N=17	N=17	N=8	N=17
	p=.010	p=.169	p=.131	p=.516	p=.970	p=.012	p=.001
Log(ATP)	.4934	.5913	.5173	–.0037	.1043	.9115	.7101
	N=14	N=14	N=14	N=14	N=14	N=8	N=14
	p=.073	p=.026	p=.058	p=.990	p=.723	p=.002	p=.004
Log(CHAB)	.0017	–.0281	.1510	–.5989	–.4666	.4238	.6343
	N=8	N=8	N=8	N=8	N=8	N=8	N=8
	p=.997	p=.947	p=.721	p=.117	p=.244	p=.295	p=.091
Log(NRB)	.4102	.3655	.4416	–.2319	–.0995	.8007	.7890
	N=9	N=9	N=9	N=9	N=9	N=8	N=9
	p=.273	p=.333	p=.234	p=.548	p=.799	p=.017	p=.011
Log(IRB)	.3850	.0853	.3359	–.2160	.0016	.5492	.3225
	N=17	N=17	N=17	N=17	N=17	N=8	N=17
	p=.127	p=.745	p=.188	p=.405	p=.995	p=.159	p=.207
Log(MRB)	.3162	–.1122	.1380	–.1828	–.0672	.7615	.1763
	N=18	N=18	N=18	N=18	N=18	N=8	N=18
	p=.201	p=.658	p=.585	p=.468	p=.791	p=.028	p=.484
Log(SRB)	.3847	–.1566	–.1168	–.0878	.1365	.6073	.4292
	N=18	N=18	N=18	N=18	N=18	N=8	N=18
	p=.115	p=.535	p=.644	p=.729	p=.589	p=.110	p=.076
Log(AA)	.5609	–.1750	.0241	–.2081	–.1263	.8079	.4495
	N=16	N=16	N=16	N=16	N=16	N=8	N=16
	p=.024	p=.517	p=.930	p=.439	p=.641	p=.015	p=.081
Log(HA)	.5375	–.1344	.1285	–.1589	.0168	.8571	.5258
	N=16	N=16	N=16	N=16	N=16	N=8	N=16
	p=.032	p=.620	p=.635	p=.557	p=.951	p=.007	p=.036
Log(AM)	.0024	.2219	.4077	.2887	.3666	.1239	–.0429
	N=14	N=14	N=14	N=14	N=14	N=6	N=14
	p=.993	p=.446	p=.148	p=.317	p=.197	p=.815	p=.884
Log(HM)	–.0708	.2571	.1758	.0268	.1020	.9275	.2116
	N=14	N=14	N=14	N=14	N=14	N=4	N=14
	p=.810	p=.375	p=.548	p=.928	p=.729	p=.072	p=.468
MPN/TNC	.8228	.0870	.1578	.1903	.2512	.8699	.4596
	N=17	N=17	N=17	N=17	N=17	N=8	N=17
	p=.000	p=.740	p=.545	p=.464	p=.331	p=.005	p=.063
Log(SO_4^{2-})	.3278	.7525	.8063	–.0266	–.0237	.1005	.1611
	N=18	N=18	N=18	N=18	N=18	N=8	N=18
	p=.184	p=.000	p=.000	p=.916	p=.926	p=.813	p=.523
Fe (mg L^{-1})	.9996	.3914	.3969	.1758	.2043	.7711	.4863
	N=18	N=18	N=18	N=18	N=18	N=8	N=18
	p=0.00	p=.108	p=.103	p=.485	p=.416	p=.025	p=.041
Log(Fe^{2+})	.6116	.5506	.7353	–.0316	.0580	.6829	.5168
	N=18	N=18	N=18	N=18	N=18	N=8	N=18

Variable	**Variable**						
	Fe^{2+} (mg L^{-1})	**Mn^{2+} (mg L^{-1})**	**Log(Mn^{2+})**	**S^{2-} (mg L^{-1})**	**Log(S^{2-})**	**TOC**	**Log(DOC)**
	p=.007	p=.018	p=.001	p=.901	p=.819	p=.062	p=.028
Fe^{2+} (mg L^{-1})		.3915	.4006	.1716	.2046	.7663	.4856
		N=18	N=18	N=18	N=18	N=8	N=18
		p=.108	p=.099	p=.496	p=.415	p=.027	p=.041
Mn^{2+} (mg L^{-1})	.3915		.8438	–.1172	–.0954	.7178	.3095
	N=18		N=18	N=18	N=18	N=8	N=18
	p=.108		p=.000	p=.643	p=.707	p=.045	p=.211
Log(Mn^{2+})	.4006	.8438		–.0994	–.1274	.6638	.2673
	N=18	N=18		N=18	N=18	N=8	N=18
	p=.099	p=.000		p=.695	p=.615	p=.073	p=.284
S^{2-} (mg L^{-1})	.1716	–.1172	–.0994		.8530	.3369	–.1963
	N=18	N=18	N=18		N=18	N=8	N=18
	p=.496	p=.643	p=.695		p=.000	p=.415	p=.435
Log(S^{2-})	.2046	–.0954	–.1274	.8530		.2649	.0417
	N=18	N=18	N=18	N=18		N=8	N=18
	p=.415	p=.707	p=.615	p=.000		p=.526	p=.870
TOC (mg L^{-1})	.7663	.7178	.6638	.3369	.2649		.8688
	N=8	N=8	N=8	N=8	N=8		N=8
	p=.027	p=.045	p=.073	p=.415	p=.526		p=.005
Log(DOC)	.4856	.3095	.2673	–.1963	.0417	.8688	
	N=18	N=18	N=18	N=18	N=18	N=8	
	p=.041	p=.211	p=.284	p=.435	p=.870	p=.005	
E_h SO_4^{2-}/FeS	.2814	.8055	.8705	–.0307	.0024	.3668	.2161
	N=18	N=18	N=18	N=18	N=18	N=8	N=18
	p=.258	p=.000	p=.000	p=.904	p=.993	p=.371	p=.389
E_h Chemmac	–.2575	.6358	.6664	–.1729	–.1557	–.1676	–.3276
	N=13	N=13	N=13	N=13	N=13	N=6	N=13
	p=.396	p=.020	p=.013	p=.572	p=.611	p=.751	p=.275
DWR (%)	–.0393	.0352	.0048	–.3287	–.3266	–.6565	–.1331
(Drilling water	N=18	N=18	N=18	N=18	N=18	N=8	N=18
residual)	p=.877	p=.890	p=.985	p=.183	p=.186	p=.077	p=.599
Log Fe^{2+}/S^{2-}	.7942	.4665	.6325	–.7136	–.8601	.5306	.2635
	N=16	N=16	N=16	N=16	N=16	N=6	N=16
	p=.000	p=.069	p=.009	p=.002	p=.000	p=.279	p=.324

Variable	**Variable**			
	E_h SO_4^{2-}/FeS	**E_h Chemmac**	**DWR (%)**	**Log Fe^{2+}/S^{2-}**
Elevation (m)	.3897	.0852	–.0862	.7940
	N=18	N=13	N=18	N=16
	p=.110	p=.782	p=.734	p=.000
Log(TNC)	.3004	–.2115	–.0264	.5789
	N=17	N=12	N=17	N=15
	p=.241	p=.509	p=.920	p=.024
Log(ATP)	.4379	–.1673	–.0344	.2479
	N=14	N=10	N=14	N=12
	p=.117	p=.644	p=.907	p=.437
Log(CHAB)	–.1770	–.3169	–.5100	.8682
	N=8	N=6	N=8	N=6
	p=.675	p=.541	p=.197	p=.025
Log(NRB)	.0826	–.3226	–.4284	.6715
	N=9	N=6	N=9	N=7
	p=.833	p=.533	p=.250	p=.099
Log(IRB)	.2332	–.3885	.0498	.3468
	N=17	N=12	N=17	N=15
	p=.368	p=.212	p=.850	p=.205
Log(MRB)	–.0122	–.4076	–.1613	.3529
	N=18	N=13	N=18	N=16
	p=.962	p=.167	p=.523	p=.180
Log(SRB)	–.0916	–.6929	.1005	.0716
	N=18	N=13	N=18	N=16
	p=.718	p=.009	p=.692	p=.792
Log(AA)	–.0933	–.7532	.0084	.3837
	N=16	N=11	N=16	N=14
	p=.731	p=.007	p=.975	p=.176
Log(HA)	.0509	–.6060	.0675	.2855
	N=16	N=11	N=16	N=14
	p=.852	p=.048	p=.804	p=.322
Log(AM)	.4477	.3384	–.3157	–.1113
	N=14	N=10	N=14	N=13
	p=.108	p=.339	p=.271	p=.717
Log(HM)	.4653	.2558	.1324	–.1458
	N=14	N=10	N=14	N=13
	p=.094	p=.476	p=.652	p=.634
MPN/TNC	.0408	–.4145	–.1891	.0666
	N=17	N=12	N=17	N=15
	p=.876	p=.180	p=.467	p=.814
Log(SO_4^{2-})	.8227	.5521	.0782	.3987
	N=18	N=13	N=18	N=16
	p=.000	p=.050	p=.758	p=.126
Fe (mg L^{-1})	.2767	–.2525	–.0486	.8073
	N=18	N=13	N=18	N=16
	p=.266	p=.405	p=.848	p=.000
Log(Fe^{2+})	.6171	.0793	–.0075	.8567
	N=18	N=13	N=18	N=16
	p=.006	p=.797	p=.976	p=.000

Variable	**Variable**			
	E_h SO_4^{2-}/FeS	**E_h Chemmac**	**DWR (%)**	**Log Fe^{2+}/S^{2-}**
Fe^{2+} (mg L^{-1})	.2814	–.2575	–.0393	.7942
	N=18	N=13	N=18	N=16
	p=.258	p=.396	p=.877	p=.000
Mn^{2+} (mg L^{-1})	.8055	.6358	.0352	.4665
	N=18	N=13	N=18	N=16
	p=.000	p=.020	p=.890	p=.069
Log(Mn^{2+})	.8705	.6664	.0048	.6325
	N=18	N=13	N=18	N=16
	p=.000	p=.013	p=.985	p=.009
S^{2-} (mg L^{-1})	–.0307	–.1729	–.3287	–.7136
	N=18	N=13	N=18	N=16
	p=.904	p=.572	p=.183	p=.002
Log(S^{2-})	.0024	–.1557	–.3266	–.8601
	N=18	N=13	N=18	N=16
	p=.993	p=.611	p=.186	p=.000
TOC (mg L^{-1})	.3668	–.1676	–.6565	.5306
	N=8	N=6	N=8	N=6
	p=.371	p=.751	p=.077	p=.279
Log(DOC)	.2161	–.3276	–.1331	.2635
	N=18	N=13	N=18	N=16
	p=.389	p=.275	p=.599	p=.324
E_h SO_4^{2-}/FeS		.7921	.2723	.4182
		N=13	N=18	N=16
		p=.001	p=.274	p=.107
E_h Chemac	.7921		.0669	.1688
	N=13		N=13	N=11
	p=.001		p=.828	p=.620
DWR (%)	.2723	.0669		.1976
(Drilling water	N=18	N=13		N=16
residual)	p=.274	p=.828		p=.463
Log Fe^{2+}/S^{2-}	.4182	.1688	.1976	
	N=16	N=11	N=16	
	p=.107	p=.620	p=.463	

As described in section 1.2, microbial metabolic processes will lower the redox potential (E_h) in the environment. Figure 1-24 shows the measured E_h (Chemmac) in groundwater from the different depths in the 13 boreholes studied. The values did not show a significant correlation with depth (p=0.782, Table 1-6). Elsewhere in this report E_h was calculated and the SO_4^{2-}/FeS system was deemed most relevant. However, a correlation could not be established for E_h calculated for the SO_4^{2-}/FeS pair with depth (Table 1-6). Very low E_h was observed at 200 m in KFM10A and E_h values were at their lowest, under –250 mV, in boreholes KFM10A, KFM08D and KFM01D, followed by KFM03A at a depth of 943 m. It is clear that measured and calculated E_h did not relate to depth. The correlation to microbiology for the Chemmac E_h was with AA, HA and SRB (Figure 1-25) which is reasonable because these groups of microbes generally dominated the groundwaters analysed. A similar correlation could not be found for the calculated SO_4^{2-}/FeS E_h. This variable only showed a significant relation with manganese, ferrous iron and sulphate. Possibly, Chemmac E_h values do relate to microbial processes as will be discussed later, but not calculated E_h.

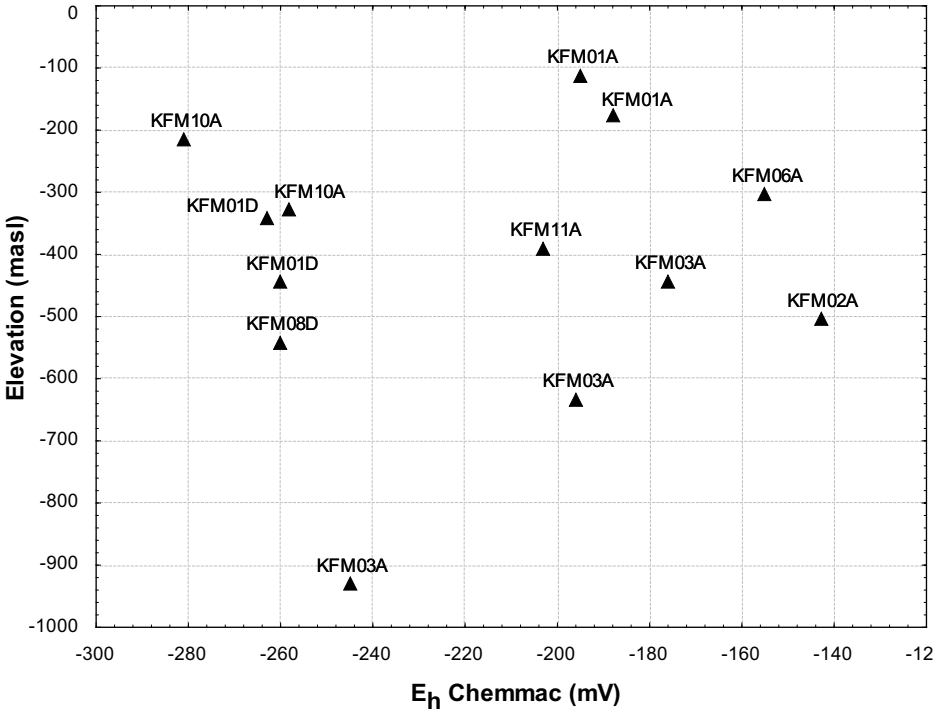

Figure 1-24. *Measured E_h versus 13 depth in the Forsmark area. Data from extended freeze 2.3 (December 2007) in Forsmark.*

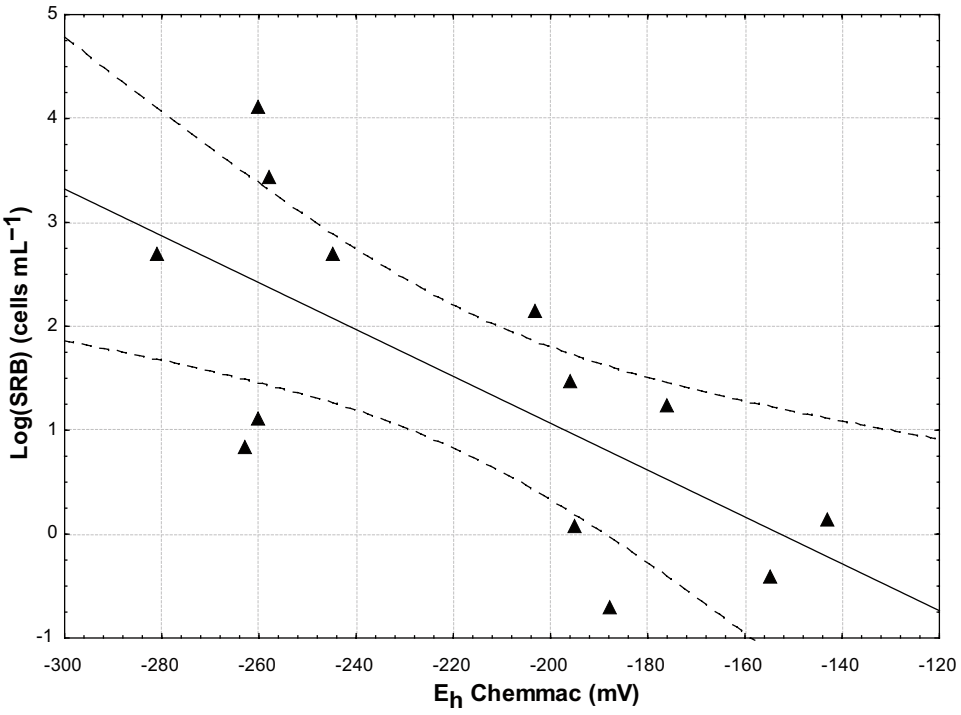

Figure 1-25. *The relation between the number of sulphate reducing bacteria and the E_h analysed with the Cemmac system. Statistics: $^{10}Log(SRB)=3.44–0.023 \times E_h$, r=–0.69, significant at p=0.0087, n=13. Dashed lines denote the 95% confidence interval. Data from extended freeze 2.3 (December 2007) in Forsmark.*

Many microorganisms use organic carbon as their energy source and electron donor (see section 1.2). Dissolved organic carbon is therefore a factor that could influence E_h. However, a significant correlation was not present for the organic carbon variables TOC, log(DOC) (Table 1-6) and DOC (not shown).

Three different methods were applied to analyse the groundwater samples; TNC returns numbers, ATP returns a measure of biomass and MPN cultivation returns a measure of diversity and numbers. It has been demonstrated here and elsewhere that TNC and ATP values correlate in Fennoscandian Shield groundwater. It was shown by /Eydal and Pedersen 2007/ that the amount of ATP in groundwater samples reflects the number of cells, biovolume and activity. When the amount of ATP in the samples was scatter plotted versus the stacked MPN values significant correlation was found (Figure 1-26). In conclusion, the outputs from three independent methods were found to correlate. ATP and TNC have been shown to correlate here (Figure 1-3) and elsewhere /Pedersen 2008/, but the demonstration of correlation between ATP and MPN cultivations is novel. This relation shows that the MPN determinations returns a reliable measure of numbers and activity of the microbial populations in the analysed groundwater

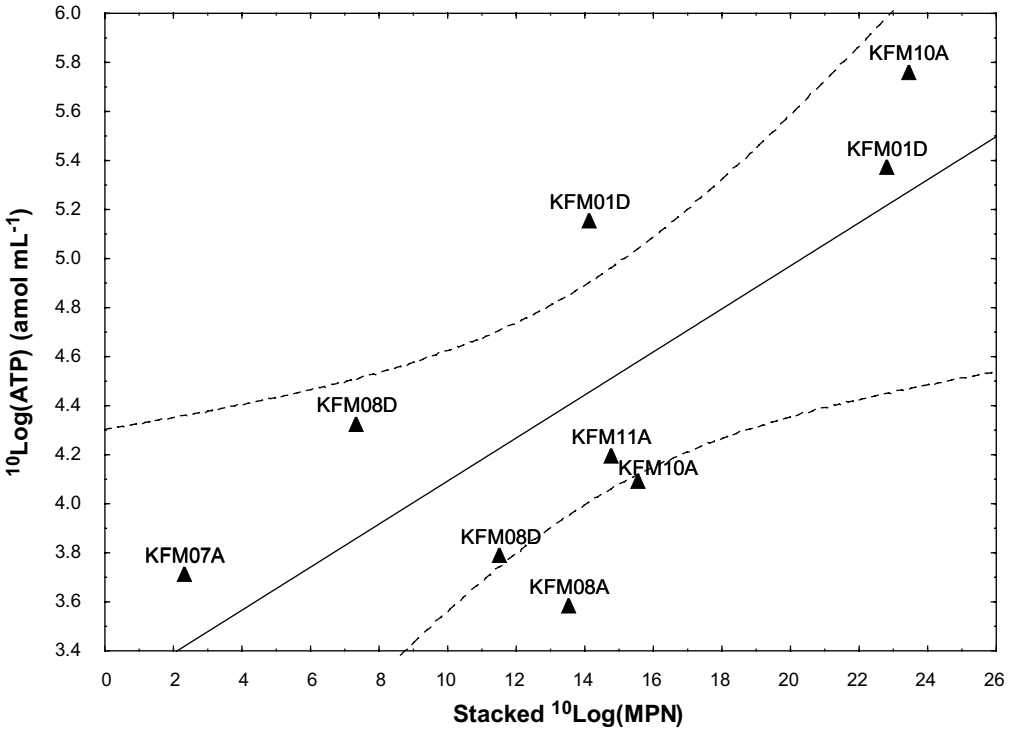

Figure 1-26. *The relation between stacked values of most probable numbers of various physiological groups of microorganisms (Figure 3-11) in deep Forsmark groundwater with the concentration of ATP. The scatter plot and the correlation only includes datasets that with full analysis of all physiological groups. The least square regression lines for ATP versus Stacked MPN is shown (^{10}Log(ATP) =0.09× ^{10}Log(MPN) + 3.2; r=0.74, p=0.02, n=9). Dashed lines denote the 95% confidence interval.*

1.15 Discussion – The microbial model

1.15.1 A theoretical model of microbial reactions in a granitic groundwater environment

Figure 1-27 shows a theoretical model of microbial reactions in a granitic groundwater environment. The reactions depicted are metabolic redox reactions involving many different physiological groups of microorganisms. Which of the groups is active is determined by the available energy, carbon sources, and electron donors. The activities of the different groups are described in Table 1-1. This model proposes a depth-related diversification of the microbial populations comparable to that found in a shallow aquatic sediment environment; the latter can be modelled as a biosphere involving oxygenic photosynthesis that creates a chemical potential and chemical equilibrium. Mineralization is occuring via several redox processes carried out by a variety of organisms /Fenchel et al. 1998/. The greatest difference between the two systems is the depth scale: the shallow aquatic sediment environment extends over a depth range of centimetres, while the deep groundwater system extends to a depth of at least 1,000 m.

1.15.2 The microbial model in Forsmark

Figure 1-28 shows the stacked ^{10}log values of MPN for all sampled sections, sorted by depth. Here it can be seen that the MPN results for KFM01D, 445 m and KFM10A, 328 m are several orders of magnitude greater than those for all other sampled sections. As well, the stacked ^{10}log values of MPN for the other sampled sections of boreholes KFM01D and KFM10A, at depths of 341 and 214 m, respectively, are higher than those found in the other samples. The reason for this is unknown, though it could be due to high drill-water content or because intersection with other water-bearing fractures allowed different groundwater types to mix. Interestingly, both IRB and SRB were high in these sections, supporting the idea that different groundwaters may have been mixing.

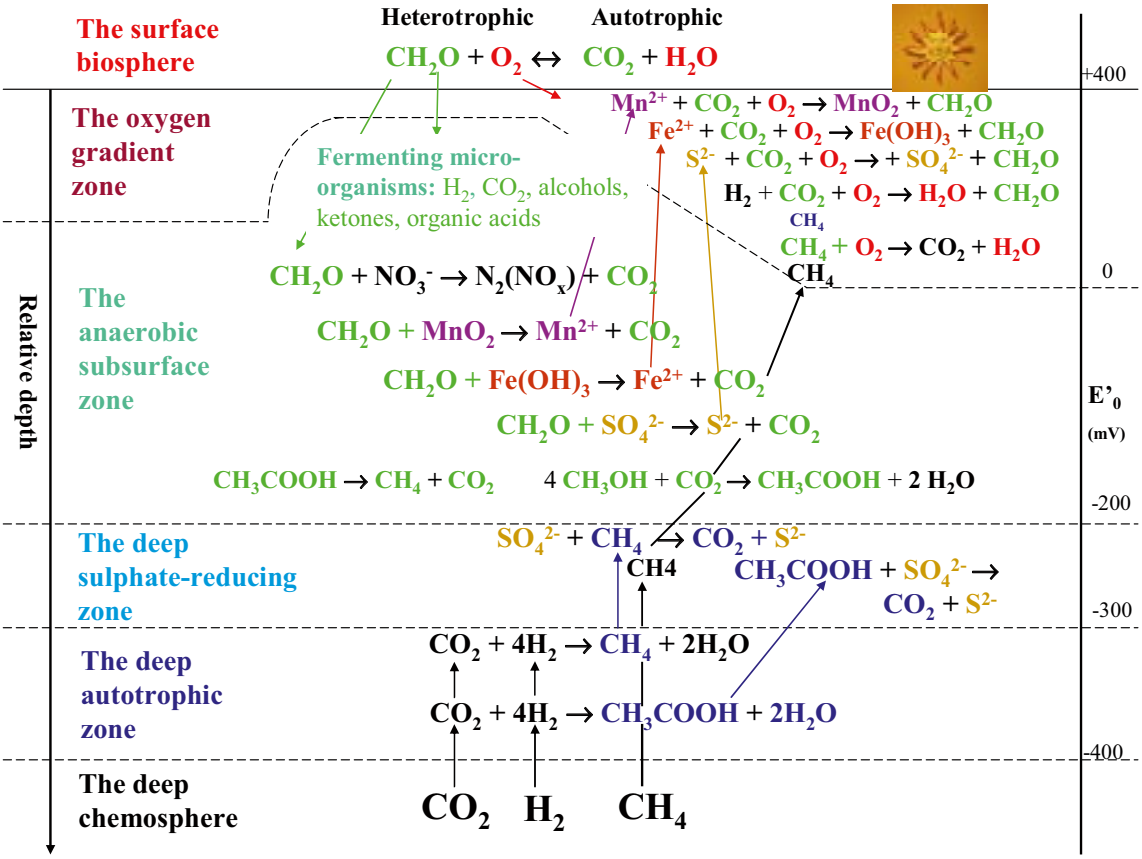

Figure 1-27. *Theoretical model of microbial reactions in a granitic groundwater environment.*

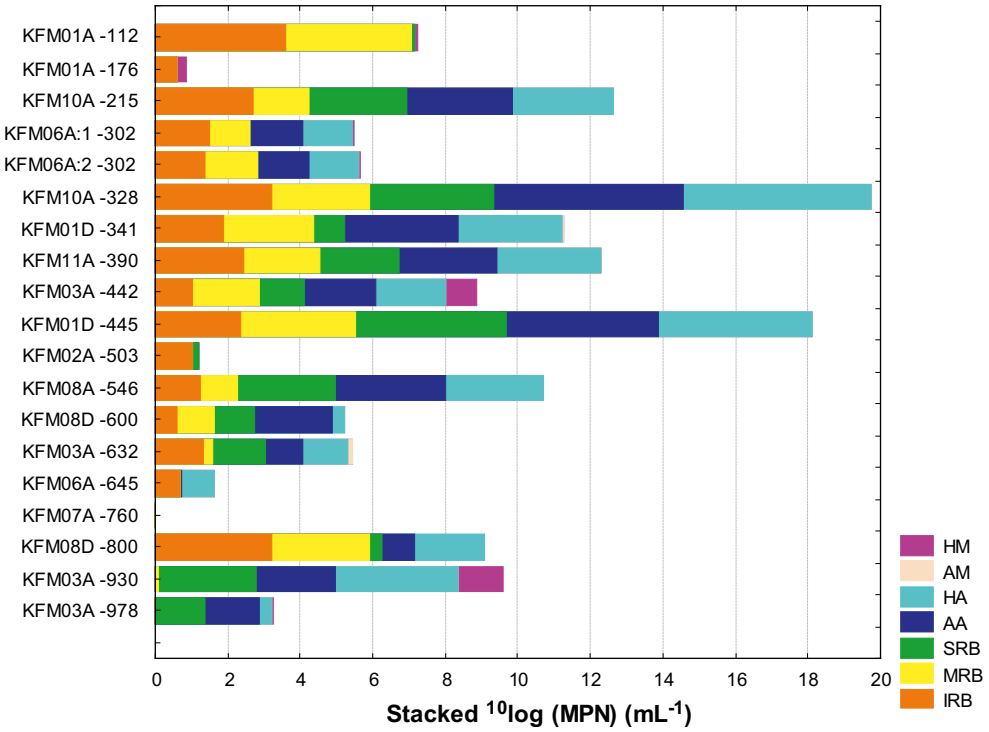

Figure 1-28. *Stacked log [10]MPN values for samples from Forsmark sorted by depth.*

Figure 1-29, on the other hand, shows the stacked log values sorted by sampling date. The highest value found was close to 20 in KFM10A, 328 m and the lowest in KFM07A, 760 m. In general, it can be seen that acetogenic bacteria are present in all sampled sections. Acetogenic bacteria even comprise the dominant group in some sections, though it can also be seen that the iron and manganese reducers dominate in the shallow sections. However, in the most recently sampled sections, for example, at a depth of 800 m in boreholes KFM01D, KFM10A, and especially in KFM08D, there were also quite large populations of iron and manganese reducers. There is no obvious explanation for this, but presumably there was a mixing of different groundwaters in these sections, creating a suitable environment for iron and manganese reducers. Another possible explanation is that, by sampling a large volume of rock, we obtained mixed groundwater from several different groundwater environments. Whether this represents natural mixing or was induced by drilling and pumping activity in the area needs to be further investigated. The sections with high stacked MPN numbers also have lower E_h values than do sections with lower stacked MPNs (see Figure 1-24). In the Olkiluoto area in Finland, such high numbers are rarely seen and only found in very shallow water /Pedersen 2008/. Unfortunately, there is one unknown in the late samples. The quality plan for drilling included a microbial test to confirm that UV disinfection of the flushing water was indeed working satisfactorily. While drilling boreholes KFM01A–KFM06A, monitoring of the microbe numbers in the flushing water were made. From the samples taken in KFM07A this monitoring was excluded on the basis that it was successful in the previous borehole /Berg et al. 2006/. UV disinfection is not an absolute method; rather, its success depends on treatment time and on the condition of the UV lamp used /Pedersen 2003, Pedersen and Kalmus 2003, Hallbeck et al. 2004, Pedersen 2005/.

Figure 1-30 presents the theoretical model of the microbial system in Forsmark, as can be interpreted from the site investigation results, which pertain to samples from 115 m down to 978 m. The microbial reactions noted in black are those that we have confirmed to be ongoing; those noted in grey must still be verified.

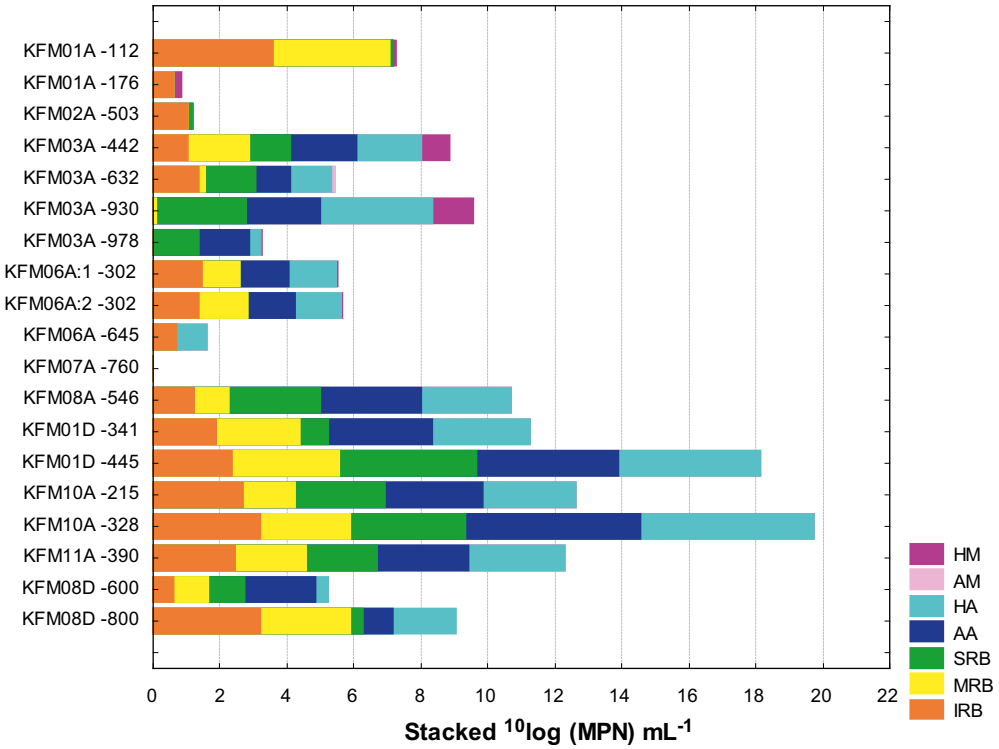

Figure 1-29. *Stacked ^{10}log MPN values for samples from Forsmark sorted by sampling date with the oldest samples starting at the top of the figure.*

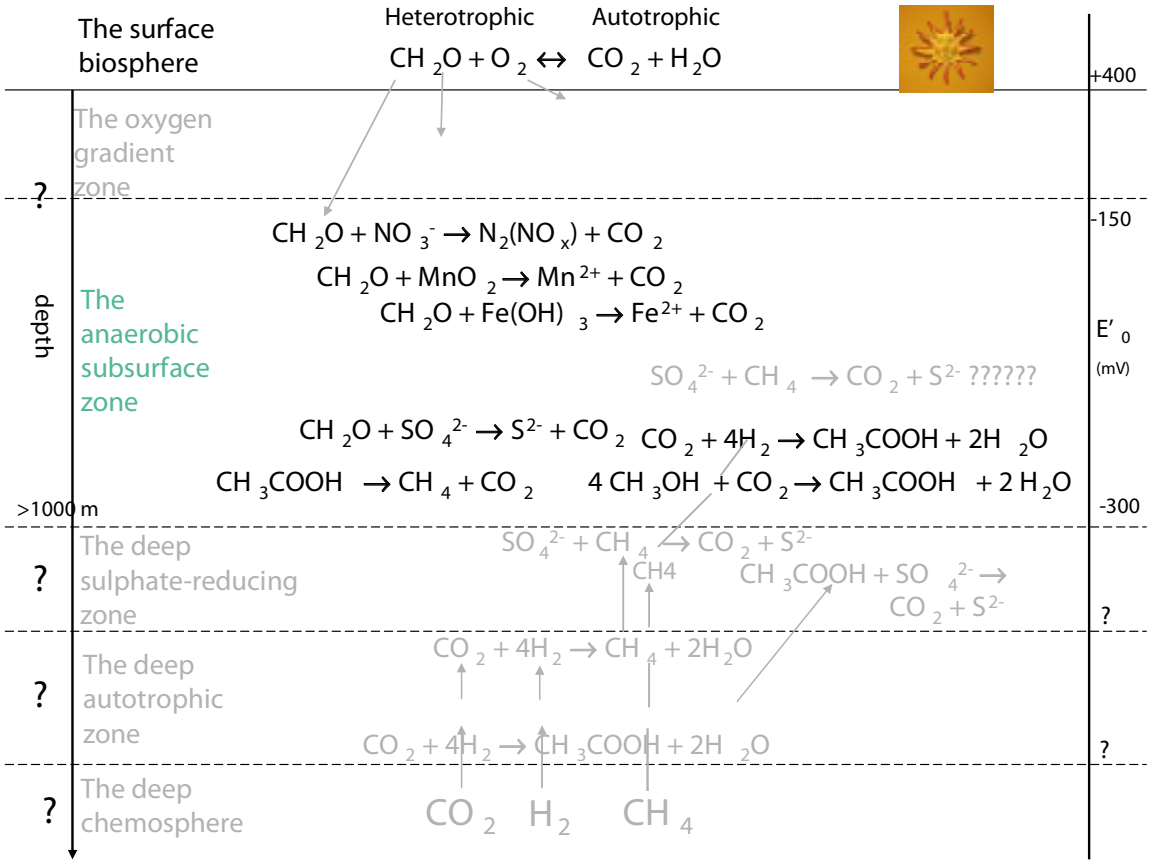

Figure 1-30. *The theoretical model of the microbial system in Forsmark.*

Anaerobic respiration

Iron and manganese-reducing bacteria dominate in the shallowest sampled sections; this finding is supported by the E_h measurements, which indicate values above −200 mV at such depths. Sulphate-reducing microorganisms dominate in deeper groundwater, as evidenced by lower E_h values of under −200 mV.

Acetogens and methanogens

In all sampled sections where the MPNs of acetogens and methanogens were determined, acetogens were found to be dominant. Methanogens were barely present in the Forsmark area, a finding supported by the low concentrations of methane measured in the area (see Figure 1-20 and section 3, "Gases", in this report). The acetogens, a group of organisms that can live on hydrogen gas and organic one-carbon compounds and/or carbon dioxide, seem to create a background level of organic carbon in granitic groundwater /Pedersen 2001, Lin et al. 2005/. The source of energy for the formation of this background level of organic carbon can be either the sun in a surface system or radio- or thermocatalytically derived hydrogen gas in deep, sub-surface systems /Lin et al. 2005/.

Groundwater chemistry is of course a combination of microbially mediated and chemical processes. Below follows the reactions that are involved in the final sulphide concentration in groundwater. The reactions are categorized as either microbial or inorganic.

Microbial processes

As discussed above, one basic source of energy for microbial growth in granitic groundwater is hydrogen. In Forsmark, acetogens are the group that utilizes hydrogen in producing acetate (Eq. 1-1). The acetate can then be used by anaerobic organisms, which in Forsmark consist of iron and manganese reducers in the shallow groundwater. Since manganese does not easily form sulphide compounds in groundwater, the focus here is on iron reduction (Eq. 1-2). In the deeper groundwaters, sulphate reducers use the acetate in their respiration, with or without hydrogen gas (Eq. 1-3). The sulphate reducers can also use other carbon sources in reducing sulphate (Eq. 1-4). There is one microbial sulphate production process that has not been detected in the Forsmark area, namely, anaerobic sulphate reduction with methane (Eq. 1-5).

AA: $H_2 + CO_2 \Rightarrow$ acetate (Eq. 1-1)

IRB: acetate + $Fe^{3+} \Rightarrow Fe^{2+} + CO_2$ (Eq. 1-2)

SRB: acetate + SO_4^{2-} (+ H_2) $\Rightarrow H_2S + CO_2$ (Eq. 1-3)

SRB: DOC + $SO_4^{2-} \Rightarrow H_2S + CO_2$ (Eq. 1-4)

AM + SRB: $CH_4 + SO_4^{2-} \Rightarrow H_2 + CO_2 + SO_4^{2-} \Rightarrow H_2S + CO_2$ (Eq. 1-5)

Inorganic processes (pH > 6.5)

The sulphide produced via Eqs. 1-3 and 1-4 will react with compounds in the groundwater environment. It can reduce ferric iron present in fracture-filling materials and in minerals, producing ferrous iron, elemental sulphur, and hydroxide ions (see Eq. 1-6). It can either precipitate or form colloids with ferrous ions, forming iron sulphide (Eq. 1-7). The iron sulphide can react with elemental sulphur to produce Fe_3S_4. The precipitation reactions all reduce the amount of soluble sulphide in the water, which explains the low sulphide levels in groundwater in Forsmark (see Figure 1-18). It also explains the good correlation between sulphide and the iron sulphide ratio displayed in Figure 1-31. It is only in a groundwater environment containing small amounts of iron that the sulphide concentration can increase.

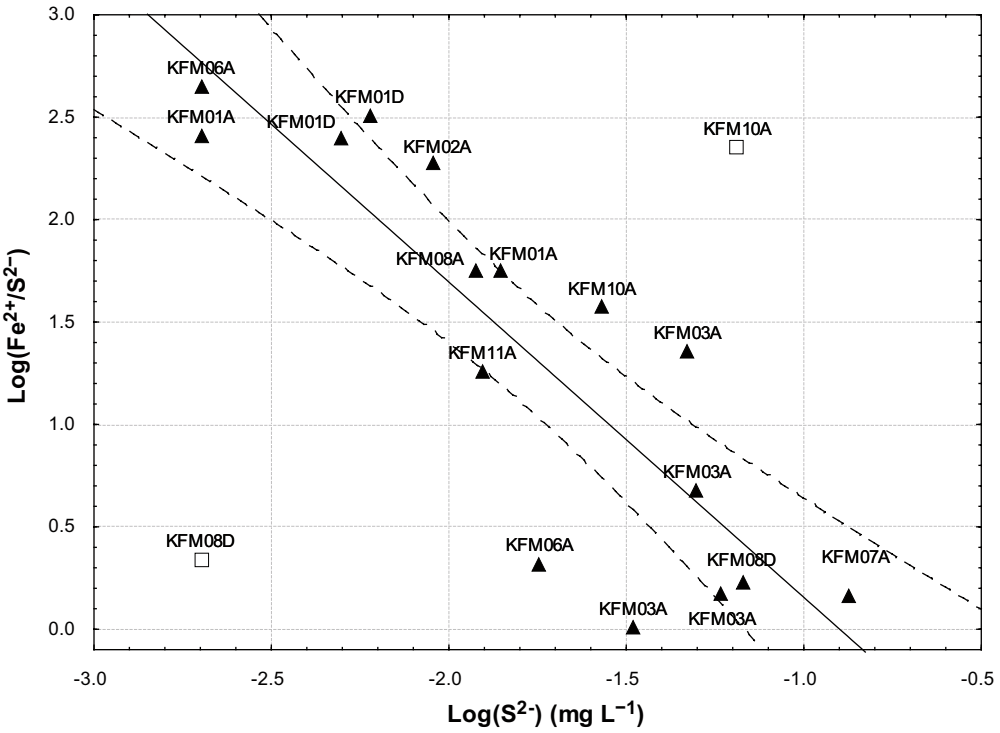

Figure 1-31. *The relation between the concentration of sulphide and the ratio of Fe^{2+}/S^{2-}. Statistics: $^{10}Log(Fe^{2+}/S^{2-})=1.39–1.54 \times {}^{10}Log(S^{2-})$, r=–0.86, significant at p=0.00002, n=16.. Dashed lines denote the 95% confidence interval. Data represented by squared symbols were not included in the correlation calculations. Data from extended freeze 2.3 (December) in Forsmark.*

$$H_2S + 2FeOOH \Rightarrow S^0 + 2Fe^{2+} + 4OH^- \quad \text{(Eq. 1-6)}$$

$$H_2S + Fe^{2+} \Rightarrow FeS + 2H^+ \quad \text{(Eq. 1-7)}$$

$$3FeS + 3S^0 \Rightarrow Fe_3S_4 + 2S^0 \Rightarrow 3FeS_2 \quad \text{(Eq. 1-8)}$$

1.15.3 Limitations of microbial processes

Several reviewers have requested discussion of the limitations of microbial activity in groundwater. They have suggested that nutrients such as nitrogen and phosphorous should be limiting in the deep subsurface.

Nitrogen

All living cells need reduced nitrogen with which to synthesize amino acids and the nitrogen bases of the nucleotides. The soluble sources of this are ammonium and nitrate, which are found in limited amounts in deep groundwater. Microorganisms have another option when it comes to incorporating nitrogen into the cell, namely, nitrogen fixation. This ability is widespread in microbial groundwater populations, so nitrogen availability will rarely limit growth.

Phosphorous

Microorganisms utilize phosphorous in the form of phosphate, which is found in low amounts soluble in groundwater. It has been demonstrated that microbes can weather phosphate from phosphate-rich minerals, such as apatite, in rock /Bennett et al. 2001/. Microorganisms also recycle the phosphate available in the microbial community during the succession of different populations.

1.16 Conclusions

- The data on total number of cells (TNC) were in the range of the cell numbers earlier found in boreholes in Fennoscandian Shield groundwater.
- When ATP was analysed concomitantly with TNC, a good correlation was obtained. The ATP/TNC ratio is a good indicator of the metabolic activity of cells in groundwater. The average microbial population of Forsmark was more active than the average Fennoscandian shield population.
- The results of fractionated filtration indicated that most of the organic material was smaller than 1,000 D in size and that only a minor part was in the >5,000 D fraction.
- The anaerobic cultivation methods presented here represent the culmination of almost 10 years of development, testing, and adaptation for deep groundwater. The use of multiple, liquid anaerobic media has overcome much of the discrepancy found between TNC and cultivations that use agar media only. This success and usefulness of the cultivation methods are reflected in the maximum MPN cultivability of 70% of the TNC in the sample from the borehole KFM10A in the 328 m section and the 0.02–70% MPN cultivability range in all groundwater samples.
- The relatively high numbers of IRB imply that they are important for the geochemistry in the Forsmark area. Since most IRB use partially oxidized organic matter, such as short-chain organic acids, as their sources of energy, electron, and carbon, they participate in the degradation of organic matter originating from the ground surface.
- An excellent correlation was found between IRB and MRB. These organisms can toggle between the electron acceptors ferric iron and manganese(IV) depending on availability. This correlation also attests the stability and reproducibility between the different physiological MPN groups applied.
- The data obtained on microbial diversity and numbers indicated that at the shallowest depths with relatively high E_h values iron- and manganese-reducing bacteria dominated, while sulphate reducers dominated at greater depths.
- Acetogens were the dominant microorganisms in the sections studied; there were often one or two orders of magnitude more acetogens than the second most common organism type, which was either sulphate reducer or iron/manganese reducers. Acetogenic activity results in production of acetate.
- Sulphide concentration in groundwater in Forsmark appears to be controlled by the presence of ferrous iron. The low observed values could also relate to heavy pumping before sampling.
- There were generally good crosswise correlations between the different cultivation and biomass results. Many of these parameters also showed good correlations with TOC and DOC.
- The drill water residual (DWR) was not found to correlate with any of the included variables.
- The only correlation with chemistry for the measurement of E_h with the Chemmac electrodes was with AA, HA and SRB which is reasonable because these groups of microbes generally dominated the numbers of microbes analysed in Forsmark groundwater.

2 Colloids

2.1 Introduction

Particles in the size range from 1 to 1×10^{-3} µm are regarded as colloids /Stumm and Morgan 1996/. Their small size prohibits them from settling, which gives them the potential to transport radionuclides in groundwater. The aim of the study of colloids in the Forsmark 2.3 site investigation was to quantify and determine the composition of colloids in groundwater samples from the boreholes.

Radionuclides can sorb (adhere) to colloidal particles and be transported with them. It is therefore important to estimate to what extent such particles can occur or be formed in the groundwater and for what time periods these particles can be stable. A summary of the reasons behind analysis of colloids can be found in the SR-CAN Technical Report TR-06-19 (section 5.9). In summary, SR-CAN concluded that "Radionuclides in the groundwater can occur sorbed on colloids, and that the possibility that a small fraction will be bound irreversibly to mobile natural colloidal particles cannot be entirely excluded. However, as long as dose calculations are dominated by weakly or non-sorbing radionuclides, the overall consequence of colloid enhanced transport for the safety of the repository is negligible".

There are both inorganic and organic colloids, and the site investigation measured both types. Microorganisms must also be considered as colloids, as there are many groundwater microorganisms ≤1 µm in size. The results of the organic colloid analyses are presented in Section 1 of this report, "Microbiology and microbial model". In addition, a recent study of groundwater in the Äspö tunnel has found a variety of viruses in the water; these are protein particles, approximately 200 nm in diameter, that infect microbial cells.

2.2 Methods

Details about the methods and the procedures for each borehole can be found in the respective P-report for hydrogeochemical Progress Report (www.skb.se/publications). Two different methods were used in collecting and analyzing colloids. The first included filtering the groundwater through a series of connected filters in a closed system under pressurized argon. The final filters had pore sizes of 0.2 and 0.05 µm, and were installed after a 0.4-µm prefilter. The mineral composition of the colloids collected on the filters was determined using inductively coupled plasma analysis (ICP), and the quantities of the analysed elements were recalculated in µg L^{-1} (ppb), taking account of the water flow (mL h^{-1}) registered through the filters. The elements analysed were calcium (Ca), iron (Fe), sulphur (S), manganese (Mn), aluminium (Al), and silicon (Si). The second method was fractionation using a defined cut-off membrane filter (i.e. of a particular pore size) concomitant with the analysis of organic colloids; two different filter pore sizes were used, 1,000 D and 5,000 D. The elements Fe, Si, Al, S, U, and Mg were reported to the SICADA database. The sample descriptions and colloid filtering data are compiled in Table 2-1, while data regarding the colloid fractionation are found in section 2.8.

Two other analysis methods were used for some samples during the last sampling campaign in Forsmark, namely, laser-induced breakdown colloid detection (LIBD) /Berg et al. 2006/ and colloid analysis by means of micro-filtration plus scanning electron microscopy and energy-dispersive spectroscopy (SEM/EDS) /Nilsson and Degueldre 2007/. The results of these investigations are presented in sections 2.9 and 2.10.

2.3 Databases

The colloid filtration and colloid fractionation data in the SICADA database were compiled by Maria Gimeno and distributed to the author via the CHEMNET web page. The LIBD data were taken from /Berg et al. 2006/ and the SEM/EDS investigation was described in /Nilsson and Degueldre 2007/.

2.4 Evaluation of colloid data from the filtration method

When evaluating the primary data, we decided to exclude the silicon data for borehole KFM01A, 112 m in some of the analyses, because they were extremely likely due to a sampling artefact (see Table 2-1). In addition, no total amount of colloids are available for this borehole. All other available data were used in the evaluation.

/Laaksoharju et al. 1995/ calculated calcium values as calcite and sulphur values calculated as pyrite were both subtracted from the total amount of colloids. In our presentation, the calcite values were subtracted from the total amount of colloids, while the sulphur values were not recalculated as pyrite because this compound could not be confirmed. Sulphur is therefore represented as sulphur as given in SICADA. Calcium and sulphur colloids are commonly regarded as pressure drop related and their actual concentrations in the sampled groundwater can not be safely inferred from the data.

2.4.1 Colloids versus depth

In evaluating the background levels of colloids in groundwater, colloid concentration versus depth was examined. It can be seen in Figure 2-1 that the colloid concentration was highest at the shallowest depth, i.e. 112 m, though the concentration was also high in KFM03A, 442 m and KFM10A, 328 m. The lowest concentration was found at a depth of 645 m in KFM06A. The average colloid concentration found in this study was 58.4 ± 62.6 µg L^{-1}, a finding in agreement with the results of colloid studies from Switzerland (30 ± 10 and 10 ± 5 µg L^{-1}) /Degueldre, 1994/ and Canada (300 ± 300 µg L^{-1}) /Vilks et al. 1991/ that used the approach as was used here.

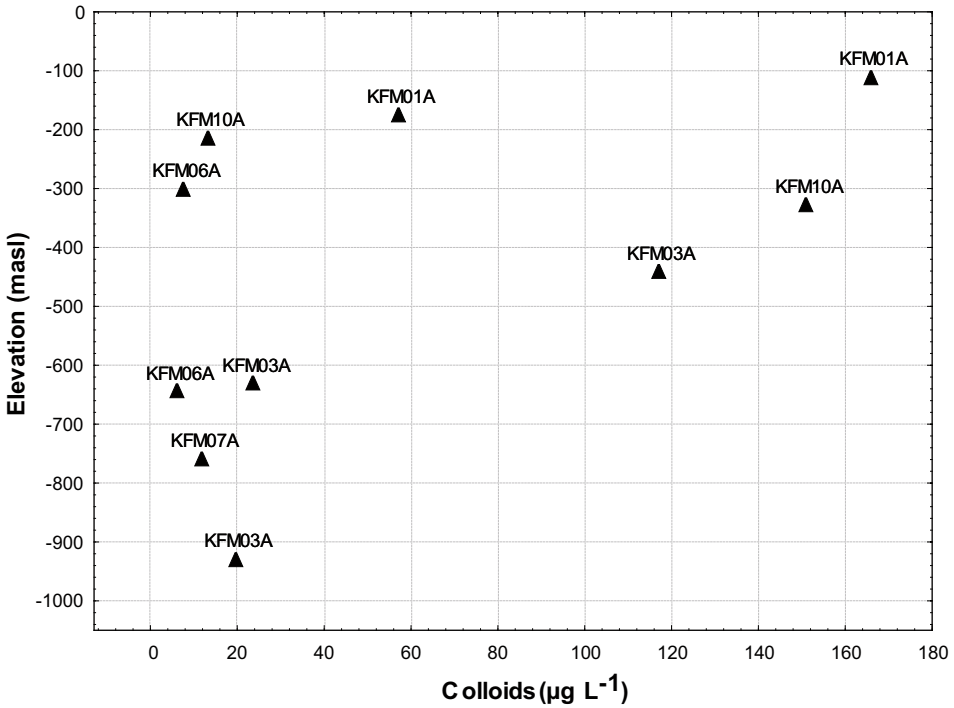

Figure 2-1. *Colloid concentration (µg L^{-1}) plotted against depth in the Forsmark area. Data from data freeze 2.3. Data from Table 2-1 but without silica data for KFM01A, 112 m. Data from extended freeze 2.3 (December) in Forsmark.*

Table 2-1. Elemental analyses of the 0.05- and 0.2-µm colloid fractions and the 0.4-µm precipitation fraction from the Forsmark area.

Colloid phase	Borehole and filter pore size								
	KFM01A, –112 m Filter pore size (µm)			KFM01A, –176 m Filter pore size (µm)			KFM02A, –503 m Filter pore size (µm)		
	0.05	0.2	0.4	0.05	0.2	0.4	0.05	0.2	0.4
Ca as calcite $CaCO_3$ (µg L^{-1})	0.89	b.d.	1.36	0.21	0.10	0.14	d.m.	d.m.	0.20
Fe as $Fe(OH)_3$ (µg L^{-1})	5.74	12.44	443.47	0.38	0.51	9.06	d.m.	d.m.	3.64
S as sulphur (µg L^{-1})	61.25	b.d.	40.95	22.10	15.5	18.48	d.m.	d.m.	b.d.
Mn as $Mn(OH)_2$ (µg L^{-1})	b.d.	b.d.	b.d.	b.d.	b.d.	b.d.	d.m.	d.m.	0.405
Al as K-Mg-Illite clay: $K_{0.6}Mg_{0.25}Al_{2.3}Si_{3.5}O_{10}(OH)_2$ (µg L^{-1})	71.36	14.9	29.45	10.39	8.30	20.21	d.m.	d.m.	2.90
Si as SiO_2 (µg L^{-1})	365.91	601.33	729.93	b.d.	b.d.	b.d.	d.m.	d.m.	b.d.
Sum, ppb, (µg L^{-1})	505.15	628.67	1,245.16	33.08	24.41	47.8			7.145
Sum omitting calcite (µg L^{-1})	504.26	628.67	1,243.8	32.87	24.31	47.66			6.945
Sum omitting calcite and sulphur (µg L^{-1})	443.01	628.67	1,202.85	10.77	8.81	29.18	–	–	6.945

b.d. = below detection limit; d.m. = data missing because of broken filters

Colloid phase	Borehole and filter pore size								
	KFM03A, –441 m Filter pore size (µm)			KFM03A, –632 m Filter pore size (µm)			KFM03A, –930 m Filter pore size (µm)		
	0.05	0.2	0.4	0.05	0.2	0.4	0.05	0.2	0.4
Ca as calcite $CaCO_3$ (µg L^{-1})	0.49	1.30	0.50	1,412	d.m.	628	1,689	d.m.	1,214
Fe as $Fe(OH)_3$ (µg L^{-1})	3.06	4.59	27.5	1.1	d.m.	5.0	1.0	d.m.	3.05
S as sulphur (µg L^{-1})	30	72	16	28	d.m.	b.d.	b.d.	d.m.	b.d
Mn as $Mn(OH)_2$ (µg L^{-1})	0.65	1.78	1.46	0.2	d.m.	0.2	0	d.m.	0
Al as K-Mg-Illite clay: $K_{0.6}Mg_{0.25}Al_{2.3}Si_{3.5}O_{10}(OH)_2$ (µg L^{-1})	2.5	2.5	172.2	4.1	d.m.	18.7	18.7	d.m.	0.5.
Si as SiO_2 (µg L^{-1})	b.d.	b.d.	b.d.	b.d	d.m.	b.d.	b.d.	d.m.	b.d.
Sum, ppb, (µg L^{-1})	36.7	82.17	217.66	1445	–	651.9	1,708.7	–	1,217.55
Sum omitting calcite (µg L^{-1})	36.21	80.87	217.16	33.4	–	23.9	19.7	–	3.55
Sum omitting calcite and sulphur (µg L^{-1})	6.21	8.87	201.16	5.4	–	23.9	19.7	–	3.55

b.d. = below detection limit; d.m. = data missing because of broken filters

Colloid phase	Borehole and filter pore size								
	KFM03A, –978 m Filter pore size (μm)			KFM06A, –302 m Filter pore size (μm)			KFM06A, –645 m Filter pore size (μm)		
	0.05	0.2	0.4	0.05	0.2	0.4	0.05	0.2	0.4
Ca as calcite $CaCO_3$ (μg L^{-1})	d.m.	d.m.	657.5	232.5	b.d.	191	977	981	484
Fe as $Fe(OH)_3$ (μg L^{-1})	d.m.	d.m.	3.05	2.1	0.6	3.9	1.2	1.3	3.15
S as sulphur (μg L^{-1})	d.m.	d.m.	b.d	b.d.	b.d.	b.d.	b.d.	b.d.	b.d.
Mn as $Mn(OH)_2$ (μg L^{-1})	d.m.	d.m.	0	0.1	0	0.1	0	0	0.55
Al as K-Mg-Illite clay: $K_{0.6}Mg_{0.25}Al_{2.3}Si_{3.5}O_{10}(OH)_2$ (μg L^{-1})	d.m.	d.m.	4.2	3.3	1.7	7.9	2.1	1.7	7.05
Si as SiO_2 (μg L^{-1})	d.m.	d.m.	b.d.	b.d.	b.d.	b.d.	b.d	b.d.	b.d
Sum, ppb, (μg L^{-1})	–	–	664.75	238.0	2.3	202.9	980.3	984	494.75
Sum omitting calcite (μg L^{-1})	–	–	7.25	5.5	2.3	11.9	3.3	3.0	10.75
Sum omitting calcite and sulphur (μg L^{-1})	–	–	7.25	5.5	2.3	11.9	3.3	3.0	10.75

b.d. = below detection limit; d.m. = data missing because of broken filters

Colloid phase	Borehole and filter pore size								
	KFM07A, –760 m Filter pore size (μm)			KFM10A, –215 m Filter pore size (μm)			KFM10A, –328 m Filter pore size (μm)		
	0.05	0.2	0.4	0.05	0.2	0.4	0.05	0.2	0.4
Ca as calcite $CaCO_3$ (μg L^{-1})	877	1,807	1,572	230.2	247.8	b.d.	b.d.	b.d.	b.d.
Fe as $Fe(OH)_3$ (μg L^{-1})	1.8	2.5	2.4	5.2	5.2	11.3	72.2	61.4	28.5
S as sulphur (μg L^{-1})	b.d.	b.d.	b.d.	b.d.	b.d.	15.8	11.0	b.d.	9.0
Mn as $Mn(OH)_2$ (μg L^{-1})	b.d.	b.d.	b.d.	b.d.	b.d.	b.d.	0.146	0.162	0.218
Al as K-Mg-Illite clay: $K_{0.6}Mg_{0.25}Al_{2.3}Si_{3.5}O_{10}(OH)_2$ (μg L^{-1})	4.95	2.5	8.3	1.2	1.7	3.5	2.7	3.6	15.5
Si as SiO_2 (μg L^{-1})	b.d.	b.d	b.d	b.d.	b.d.	b.d.	b.d.	b.d.	b.d.
Sum, ppb, (μg L^{-1})	884	1,812	1,583	236.6	254.7	30.6	86.0	65.2	53.2
Sum omitting calcite (μg L^{-1})	7	5	11	6.4	6.9	30.6	86.0	65.2	53.2
Sum omitting calcite and sulphur (μg L^{-1})	7	5	11	6.4	6.9	14.8	75.0	65.2	44.2

b.d. = below detection limit

2.5 Colloids and chloride

Figure 2-2 shows the amount of colloids versus chloride. In groundwater with a high chloride concentration the amount of colloids usually decreases, because a higher ion strength increases the precipitation of various solid particles. The chloride concentrations in this dataset were relatively constant at approximately 5,000 mg L^{-1}. The highest amount of colloids was found in borehole KFM01A at a depth of 112 m, where the chloride concentration was 4,563 mg L^{-1}; the lowest amounts were found in borehole KFM06A.

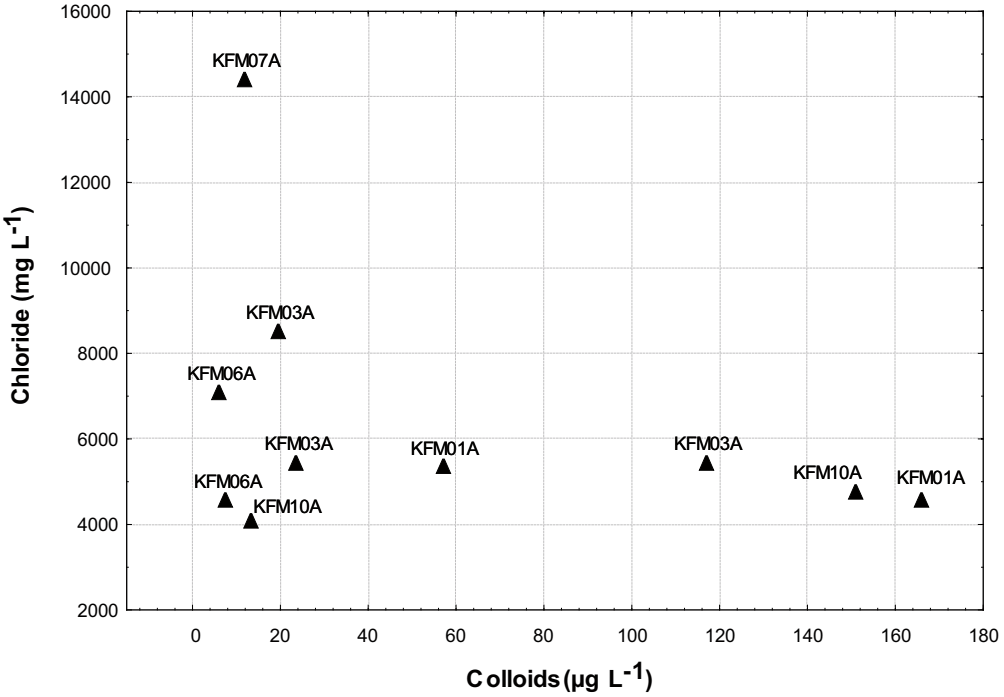

Figure 2-2. *Colloid concentration (µg L^{-1}) plotted against amount of chloride in the groundwater in Forsmark. Data from data freeze 2.3.*

2.6 Colloids and iron

High ferric iron concentrations in groundwater force the precipitation of other compounds due to the ability of iron to co-precipitate, producing larger particles; thus, the amount of colloids should decrease with increasing iron concentration. Figure 2-3 shows colloid concentration versus iron content in groundwater in Forsmark. The data do not correspond well with the theory, although the most colloids were found in water from a depth of 112 m in borehole KFM01A, there was no correlation. In particular, in KFM10A at a depth of 328 m there are both high amounts of colloids and the highest iron concentration found in Forsmark; the colloids here mostly consist of iron, as can be seen in Figure 2-4.

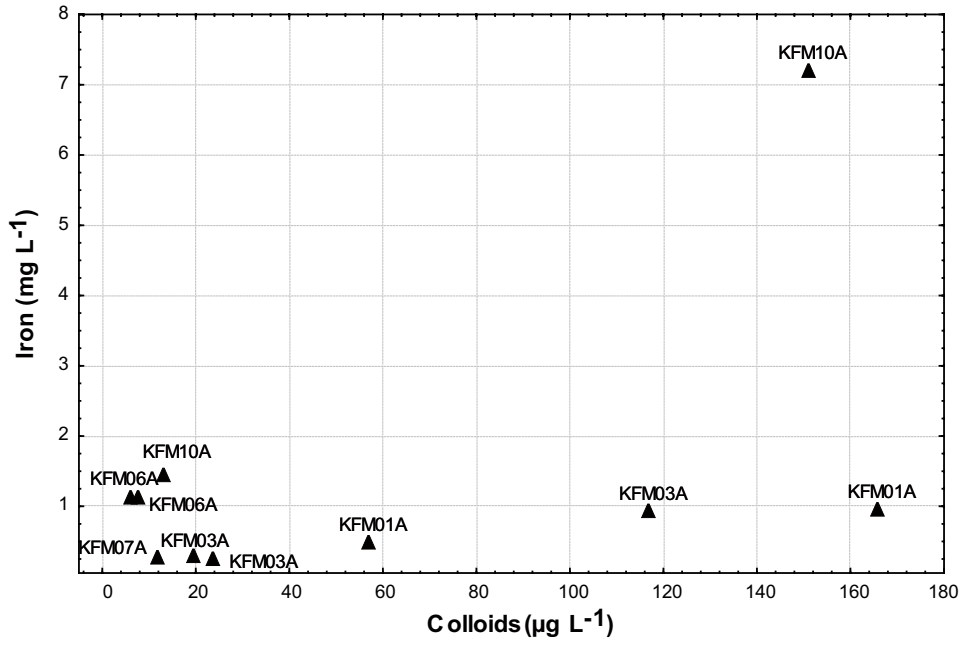

Figure 2-3. *Colloid concentration (µg L^{-1}) plotted against iron concentration in the groundwater in Forsmark. Data from data freeze 2.3.*

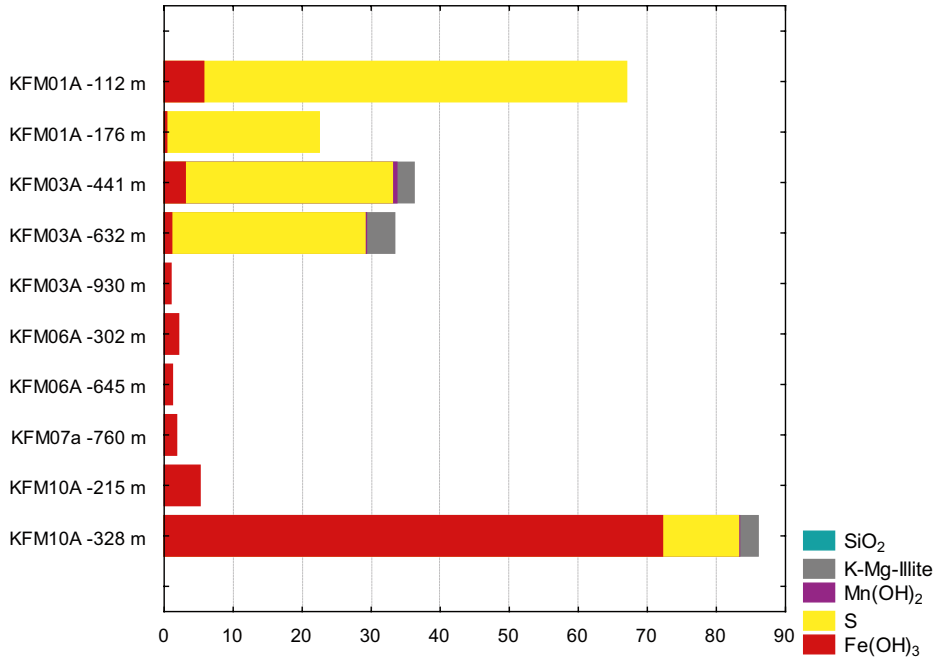

a.

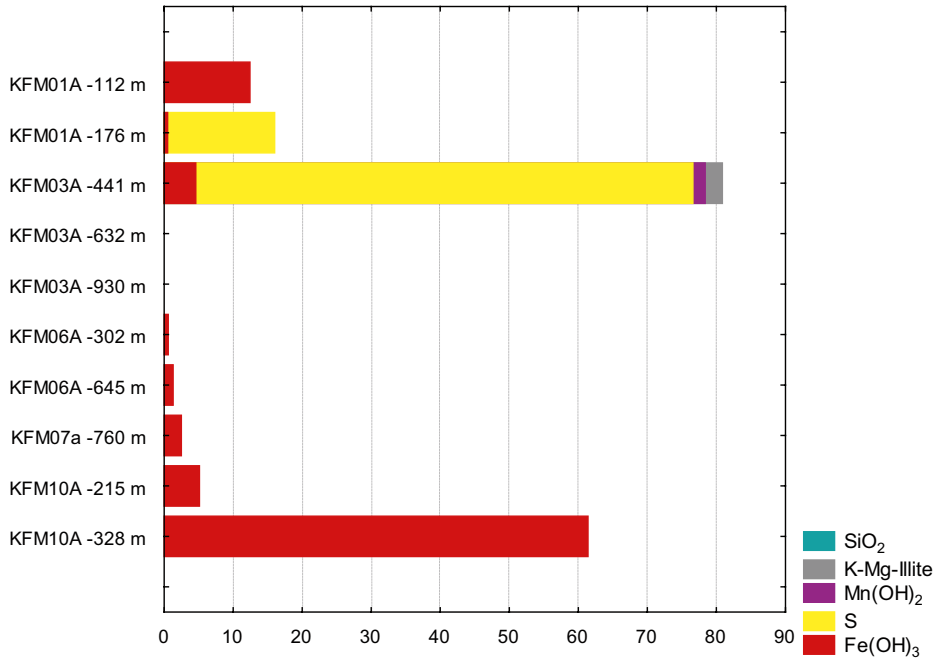

b.

Figure 2-4. *Colloid composition in groundwater in Forsmark. Stacked amounts of minerals in two colloid fractions: a) colloids ≤ 0.05 µm and b) colloids ≤ 0.2 µm.*

2.7 Composition of colloids – size distribution

To understand the size distribution of the various colloidal minerals, the stacked amounts of these minerals were plotted for both pore sizes (Figure 2-4, a and b). In this figure it can be seen that most of the colloids were either sulphur or iron. The question that then arises is whether these were "real" colloids or were simply the results of sampling artefacts (i.e. sulphur colloids can be formed because of pressure release and iron colloids because of oxidation). The filtration method indicated higher amounts of colloids than did the fractionation method, as can be seen in next section.

2.8 Inorganic colloids – fractionation

Fractionation filtration was performed on groundwater sampled from 16 sections of eight boreholes (see Table 2-1, Table 2-2); when using this method, the 1,000–5,000 D fraction was considered as the colloid fraction.

Iron colloids were found in borehole KFM01D at depths of 341 and 445 m, at concentrations of 0.121 and 0.040 µg L^{-1}, respectively. In boreholes KFM07A at 760 m and KFM08A at 546 m iron colloids found at concentrations of 0.005 and 0.030 µg L^{-1}, respectively. Uranium colloids were found in borehole KFM02A at depths of 116 and 503 m, at concentrations of 1.20 and 6.1 µg L^{-1}, respectively, in borehole KFM03A at 632 m at a concentration of 2.70 µg L^{-1} and in borehole KFM10A at 328 m at a concentration of 0.16 µg L^{-1}.

Table 2-2. Boreholes and section elevation from which colloid fractionation samples were taken in Forsmark.

Borehole and section	Borehole and section
KFM01A, −112 m	KFM06A, −302 m
KFM01A, −176 m	KFM06A, −645 m
KFM02A, −116 m	KFM07A, −760 m
KFM02A, −503 m	KFM08A, −546 m
KFM03A, −379 m	KFM01D, −341 m
KFM03A, −441 m	KFM01D, −445 m
KFM03A, −632 m	KFM10A, −215 m
KFM03A, −978 m	KFM10A, −328 m

2.9 Laser-induced breakdown colloid detection

Laser-induced breakdown colloid detection (LIBD) was used to analyze groundwater samples from boreholes KFM06A, KFM08A, KFM08D, KFM01D, KFM10A, and KFM11A in Forsmark. The method is described in the P- report on borehole KFM06A /Berg et al. 2006/. Table 2-3 presents the most important results. The results represent the means of several measurements and are presented together with the standard deviation, ±SD.

In samples from boreholes KFM06A, KFM08A, and KFM01D , the number of colloids was $2–6\times10^5$ mL^{-1} (see Table 2-3 and Figure 2-4). In KFM10A there were ten times more colloids, approximately 2×10^6 mL^{-1}. The mean size of the colloids was approximately 200 nm except in the 445-m section of KFM01D, which contained large and heavy colloids with a mean colloid diameter of 861 ± 113 nm. The samples from borehole KFM08D, on the other hand, had 1×10^7 to up to 1.9×10^8 colloids per millilitre. In the borehole section at −541 m, the colloid mass concentration was over 1,000 µg L^{-1}. These high values may possibly come from some kind of sampling artefact, e.g. pumping effects. Based on SEM pictures it was suggested that the large particles were conglomerates of small colloids. EDX analyses showed that the colloids mostly consisted of aluminium, silica, iron, and calcium.

Table 2-3. Results of LIBD analyses of groundwater samples from Forsmark. Data from data freeze 2.3.

Borehole and elevation	Number of colloids (mL^{-1})	Colloid diameter (nm)	Colloid mass concentration (µg L^{-1})
KFM06A, −302 m			
SKB PVB 9506-5*, *n* = 2	$4.0\times10^5 \pm 2.3\times10^5$	167 ± 71	2.35 ± 1.5
SKB PVB 9506-6, *n* = 2	$4.6\times10^5 \pm 3\times10^5$	188 ± 117	4.0 ± 4
KFM08A, −546 m			
SKB PVB 201, *n* = 2	$2.6\times10^5 \pm 5\times10^4$	361 ± 27	17 ± 0.5
SKB PVB 203, *n* = 2	$6.3\times10^5 \pm 2.7\times10^5$	197 ± 35	6.4 ± 0.6
KFM08D, −541 m			
SKB PVB 204,	2.0×10^7 (*n = 1)*	–**	2,469 ± 1,301 (*n= 5)*
SKB PVB 203	1.9×10^8 (*n = 3*)	–	1,099 ± 298 (*n = 4)*
KFM08D, −664 m			
SKB PVB 9506-8	$1.0\times10^7 \pm 1.1\times10^7$ (*n = 3*)	–	27 ± 12
SKB PVB 028	$1.7\times10^7 \pm 1.8\times10^7$ (*n = 2*)	–	84 ± 25
KFM01D, −341 m			
SKB PVB 220, *n* = 2	$2.0\times10^5 \pm 2\times10^4$	300 ± 60	8.5 ± 6
KFM01D, −445 m			
SKB PVB 9506-10, *n* = 5	$3.4\times10^5 \pm 3\times10^5$	861 ± 113	155 ± 38
KFM10A, −328 m			
SKB PVB 026, *n* = 5	$2.11\times10^6 \pm 7.7\times10^5$	228 ± 31.7	40 ± 10
SKB PVB 9506-8, *n* = 6	$1.7\times10^6 \pm 5.4\times10^5$	241 ± 24	31 ± 5
KFM11A, −391 m			
SKB PVB 220 n = 4	$2.0\times10^6 \pm 7\times10^5$	–	124 ± 15

* PVB sampler no.
** not calculated

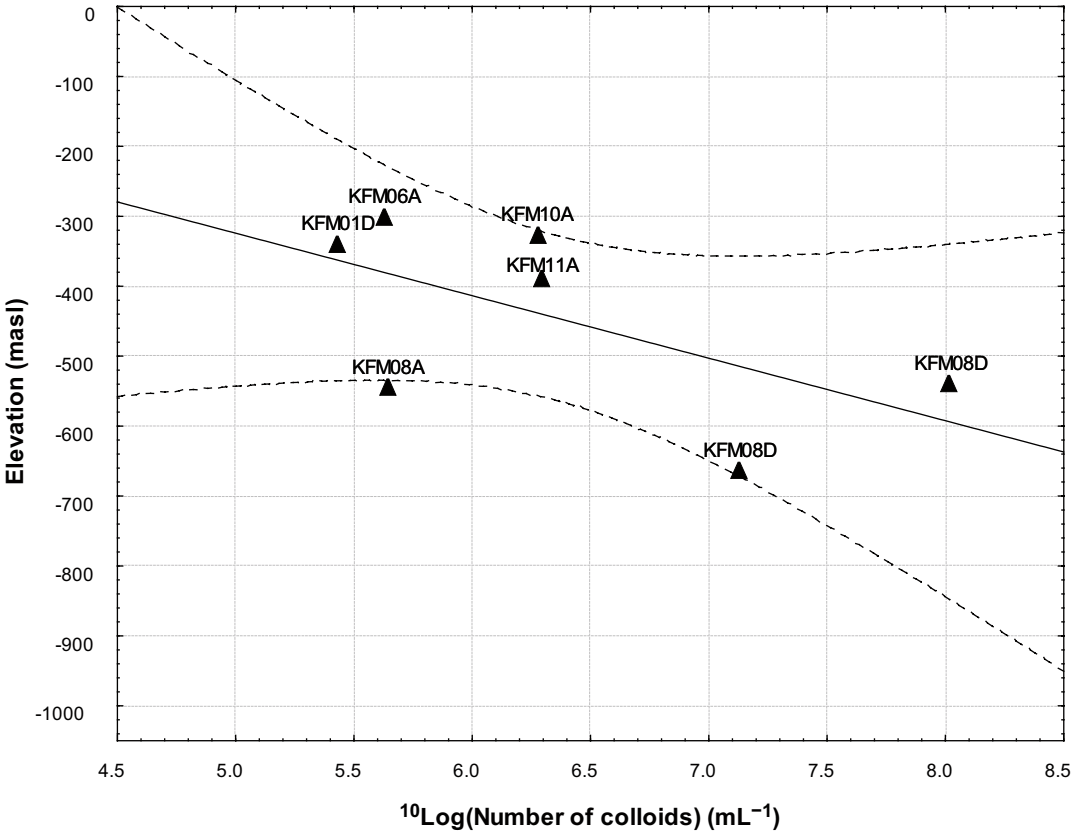

Figure 2-5. *Number of colloids in groundwater from the Forsmark area.*

2.10 Colloid analyses by means of micro-filtration plus scanning electron microscopy and energy-dispersive spectroscopy

One sample from a depth of 391 m in borehole KFM11A was examined using micro-filtration plus scanning electron microscopy and energy-dispersive spectroscopy (SEM/EDS). The sampling, analysis, and data handling are described by /Nilsson and Degueldre 2007/. The colloid concentration was determined to be approximately 1 µg L^{-1} for sizes of 50–500 nm, while the number of particles larger than 100 nm was approximately 10^6 mL^{-1}. The colloids were assumed to be clay, based on the chemical composition with an average size less than 200 nm.

2.11 Microbes and viruses as possible colloids

Microorganisms vary considerably in size. In groundwater, many of them are $\leq 10^{-3}$ mm and should be considered as colloids /Laaksoharju and Wold, 2005/. In addition, many microorganisms have negatively charged groups, such as hydroxyl and carboxyl groups, on their surfaces; this allows positively charged ions and compounds in groundwater to bind easily to free-living microbes. Figure 2-6 shows the relationship between number of colloids and number of cells. Though the amount of data is admittedly small, the data for boreholes KFM06A, KFM08A, and KFM10A correlate very well with each other. The figure indicates that there are nearly ten times more colloids than cells. The data for borehole KFM10, at a depth of 328 m, is particularly interesting, since the numbers of both cells and colloids are high compared to the numbers from the same depth of other boreholes.

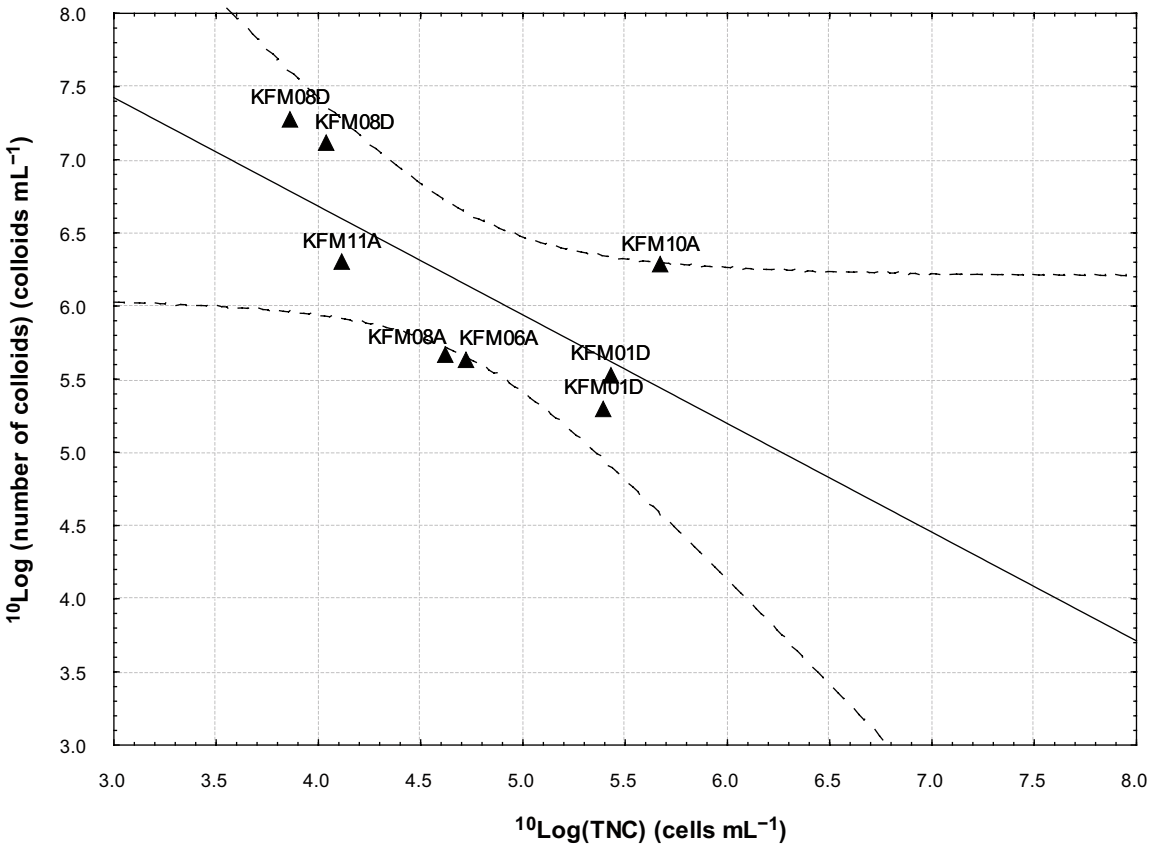

Figure 2-6. *The relation between total number of cells (TNC) and the number of colloids (confer Table 2-3). Statistics:* $^{10}Log(colloids) = -9.65 - 0.74 \times {}^{10}Log(TNC)$, *r=–0.70, not significant at p<0.05, n=8. Regression bands show 0.95 confidence intervals. Data from extended freeze 2.3 (December 2007) in Forsmark.*

A recent study of groundwater in the Äspö tunnel has revealed the presence of many different types of microbial viruses /Kyle et al. 2008/. Figure 2-7 shows some of the different types of viruses found in the Äspö groundwater; on average, the viruses were approximately 200 nm in diameter. To detect biological species with scanning electron microscopy, special treatment 0f the sample is needed.

The study has also found that there were approximately ten times more viruses than microbial cells in groundwater in the Äspö tunnel (see Figure 2-8), the same as the ratio between colloids and cells in Forsmark. There was a strong negative correlation between salinity and the number of viruses, similar to that between colloids and salinity. The finding of viruses in groundwater suggests a biological origin for many colloids.

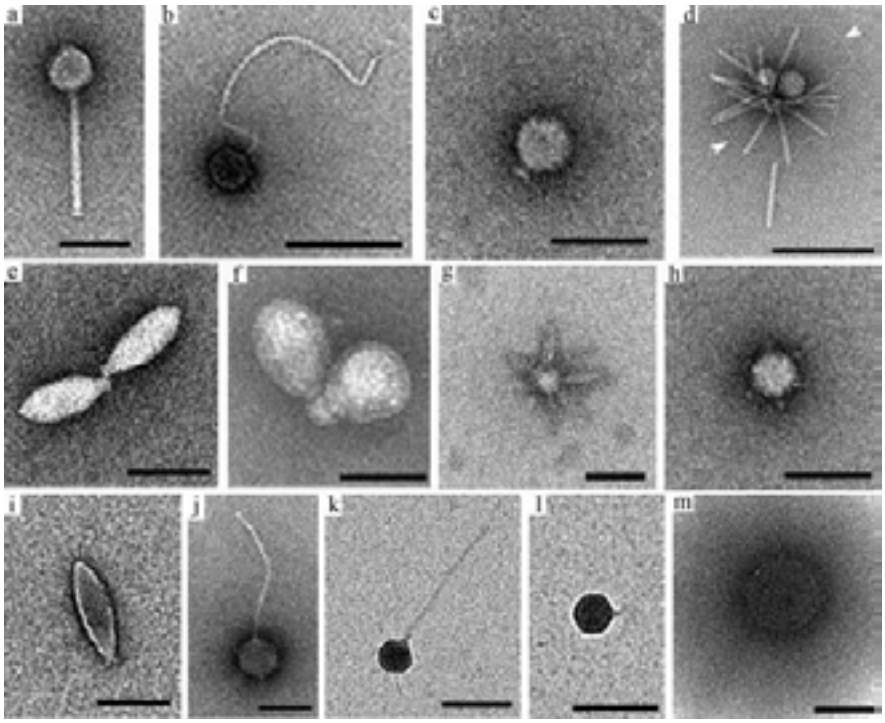

Figure 2-7. *Transmission electron micrographs of viruses from Äspö groundwater. Scale bar indicates 125 nm, except in a and d where it indicates 250 nm.*

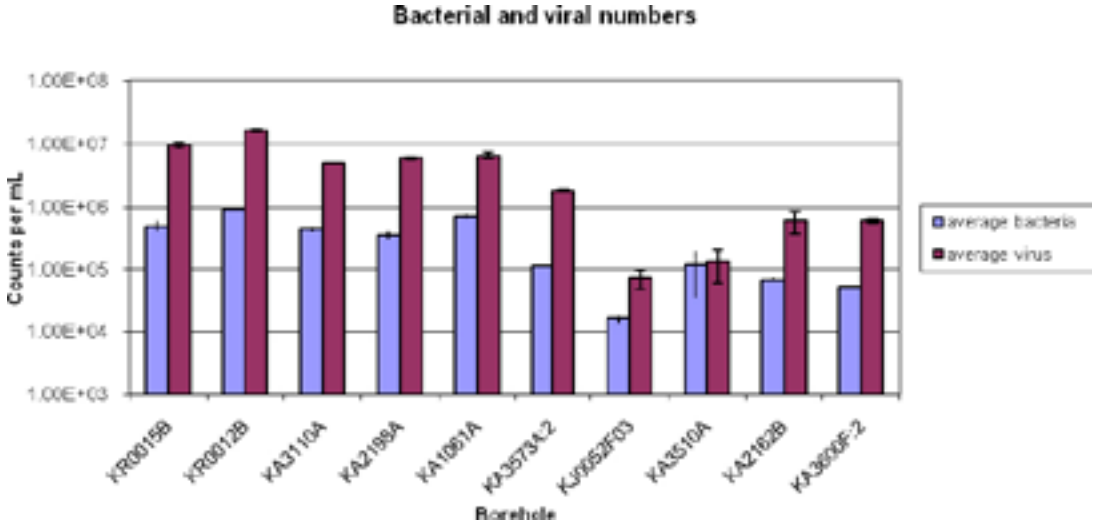

Figure 2-8. *Numbers of microbial cells and viruses in Äspö groundwater.*

2.12 Conclusions

- The number of colloids found in Forsmark groundwater was 2–6×10^5 mL^{-1}, except in borehole KFM10A, at a depth of 328 m, where the number was 2×10^6 mL^{-1} and in borehole KFM08D where the number of colloids were between 1×10^7 and 2×10^8 mL^{-1}.
- The filtration and fractionation method showed that the colloids were composed mostly of iron and sulphur. Uranium colloids were found in boreholes KFM02A and KFM06A, in line with the high uranium concentrations found in the groundwater from these boreholes see /Smellie et al. 2008/ LIBD with EDX on the other hand showed that the colloids were composed mostly of aluminium, silica and iron.
- The mass concentration of the colloids differs considerably depending on the detection method used: the highest values were obtained using the filtration method, while fractionation gave very low values. However, filtration values are in the same order of magnitude as are the LIBD values, and most of the samples were found to contain below 100 µg L^{-1} of colloids.
- The number of colloids corresponds to the number of microbial cells measured. Viruses have also been found in groundwater, in numbers close to the measured number of colloids; this indicates that many colloids are of biological origin.

3 Gases

3.1 Introduction

Dissolved gases in groundwater contribute to the mass of dissolved species. The gases can be defined as chemically active or inactive. Biological processes are included within the term "chemically active". Chemically active species are oxygen and hydrogen sulphide with its anionic dissociation products HS^- and S^{2-} and carbon dioxide (HCO_3^- and CO_3^{2-}), methane and hydrogen. Chemically inactive, inert, gases are the noble gases and to some extent nitrogen. Nitrogen fixation and denitrification by microorganisms may possibly influence the pool of nitrogen gas in groundwater, making nitrogen a gas difficult to define as purely (bio)chemically active or inactive. Finally gases such as ethane and propane and their reduced forms can be found in deep groundwater.

The distribution and composition of dissolved gases in deep groundwater are important to understand in the safety assessment of a deep geological nuclear waste repository: The main reasons are:

- Microbubbles of gas may potentially transport radionuclides from the repository to the surface. This will be important in the case where the total amount of dissolved gases approach their saturation limit in groundwater.
- The chemically active gases oxygen, hydrogen sulphide and carbon dioxide are parts of fundamental redox couples that participate in several solid-aqueous phase transformations such as the precipitation of ferric iron oxides, iron sulphide and calcite.
- The (bio)chemically active gases, methane and hydrogen, may serve as sources of energy to various microbiological processes as well as being produced by microbial processes.
- The chemically inert noble gases can function as conservative tracers in the evaluation of groundwater systems.

The above listed items are briefly reviewed below.

3.1.1 Observations of gas in Fennoscandian shield groundwater

Earlier studies of groundwater in the Fennoscandian Shield have reported high amounts of dissolved gases at some locations. Upwelling of large gas volumes through major fault zones have been reported from the Åland sea, northern Baltic proper /Söderberg 1993/. The groundwater of Olkiluoto has more than 1,000 mL dissolved gases L^{-1} when the depth approaches 800 m /Pitkänen and Partameis 2007/. In general, western Finland groundwater show high volumes of 100 to 500 mL dissolved gases L^{-1} over a depth range from 100 to 500 m /Pedersen 2001, Sherwood Lollar et al. 1993a/. The Äspö hard rock laboratory has smaller volumes, typically ranging from 20 to 60 mL dissolved gases L^{-1}, but the data set is still somewhat limited /Pedersen 2001, 2005ab/.

3.1.2 Microbubbles of gas

The occurrence of gas bubbles small enough to travel upwards in fractured rock has been proposed /Goodfield and Rodwell 1998/. It was suggested that the gas/water interface of such bubbles can adsorb particles of various types in the groundwater. Radionuclides can attach to colloids, such as dispersed bentonite. If colloid-radionuclide particles sorb in the gas/water interface of microbubbles in groundwater, rapid upward transport may occur, as have been suggested for various trace metals /Malmqvist and Kristiansson 1984/. The bubbles will move

rapidly upwards in the groundwater and can cause dispersion of radionuclides over large areas of the ground surface. The mechanisms of origin of gas bubbles can be several. During the transport of groundwater to the surface, the pressure decreases and the solubility of the various gases contained in the water also decreases; if there is a decrease of pressure perhaps due to a tectonic event, gas bubbles may form /Goodfield and Rodwell 1998/. Therefore, it is important to analyse the total amount of gas in groundwater. Groundwater with gas amounts that sum up towards saturation will be prone to gas bubble formation even at a small pressure drop. When gas is produced in the repository by anaerobic corrosion of metals, the sum of background groundwater gas volume and the corrosion gases will reveal when bubbles may form. In addition it has been suggested that alpha-particles generated in radioactive decay, mainly of uranium and thorium, could induce bubble formation at depth /Goodfield and Rodwell 1998/. In a site investigation it is therefore very important to evaluate the presence of gas in groundwater and include these data in hydrogeochemical models. A special case may occur if migrating radionuclides reaches a major fault with upwelling gas of the types described by /Söderberg 1993, Söderberg and Flodén 1991 and Flodén and Söderberg 1994/. Microbubble gas transport of radionuclides could then occur in the fault as depicted in Figure 3-1.

3.1.3 Biochemically active gases

Some gases are involved in microbiological reactions, for example, methane, carbon dioxide, and hydrogen. Methane is produced by methanogens in reduced environments and can be used as a substrate by methanotrophic bacteria. Carbon dioxide is used as a carbon source and terminal electron acceptor by autotrophic organisms and is the end product of microbial degradation of organic carbon compounds. Concortia of methanogens and sulphate reducing bacteria can oxidize methane anaerobically /Boetius et al. 2000/. Hydrogen is used as an energy and electron source by methanogens, acetogens, and other autotrophic microorganisms, such as sulphate reducers. It is also one of the end products of microbiological fermentation.

Analysis of stable isotopes can give information if gases such as if methane is of a biogenic or non-biogenic origin /Sherwood Lollar et al. 1993ab/. Analyses of stable isotopes were, however, not performed in the Forsmark site investigations.

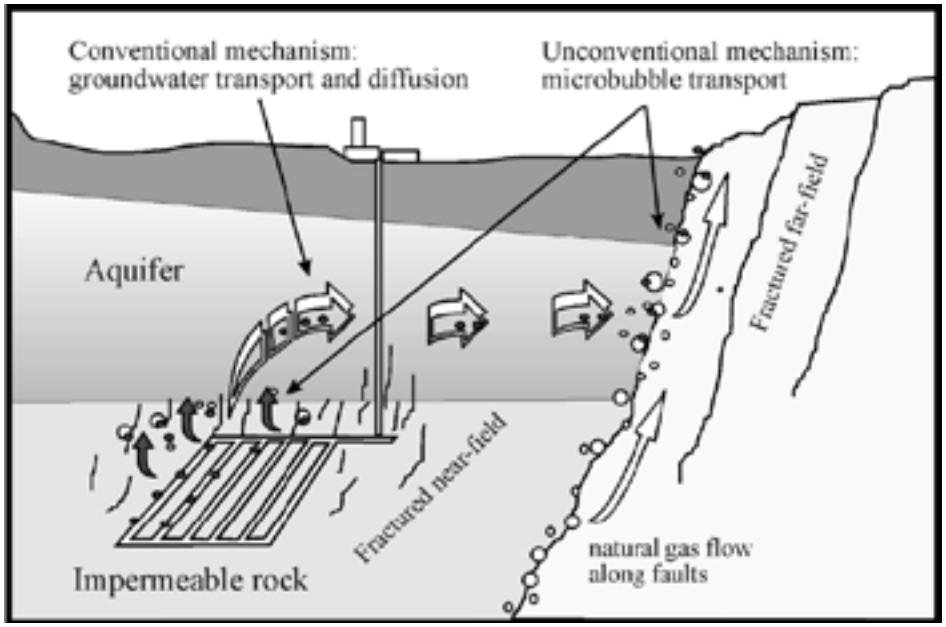

Figure 3-1. *Sketch of a possible layout for a nuclear waste repository and radionuclide migration. Currently available migration models are based on groundwater transport and diffusion. Yet there is evidence indicating the possibility of a faster nuclide transport by gas microbubbles, generated in the repository itself (near-field) or naturally occurring in water conducting faults (far-field) [Image and text from /Etiope 1998/].*

3.1.4 Origin of gases, tracer properties

Gases in groundwater have various origins. Amounts of gas are found in many Fennoscandian Shield groundwaters in concentrations that are too high to be explained by equilibria with air. This suggests that the amount of the gas, not possible to explain with exchange with the atmosphere, comes from deeper in the Earth. Gases that were trapped in the mantle during the accretion of the planets are continuously being released /Apps and van de Kamp 1993/. Because it is so light, He leaves the atmosphere, while other, heavier gases remain longer. Nitrogen, hydrogen, helium and cvarbon dioxide are continuously released from the mantle and migrate from the upper mantle to the crust, and finally to the atmosphere.

3.2 Available Forsmark 2.3 gas data

During the investigation of the Forsmark site, up to 12 gases were analyzed. They were helium, argon, nitrogen, carbon dioxide, methane, carbon monoxide, oxygen, hydrogen, ethyne, ethene, ethane, and propane. The gas contents were analysed in groundwater from 16 depths of ten boreholes, KFM01A, KFM02A, KFM03A, KFM06A, KFM07, KFM08A, KFM01D, KFM08D, KFM10A and KFM11A. Table 3-1 presents a summary of the boreholes, depth sections, and available data for this report.

In two sample occasions (KFM02A-512 m and KFM10A-328 m) dual sample vessels were collected and analysed with either nitrogen or argon in the pressure compartment (indicated in Table 3-1) as discussed next.

3.3 Data quality

The gas sampling and analysis procedures are described in SKB internal documents. According to the laboratory that performed the analyses (Paavo Ristola OY, Ramboll Finlandia), the precision of the method is 20%. The sampling of gas was performed using the PVB pressure vessel. This vessel has a piston that separates the groundwater sample from the lower compartment filled with argon or nitrogen gas. The results presented here in the figures are all from PVB with nitrogen in the lower compartment. This gas will balance the pressure of the groundwater when sampled, which reduces large shifts in pressure in the sample that would result in degassing. There have occasionally been some problems with leakage of pressure gas into the sample, which elevates the argon or nitrogen concentration of the sample. This effect is difficult to track. One possibility is to take two samples with nitrogen and argon respectively. This was done twice and in both cases, a reverse relationship between argon and nitrogen was observed (Table 3-2). Argon was elevated in the sampler with argon as pressure gas relative to the vessel with nitrogen and the opposite when nitrogen was used. This contamination effect becomes almost impossible to compensate for in the calculations of gas concentrations unless two samples are taken every time (not done here), because the degree of contamination for one of the two gases will remain unknown. The best possible way, presently, is to judge a sample result in relation to several other results for samples from similar depths. A large discrepancy between a particular sample result and the average result for samples from the same depth region indicates a sampling artefact. Several possible such cases can be found in Figure 3-2. KFM07A, 08A, 10A (215 m) and 11A all fall out of the general increasing correlation trend with depth. These samples contain more nitrogen, and also more total gas (Figure 3-2) than do all other samples in relation to depth, which may suggest leaking PVB vessels. As a result of this, all other gases in these potentially contaminated samples were diluted, so the results underestimate the actual values of all other gases. Stable isotope data on nitrogen (and the other gases) would have helped to confirm or reject if nitrogen contamination from the pressure vessel was problem. However, KFM10A at 215 m seems definitely to be contaminated with nitrogen as judged from the large amount of gas relative to the depth. It is recommended that the pressure gas is changed to neon in the future, which can be analysed and used for back-calculation if a leak is indicated.

Table 3-1. Boreholes, sample ID, elevation, sampling date, and gas volume and composition available in SICADA for analysis in Forsmark model version 2.3. All volumes are at a standard temperature (20 °C) and pressure (1 atmosphere).

Borehole	ID No	Elevation secmid (m)	Sampling date	(mL L^{-1})						(µL L^{-1})						
				Total gas	N_2	CO_2	CH_4	Ar	He	H_2	CO	C_2H_2	C_2H_4	C_2H_6	C_3H_6	C_3H_8
KFM01A	4724	176	2003-03-31	57.8	54	1.2	0.12	1.0	1.0	5.4	0*	0	0.08	1.4	0	1.5
KFM02A-N_2	8010	503	2003-09-29	83.2	77	3.9	0.03	1.1	0.8	22	0	0	0.13	0.25	0	0
KFM02A-Ar	8016	503	2003-09-29	73.5	63	4	0.04	4.9	0.8	199	0	0.06	0.15	0.20	0.1	0
KFM03A	8284	442	2004-04-27	80.2	76	1.5	0.03	0.9	1.4	213	0	0.06	0.11	0.17	0	0
KFM03A	8273	631	2004-02-23	89.0	78	0.57	0.07	1.0	9.5	0	0	0	0.06	0.6	0	0
KFM03A	8281	930	2004-03-29	124.5	105	0.16	0.06	1.4	17	44	0	0	0.14	0.37	0	0.22
KFM03A	8152	978	2003-12-08	127.5	105	0.03	0.05	1.5	21	0	0	0	0	0.56	0	0.25
KFM06A	8785	645	2005-01-31	105.5	76	0	0.09	1.0	28	0	0	0.37	0.38	0.88	0.2	0.39
KFM07A	8879	760	2005-04-25	160	132	0	0.04	1.7	26	0	0	0	0	0.66	0	0
KFM08A	12000	546	2005-10-31	135.0	118	0.08	0.03	1.53	15	0	0	0.1	0.1	0.07	0.1	0.21
KFM01D	12326	341	2006-07-03	91.2	64	0.20	0.14	1.1	26	0	0	0	0.09	2.5	0	0.57
KFM01D	12354	445	2006-07-30	112.4	64	0.04	4.6	0.85	43	0	0	0	0	6.8	0	1.3
KFM10A-N_2	12517	328	2006-10-30	68	65	1.9	0.03	0.76	0.33	0	0	0	0.28	0.37	0.12	0.14
KFM10A-Ar	12517	328	2006-10-30	69	59	1.5	0.03	7.9	0.33	0	0	0	0.24	0.31	0.10	0.11
KFM10A	12552	215	2006-11-26	127	123	0.06	0.06	1.3	3.1	0	0	0	0.13	0.26	0.13	0.13
KFM11A	12727	390	2007-03-12	104	99	0.42	0.10	0.88	3.4	34	0	0	0.11	0.21	0.11	0.11
KFM08D	12776	664	2007-05-02	110	85	0,03	0,06	1,40	24	0	0	0	0,11	0,55	0,22	0
KFM08D	12818	541	2007-06-19	98	73	0,02	0,09	1,70	23	0	0	0	0,10	0,49	0,20	0

* Value is 0 or below detection limit

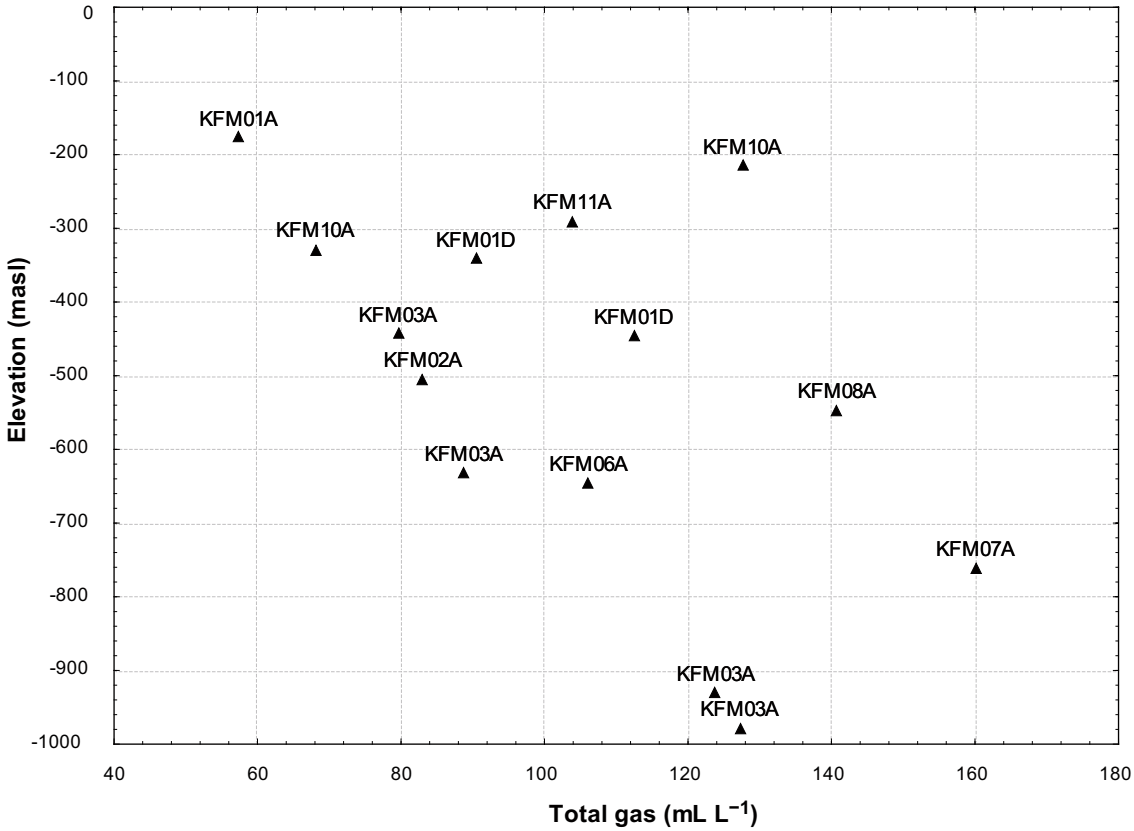

Figure 3-2. *Total volume of gas in samples from groundwater in the Forsmark area.*

Table 3-2. Ratios between nitrogen and argon in samples taken with nitrogen or argon in the PVB pressure compartment (confer Figure 3-10).

Borehole	Elevation secmid (m)	Sampling date	N_2	Ar	N_2/Ar
KFM02A-N_2	503	2003-09-29	77	1.1	70
KFM02A-Ar	503	2003-09-29	63	4.9	12.9
KFM10A-N_2	328	2006-10-30	65	0.76	85.5
KFM10A-Ar	328	2006-10-30	59	7.9	7.5

During the extraction process, there were problems with air entering the sample, which was detected as the presence of oxygen. Data reported in SICADA are not corrected for this air leakage into the samples; the data used in this report, however, are corrected for such leakage using the dissolved content of oxygen as an indicator. The oxygen could originate either from the sampling vessel or from gas extraction and analysis in the laboratory. As deep groundwater generally contains ferrous iron and sometimes sulphide, oxygen should not be present, because these two ions are not stable in oxygenated water.

3.4 Total gas volumes

Figure 3-2 shows the total volumes of gas in Forsmark groundwater samples; all volume values shown are at atmospheric pressure. This figure indicates a general trend towards increasing amount of gas with depth. The shallowest groundwater (176 m in KFM01A) contained 57.8 mL dissolved gases L^{-1}. The sample from a depth of 760 m in KFM07A contained 160 mL L^{-1} of gas, which was the largest volume of gas found in Forsmark.

3.5 Gas composition

3.5.1 Nitrogen

Figure 3-3 shows that the amount of nitrogen – the dominant gas in all samples of groundwater from Forsmark – follows the trend of the total amount of gas, and increases with depth. This corresponds to the gas content in groundwater in Olkiluoto, Finland, which also displayed an increasing trend with depth down to 1,100 m /Pitkänen et al. 2004, Pitkänen and Partamies 2007/. The highest concentration of N_2 found in the Forsmark investigation was at a depth of 760 m in borehole KFM07A, where it reached 132 mL L^{-1} of groundwater, while the lowest was 54 mL L^{-1} at a depth of 176 m in borehole KFM01A. It can not be excluded that KFM07A, 08A, 10A-215 m and 11A were contaminated with nitrogen from the PVB pressure compartment, as they have close to double the amount of nitrogen compared the rest of the data, with respect to sample depth.

The origin of nitrogen in groundwater is considered to be crustal degassing of the bedrock. It has earlier been suggested that the nitrogen gas in groundwater originates entirely from the atmosphere /Andrews et al. 1989, Pitkänen and Partemies 2007/. This assumption was made based on calculations of the N_2/Ar and $^{15}N/^{14}N$ ratios in the measured gas. The solubility of nitrogen gas in water at atmospheric pressure at 10°C is 0.024 g kg^{-1} /Aylward and Findley 2002/, which corresponds to 0.9 mmol L^{-1} or 21 mL L^{-1}. The most nitrogen gas found in Forsmark during the site investigation was 132 mL L^{-1} in a total gas volume of 160 mL L^{-1} at a pressure of one atmosphere. This corresponds to 5.7 mmol L^{-1} or 0.160 g nitrogen per litre of groundwater and is close to 6.3 times more nitrogen in the groundwater than solubility permits at atmospheric pressure. In reality the amount of nitrogen is even higher than 6.3 times, because other shallow groundwater gases, in particular carbon dioxide and oxygen, will reduce the solubility of nitrogen during the entrapment of atmospheric nitrogen. The numbers used here are thus conservative. It is deemed very unlikely that the observed excess of dissolved nitrogen

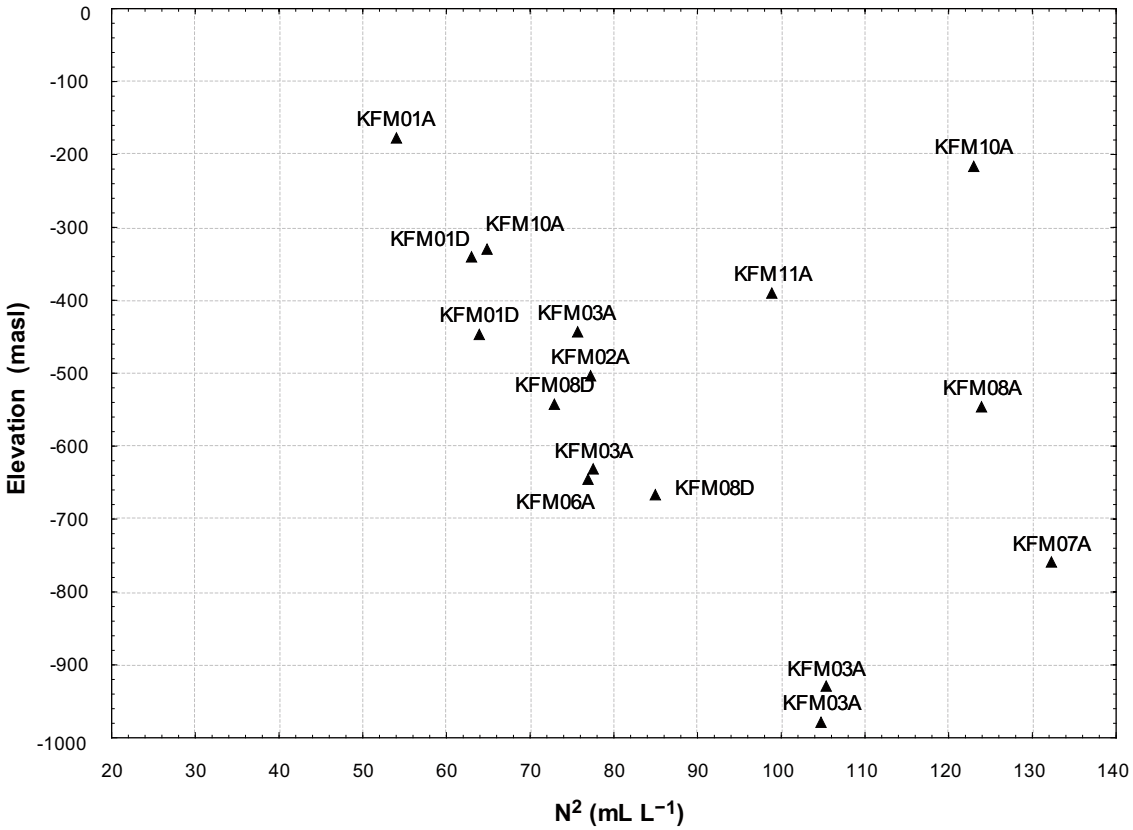

Figure 3-3. *Nitrogen concentration plotted against depth in samples from boreholes in the Forsmark area.*

in the deep Forsmark groundwater originates from atmospheric entrapment during groundwater recharge. Most dissolved nitrogen must instead originate from deep crustal sources. The increase in nitrogen concentration over depth suggests that the major part of the nitrogen comes from deep crustal sources. Actually, none of the analysed groundwater samples have nitrogen concentrations at or below the solubility limit (21 mL L^{-1}) at atmospheric pressure; the majority of the gas samples had nitrogen concentrations above this limit, supporting the suggested deep crustal origin.

Using data from /Chapoy et al. 2004/, the saturation concentration of nitrogen in a water-nitrogen system can be calculated. This calculation indicates that at a pressure of 7 MPa, which corresponds to a depth of 700 m, 1,200 mL of nitrogen gas can be dissolved in one kg of water at 10°C. All samples in Forsmark had total gas volumes below 160 mL L^{-1} of water. Although the concentration of gas generally increases with depth, the gases are not oversaturated at the depths at which they were sampled.

3.5.2 Helium

The amount of helium in groundwater from Forsmark increases with depth (see Figure 3-4, Table 3-1). There was one exception to this trend and that is borehole KFM01D. At both sampled depths in this borehole the helium values were higher than in samples from the same depths in other boreholes, i.e. 26 and 43 mL L^{-1}, respectively. It could be argued that part of these groundwaters contains gas of deep origins with a high amount of helium. These high levels may also indicate that deep groundwaters are discharging to the surface in this area. The nitrogen/helium ratio supports this conclusion (Figure 3-11).

There are four helium reservoirs on earth, namely, the air, crust, and upper and lower mantle /Apps and Van de Kamp 1993/. Since helium is not retained in the atmosphere, its concentration in air is very low (5.24 ppm by volume). The helium in the air comes from the outgassing of

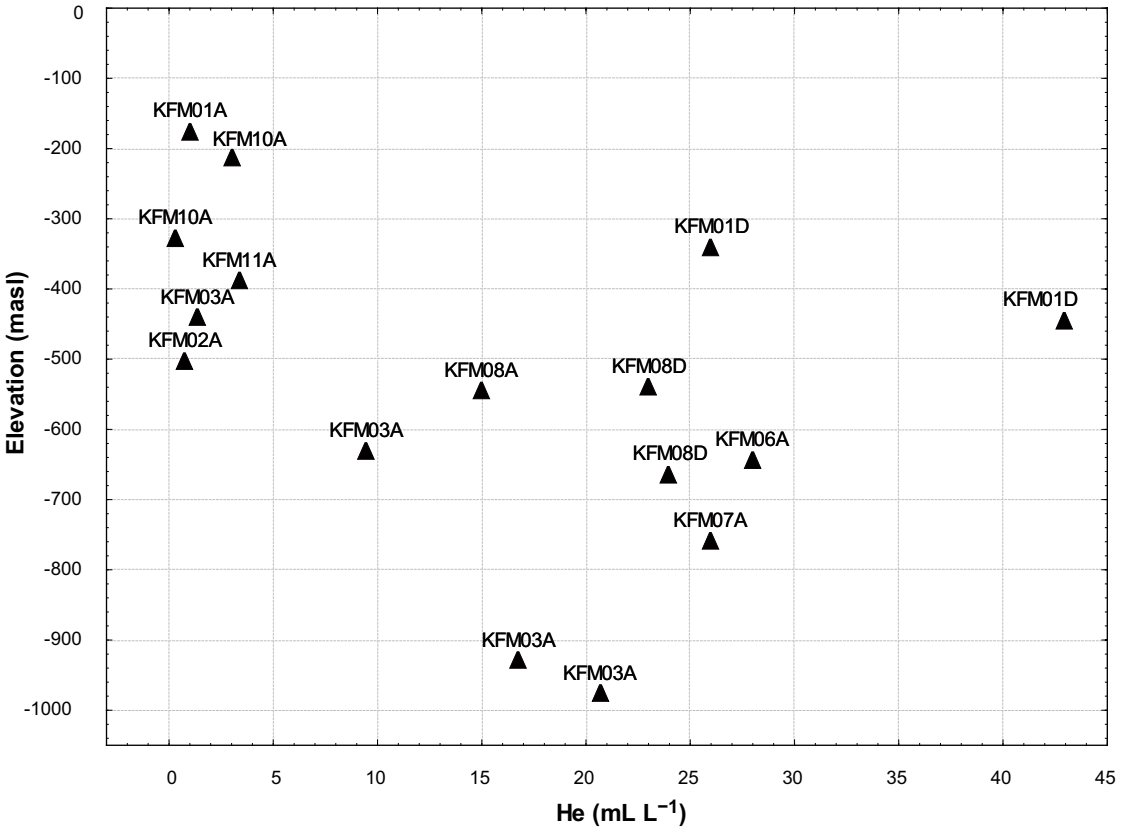

Figure 3-4. *Helium concentration plotted against depth in samples from boreholes in the Forsmark area.*

the continental crust and the degassing of the mantle. Helium is present as a mixture of two stable isotopes, helium-3 and helium-4, in relative abundances of 1.38×10^{-4} % and 99.999862%, respectively; helium-3 is mainly of primordial origin, but is also produced by the beta decay of tritium to helium-3, though this reaction is rare, while helium-4 is produced by the radioactive decay of uranium- and thorium-series radionuclides. Helium is constantly produced in the crust and the mantle by these reactions /Marshall and Fairbridge 1999/.

3.5.3 Carbon dioxide

Carbon dioxide in groundwater is a dissociation product of dissolved carbonates from fractures in the bedrock and from the biological degradation of organic material in the soil and shallow bedrock. It functions as a carbon source and electron acceptor for autotrophic methanogens and acetogens. The carbon dioxide concentrations in samples from the Forsmark area displayed a slight decreasing trend with depth (see Figure 3-5). At a depth of 990 m, the carbon dioxide concentration was very low, i.e. 0.03 mL L^{-1}. This pattern has also been observed for carbon dioxide concentrations in groundwater from the Olkiluoto site in Finland. /Pitkänen et al. 2004, Pitkänen and Partamies 2007/.

3.5.4 Methane and higher hydrocarbons

In the case of methane there was no obvious trend with depth. The amounts found were very low, between 20 and 100 µL L^{-1} (see Table 3-2, Figure 3-6). The only exception was borehole KFM01D, at a depth of 445 m, where 4,200 µL L^{-1} was measured.

Methane in groundwater can be either biotic or abiotic in origin. Biotic methane is produced by methanogenic *Archaea*, a group of prokaryotic organisms. They can utilize either C1 compounds or acetate (Eq. 3-1). They can also fix carbon dioxide, using hydrogen gas as an

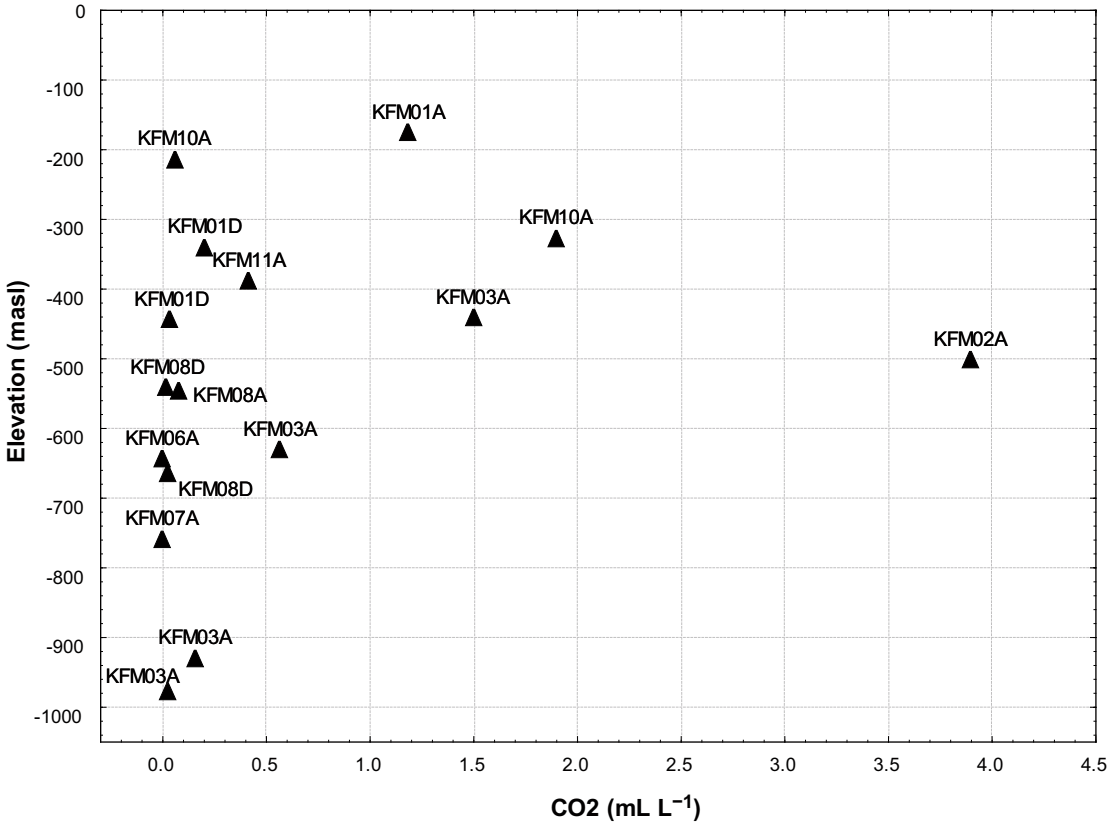

Figure 3-5. *Carbon dioxide concentration plotted against depth in samples from boreholes in the Forsmark area.*

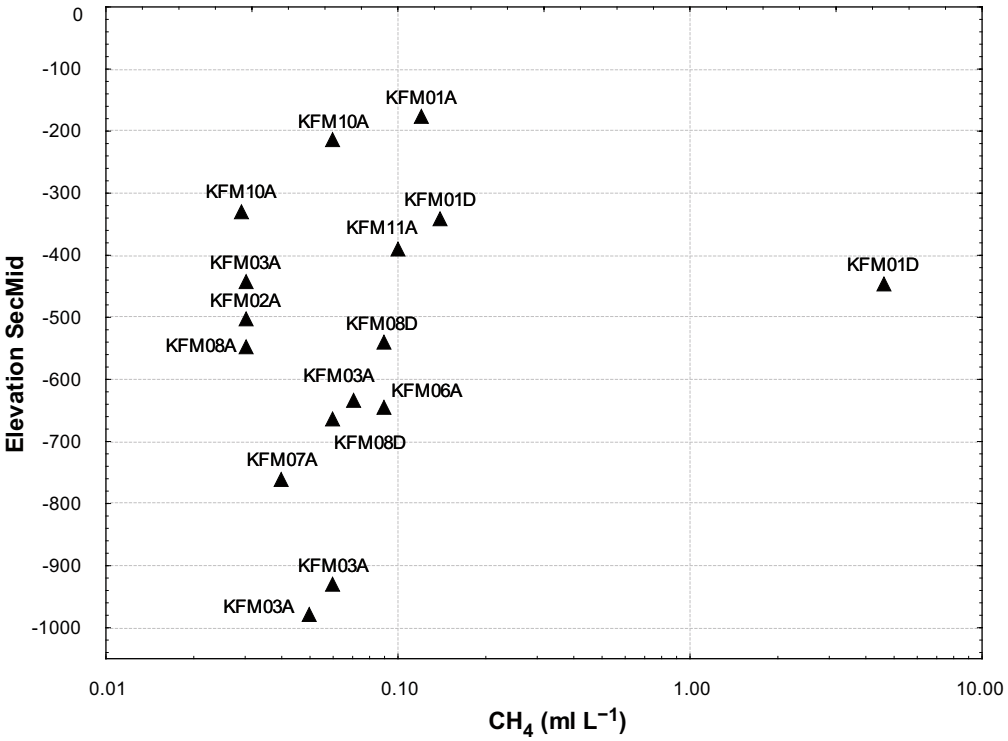

Figure 3-6. *Concentration of dissolved methane in samples from boreholes in the Forsmark area plotted against depth.*

energy and electron source (Eq. 3-2). Their substrate can be biodegraded organic matter, as in sea and lake sediments or composts, or carbon dioxide and hydrogen originating in the mantle /Apps and Van de Kamp 1993/.

$$CH_3COOH \rightarrow CH_4 + CO_2 \qquad \text{(Eq. 3-1)}$$

$$CO_2 + 4H_2 \rightarrow CH_4 + 2H_2O \qquad \text{(Eq. 3-2)}$$

Abiogenic methane is produced, for example, in hydrothermal systems during water–rock interactions involving the Fischer–Tropsch synthesis reaction (Eq. 3-2). This methane can act as a precursor for polymerization to higher hydrocarbons, such as short-chain alkanes (see below).

The isotopic carbon signature of methane can reveal its source, but no such data are available in SICADA. However, calculation of the C1/(C2 + C3) ratio also provides evidence regarding the origin of the methane (see below).

The concentration of hydrocarbons, other than methane, in groundwater in Forsmark remained relatively constant with depth and volumes were below 1 µL L^{-1} (see Figure 3-7). Three samples had higher values but were all below 8 µL L^{-1}. Abiogenic methane and higher hydrocarbons are believed to come from a deep abiogenic source and move slowly by means of diffusion towards the surface. Calculations of the C1/(C2 + C3) ratio can reveal the source of the methane found. A high ratio of over 10^3 is considered to indicate microbiological methanogenesis, while thermogenic and abiogenic methanogenesis will give a ratio of approximately 10 /Sherwood-Lollar et al. 1993a, 2002, 2005, Clark and Fritz 1997, Whiticar 1990/. Such calculations using data from Forsmark give ratios ranging from 32 to 568. This indicates that most of the methane originates from an abiogenic source, though some may have a biogenic origin. The sample containing the largest portion of biologically produced methane came from borehole KFM01D, at a depth of 445 m. To be certain as to the origin of this gas, more hydrocarbon data must be generated, together with stable isotope values for methane and other hydrocarbons.

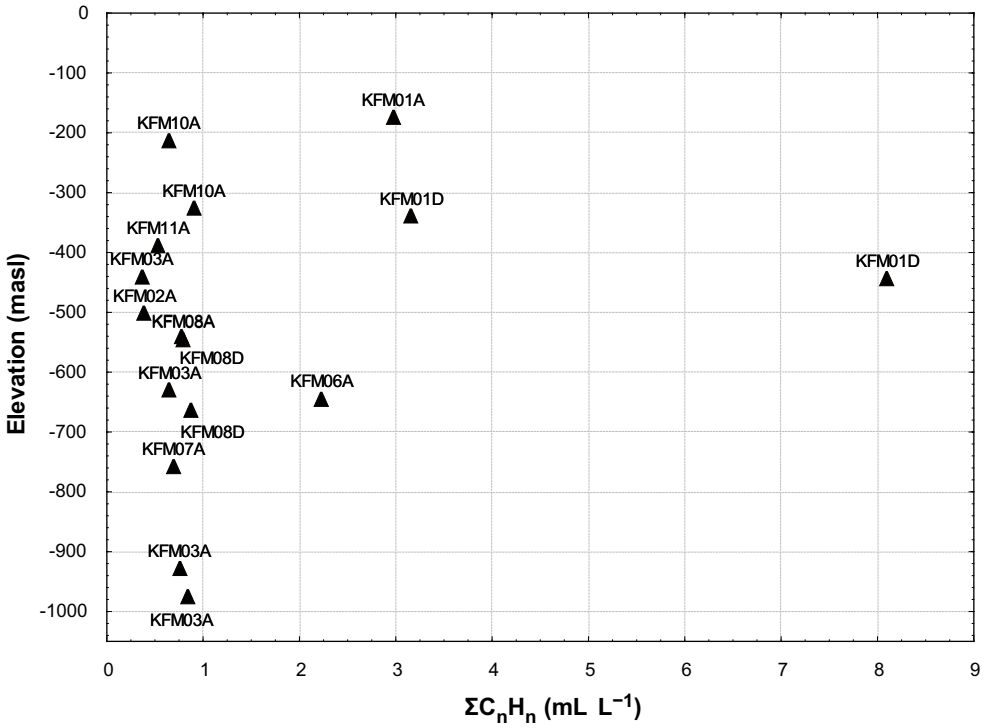

Figure 3-7. *Total concentrations of hydrocarbons (except methane), versus depth in boreholes in the Forsmark area.*

Table 3-3. The C1/(C2 + C3) ratio in groundwater from the Forsmark area.

Borehole and depth	∑ C2 + C3 (µL L⁻¹)	CH4 (µL L⁻¹)	C1/ C2 + C3
KFM01A, –176 m	3	120	40
KFM02A, –503 m a	0.4	30	75
KFM02A, –503 m b	0.5	40	80
KFM03A, –442 m	0.4	30	75
KFM03A, –632 m	0.7	70	100
KFM03A, –930 m	0.8	60	75
KFM03A, –978 m	0.8	50	63
KFM06A, –645 m	2.2	90	41
KFM07A, –760 m	0.7	40	57
KFM08A, –546 m	0.8	30	38
KFM01D, –341 m	3.2	140	44
KFM01D, –445 m	8.1	4,600	568
KFM10A, –215 m	0.6	60	100
KFM10A, –328 m	0.9	29	32
KFM11A, –390 m	0.5	100	200
KFM08D, –541 m	0.8	90	113
KFM08D, –664 m	0.9	60	67

3.5.5 Argon

The amount of argon in Forsmark was almost constant, increasing only slightly with depth; no detected value exceeded 2 mL L^{-1} (see Figure 3-8). Argon is the most common of the noble gases, accounting for 0.93% of air. It has three isotopes and 99.6% of all argon is ^{40}Ar, an isotope continuously produced in bedrock by the radioactive decay of ^{40}K. Argon is considered to be a “deep geogas” /Marshall and Fairbridge 1999/.

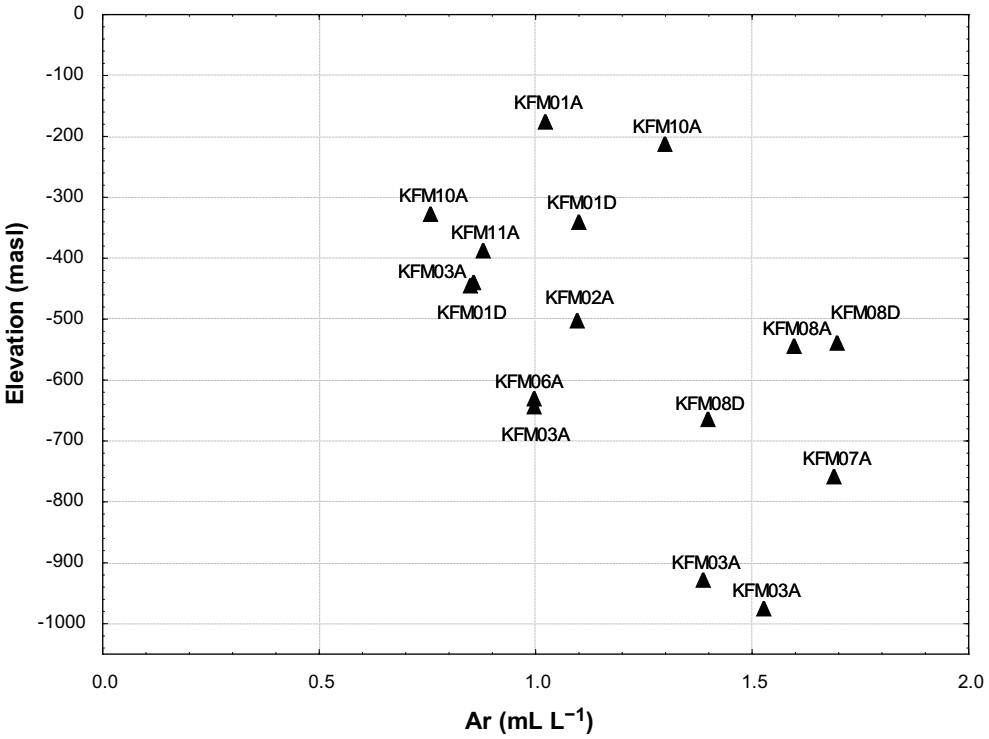

Figure 3-8. *Argon concentration plotted versus depth in samples from boreholes in the Forsmark area.*

3.5.6 Hydrogen

Hydrogen is an important gas in several anaerobic microbial metabolisms, such as methanogenesis and acetate production by acetogens. There are also autotrophic iron- and sulphate-reducing bacteria that can use hydrogen as an energy and electron source, concomitant with iron or sulphate reduction.

The hydrogen concentrations differed considerably between the two measurements made at the depth of 503 m in borehole KFM02A; a difference of the same order of magnitude can also be seen in data from the depths of 452.0 m and 642.5 m in borehole KFM03A. Measurements of hydrogen with a thermal conductivity detector, as was done here, commonly return below detection results, because the concentrations of hydrogen obviously were relatively low, and this accounts for below detection results in ten out of 16 analysed samples.

There are at least six possible processes by which crustal hydrogen is generated: (1) reaction between dissolved gases in the C-H-O-S system in magmas, especially in those with basaltic affinities; (2) decomposition of methane to carbon (graphite) and hydrogen at temperatures above 600°C; (3) reaction between CO_2, H_2O, and CH_4 at elevated temperatures in vapours; (4) radiolysis of water by radioactive isotopes of uranium and thorium and their decay daughters and by radioactive isotopes of potassium; (5) cataclasis of silicates under stress in the presence of water; and (6) hydrolysis by ferrous minerals in mafic and ultramafic rocks /Apps and Van de Kamp 1993/. The radiolysis of water has been proposed by /Lin et al. 2005/ as a possible hydrogen generation process occurring in the granitic system in the Fennoscandian Shield. In addition, hydrogen is biologically produced in microbial fermentation processes. It is important to explore the scale of these processes and the rates at which the produced hydrogen becomes available to deep microbial ecosystems.

3.6 Ratios

The present data on gas in Forsmark were influenced by a multivariate set of natural and artificial effects. Firstly, there was the documented contamination of the samples with argon or nitrogen from the pressure compartment, as discussed above. Second, there was a problem with contamination of the samples with air during analysis. Thirdly, the samples came from different areas in Forsmark, denoted FFM01, FFM02 and FFM03. It is possible that the distribution and concentrations of gases may differ significantly between these areas. The lack of stable isotope data for the analysed gases complicates the interpretation of the data set. They would have been very helpful in the separation of effects. For now, the only analytical tool available is comparison of ratios between analysed gases.

3.6.1 Nitrogen over argon

A scatter plot of the nitrogen/argon ratios shows that all samples had nitrogen/argon ratios that were greater than the water/air equilibrium value (Figure 3-10). The atmospheric nitrogen/argon ratio is 83.54 and four samples exceeded this value. High ratios above this value may suggest nitrogen of a very deep, thermogenic origin /Andrew et al. 1989/, but stable isotopes will be needed for a valid conclusion. The samples in Figure 3-10 were all collected with nitrogen in the lower PVB pressure vessel compartment. An alternative explanation to high nitrogen/argon ratios can consequently be contamination of the sample with pressure vessel nitrogen (confer Table 3-2) which depending on quality (unknown at present), would have been depleted in argon.

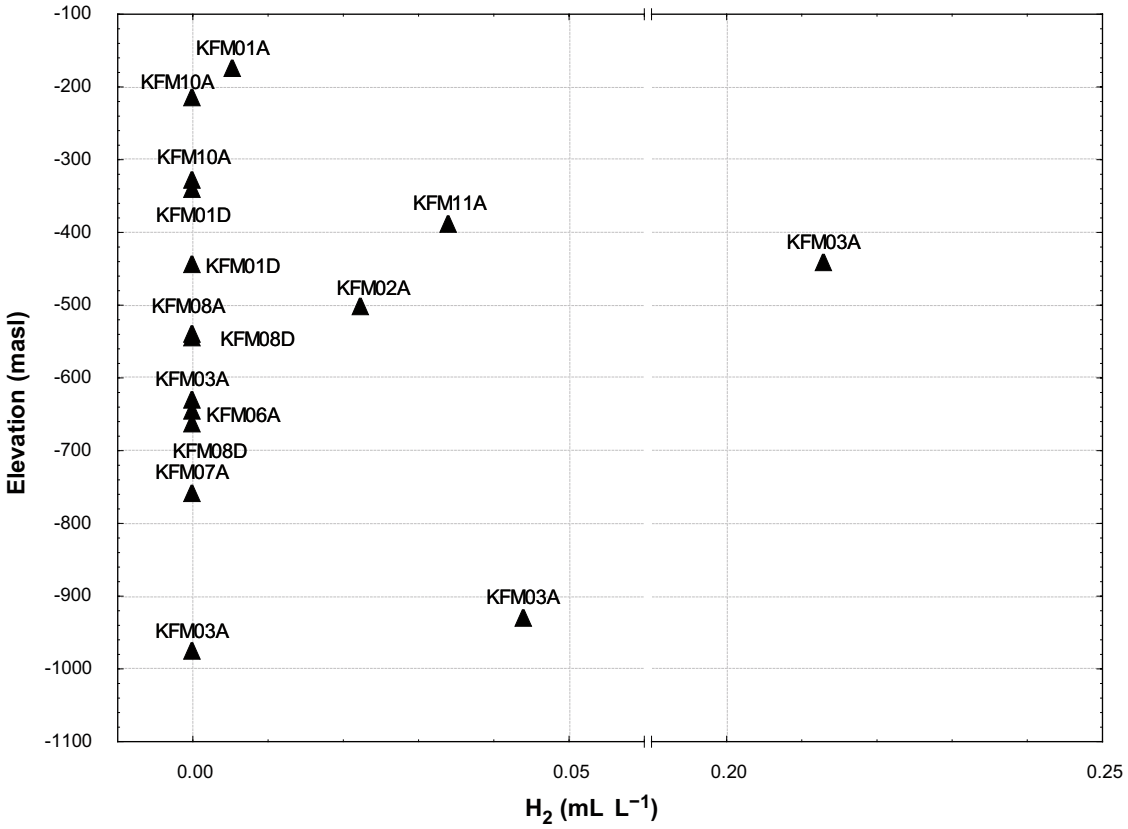

Figure 3-9. *Hydrogen concentration in groundwater from boreholes in the Forsmark area.*

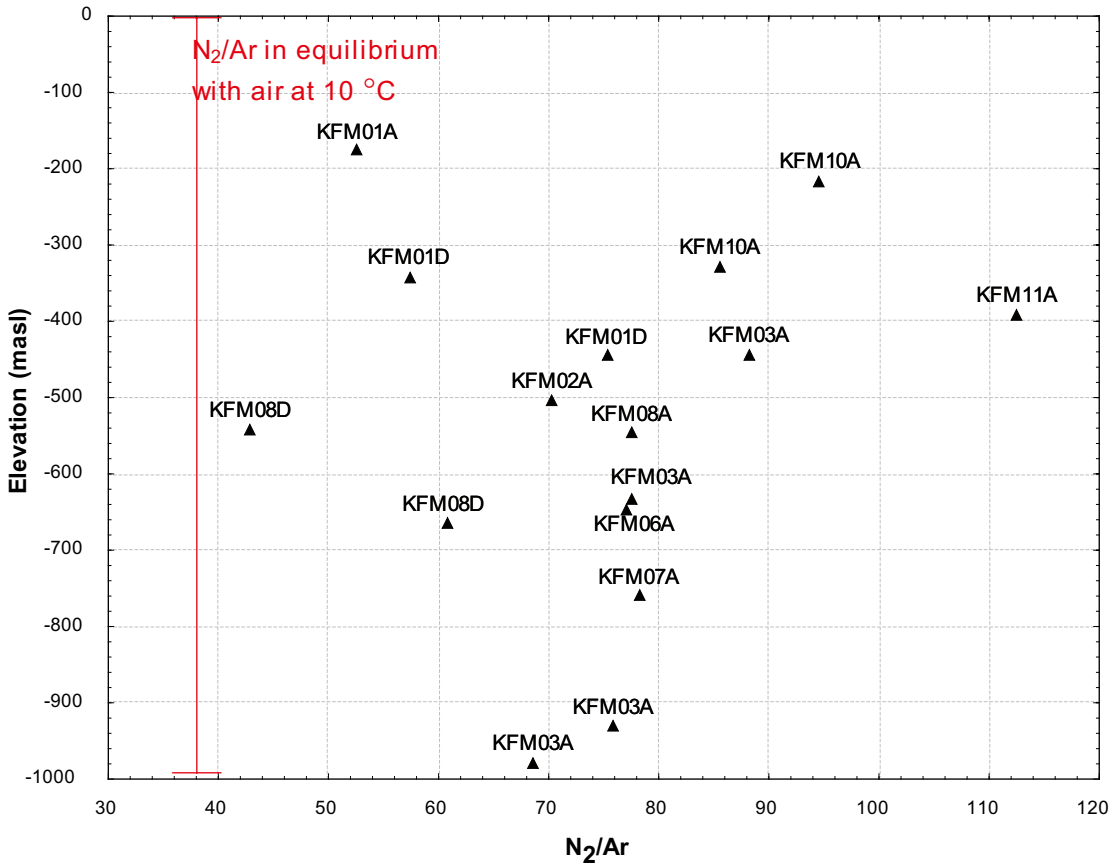

Figure 3-10. *The nitrogen/argon ratios for Forsmark groundwater gas samples.*

3.7 Nitrogen over helium

Comparing nitrogen over helium shows ten samples at similar ratios of about 10 (Figure 3-11). Six of the samples show higher ratios, all above about 500 m depth. There are several possible explanations. De-gassing to the atmosphere of helium can be assumed to be faster than that of nitrogen, because the atmospheric concentration of helium (5 ppm) is much lower compared to nitrogen (80%), which increases the gradient for helium compared to nitrogen. However, the leaking PVB problem, reflected in Table 3-2 may also explain the ratios. If there was a leak of nitrogen from the lover PVB pressure vessel compartment to the sample, the nitrogen/helium ratio would increase. This was obvious for KFM10A 328 m that was concluded to have been contaminated. It appears from Figure 3-3 that the nitrogen concentration in KFM10A 328 m is about double that found in other samples at the same depth. This would the increase the nitrogen/helium ratio by a factor of four, because the nitrogen contamination would have reduced the helium concentration by a factor of two, due to dilution. The true nitrogen/helium ratio would then have been about 50, which is closer to the bulk in Figure 3-11.

If the nitrogen/helium ratios are similar with depth, here at about 10, it suggests that nitrogen comes from deep sources. Helium is known to be produced at large depths due to radioactive decay and also to diffuse from the mantle as discussed above in relation to Figure 3-4. Nitrogen may follow in a similar process. However, stable isotope data, and tight PVB-vessels will be required for significant conclusions.

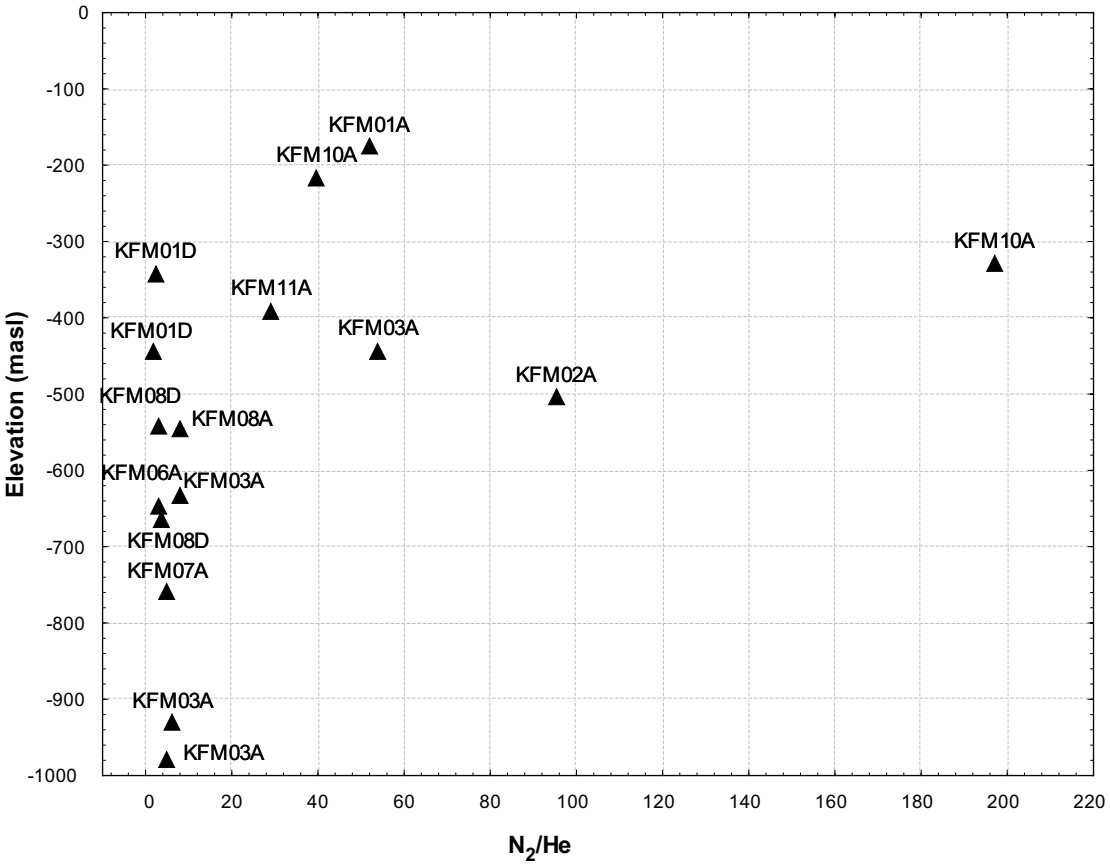

Figure 3-11. *The nitrogen/helium ratios for Forsmark groundwater gas samples.*

3.8 Methane over helium

If nitrogen is assumed to originate from deep sources as suggested above, nitrogen/methane ratios would be constant over depth if methane also is produced at depth. However, at depths above 500 m in Forsmark, the methane/nitrogen ratio increases, relative to deeper samples, which suggest ongoing methanogenesis above 500 m. Only one sample was indicated to have asignificant amount of biogenic methane as judged from C1/C2+C3 ratios. Stable isotopes will be needed for confirmation. The possible dilution effect from nitrogen in the PVB would not upset the ratios in Figure 3-12 as it would dilute helium and methane on an equal basis.

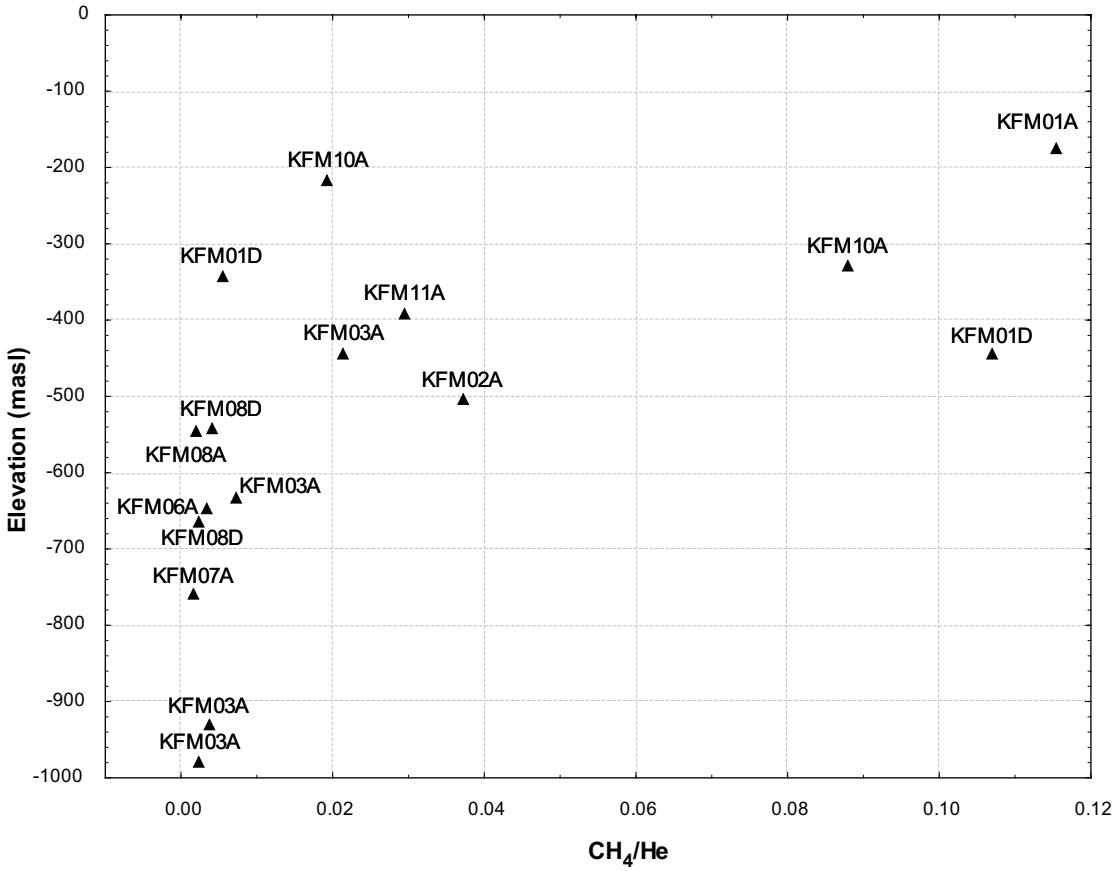

Figure 3-12. *The methane/helium ratios for Forsmark groundwater gas samples.*

3.9 Conclusions

- Although their concentrations generally increase with depth, the gases are not oversaturated at the depths at which they were sampled.
- The only sample that displays indications of biologically produced methane is from borehole KFM01D at a depth of 445 m. The methane in all other samples appears to come from abiotic sources (unless anaerobic methane oxidation is operating).
- The helium and hydrogen gases are probably mostly derived from crustal generation processes and subsequent degassing. The majority of the nitrogen appears to originate in the mantle.
- The high helium concentration found in the sample from borehole KFM01D at a depth of 445 m may be an indication of up-welling groundwater of a deep origin.
- Clarifying the origin of methane, helium argon and nitrogen calls for more data regarding deeper sections coupled with isotopic studies.

4 References

Andrews J N, Hussain N, Youngman M J, 1989. Atmosperic and radiogenic gases in groundwater from the Stripa granite. Geochimica et Cosmochimica Acta 53, 1831–1841.

Apps J.A, van de Kamp P.C, 1993. Energy gases of abiogenic origin in the Earth's crust. The future of Energy gases. U.S. Geological Survey Professional Papers. United States Government Printing Office, Washington., pp. 81–132.

Aylward G H, Findley T J V, 2002. SI Chemical Data 5th edition. John Wiley & Sons Australia, Ltd, Milton, Australia.

Bennett P C, Rogers J R, Choi W J, Hiebert F K, 2001. Silicates, silicate weathering, and microbial ecology. Geomicrobiology Journal, 18, 3–19.

Berg C, Bergelin A, Wacker P, Nilsson A-C, 2006. Forsmark site investigation. Hydrochemical characterisation in borehole KFM08A. Results from the investigated section at 683.5 – 690.8 m. SKB P-06-63, Svensk Kärnbränslehantering AB.

Boetius A, Ravenschlaug K, Schubert C J, Rickert D, Widdel F, Gleseke A, Amann R, Jörgensen B B, Witte U, Pfannkuche O, 2000. A marine microbial consortium apparently mediating anaerobic oxidation of methane. Nature, 407, 623–626.

Chapoy A, Mohammadi A H, Tohidi B, Richon D, 2004. Gas solubility measurements and modelling for the nitrogen + water system from 274.18 K to 363.02 K. Journal of Chemical Engineering data. 49, 1110–1115.

Clark I, Fritz P, 1997. Environmental isotopes in hydrogeology. Lewis Publishers, Boca Raton, 328 p.

Degueldre C, 1994. Colloid properties in groundwater from crystalline formation. Paul Scherrer Institute, Villigen, Switzerland.

Drake H.L, Küsel K, Matthies C, 2002. Ecological consequences of the phylogenetic and phisological diversities of acetogens, Antonie van Leeuwenhoek, 81 no. 1203–212,

Ekendahl S, Pedersen K, 1994. Carbon transformations by attached bacterial populations in granitic ground water from deep crystalline bed-rock of the Stripa research mine, Microbiology, 140 1565–1573.

Etiope G, 1998. Transport of radioactive and toxix matter by gas microbubbles in the ground. Journal of Environmental Radioactivity. 40, 11–13.

Eydal H.S.C, Pedersen P, 2007. Use of an ATP assay to determine viable microbial biomass in Fennoscandian Shield groundwater from depths of 3–1000 m, J Microbiol Meth, 70 363–373.

Fenchel T, King G M, Blackburn T H, 1998. Bacterial biogeochemistry. The ecophysiology of mineral cycling. Second edition. Academic Press, San Diego, USA. ISBN 0-12-103455-0.

Flodén T, Söderberg P, 1994. Shallow gas traps and gas migrations models in crystalline bedrock areas offshore Sweden. Baltica 8, 50–56.

Gascoyne M, 2005. Dissolved gases in groundwaters at Olkiluoto. Working report 2005-56. POSIVA, Finland.

Goodfield M, Rodwell W R, 1998. "Geogas" Microbubbles: a Literature Review with Reference to their Potential to Contribute to the transport of Contaminants from a Radioactive Waste Repository, Nirex Science Report S/98/016.

Greenberg A.E, Clesceri L.S, Eaton A.D, 1992. Estimation of Bacterial Density, Standard methods for the examination of water and wastewater 18th ed, 9–49. American Public Health Association, Washington.

Hallbeck L, Pedersen K, Kalmus A, 2004. Forsmark site investigation. Control of microorganism content in flushing water used for drilling of KFM05A, pp 1–19. SKB P-04-285, Svensk Kärnbränslehantering AB.

Hallbeck L, Pedersen K, 2008. Characterization of microbial processes in deep aquifers of the Fennoscandian Shield. Applied Geochemistry (in press*)*

Haveman S.H, Pedersen K, Routsalainen P, 1999. Distribution and metabolic diversity of microorganisms in deep igneous rock aquifers of Finland, Geomicrobiology Journal, 16 277–294.

Haveman S.A, Pedersen K, 2002a. Distribution of culturable anaerobic microorganisms in Fennoscandian shield groundwater, FEMS Microbiol Ecol, 39 129–137.

Haveman S.A, Pedersen K, 2002b. Microbially mediated redox processes in natural analogues for radioactive waste, J Contam Hydrol, 55 161–174.

Johnsson A, Arlinger J, Ödegaard-Jensen A, Albinsson Y, Pedersen K, 2006. Solid–aqueous phase partitioning of radionuclides by complexing compounds excreted by subsurface bacteria. Geomicrobiology Journal. 23, 621–630.

Kotelnikova S, Pedersen K, 1998. Distribution and activity of methanogens and homoacetogens in deep granitic aquifers at Äspö Hard Rock Laboratory, Sweden, FEMS Microbiology Ecology, 26 121–134.

Kyle J E, Eydal H S C, Ferris G, Pedersen K, 2008. Viruses in granitic groundwater from 69 to 450 m depth of the Äspö hard rock laboratory, Sweden. The ISME Journal. In print.

Laaksoharju M, Degueldre C, Skårman C, 1995. Studies of colloids and their importance for repository performance assessment. 95–24. Svensk Kärnbränslehantering AB.

Laaksoharju M, Wold S, 2005. The colloid investigation conducted at the Äspö Hard Rock Laboratory during 2000 – 2004. SKB TR-05-20, Svensk Kärnbränslehantering AB.

Lienert S, Short S.A, Von Guten H, 1994. Uranium infiltration from a river to a shallow groundwater. Geochimica et Cosmochimica Acta 58, 5455–5463.

Lin L-H, Slater G F, Sherwood Lollar B, Lacrampe-Couloumbe G, Onstott T C, 2005. The yield and isotopic composition of radiolytic H_2, a potential energy source for the deep subsurface biosphere. Geochimica et Cosmochemica Acta, 69:4, 893–903.

Madigan M T, Martinko J, 2006. Brock Biology of Microorganisms. 11th ed. Prentice Hall, London.

Malmqvist L, Kristiansson K, 1984. Experimental evidence for an ascending microflow of geogas in the ground. Earth & Planetary Science Letters, 70, 407–416.

Marshall C P, Fairbridge R W, 1999. Encyclopedia of Geochemistry. Kluwer Academic Publishers, Dordrecht, the Netherlands.

Meyers C R, Nealson K H, 1990. Respiration linked proton translocation coupled to anaerobic reduction of manganese (IV) and iron (III) in *Shewanella putrefaciens* MR-1. Journal of Bacteriology, 172, 6232–6238.

Morris K, Raiswell R, 2002. Biochemical cycles and remobilisation of the actinide elements., pp. 101–141 In M.J. Keith-Roach. and F.R. Livens (eds.), Interactions of microorganisms with radionuclides. Radioactivity in the environment, Vol. 2. Elsevier, Oxford, UK.

Nilsson A-C, Degueldre C, 2007. Forsmark Site Investigation.Granitic groundwater colloids sampling and characterisation. Colloid analysis from KFM11A. SKB P-07-169, Svensk Kärnbränslehantering AB.

Pedersen K, Ekendahl S, 1990. Distribution and activity of bacteria in deep granitic groundwaters of southeastern Sweden, Microbial Ecology, 20 37–52.

Pedersen K, Ekendahl S, 1992a. Incorporation of CO_2 and introduced organic compounds by bacterial populations in groundwater from the deep crystalline bedrock of the Stripa mine, Journal of General Microbiology, 138 369–376.

Pedersen K, Ekendahl S, 1992b. Assimilation of CO_2 and introduced organic compounds by bacterial communities in ground water from Southeastern Sweden deep crystalline bedrock, Microbial Ecology, 23 1–14.

Pedersen K, 2001. Diversity and activity of microorganisms in deep igneous rock aquifers of the Fennoscandian Shield. In Subsurface microbiology and biogeochemistry. Fredrickson, J. K. & Fletcher, M., Eds. New York: Wiley-Liss Inc., 97–139.

Pedersen K, 2002. Microbial processes in the disposal of high level radioactive waste 500 m underground in Fennoscandian shield rocks, pp. 279–311 In M.J. Keith-Roach and F.R. Livens (eds.), Interactions of microorganisms with radionuclides. Elsevier, Oxford, UK.

Pedersen K, 2003. Site investigation in the Forsmark area. Control of microorganisms content in flushing water used for drilling of KFM01A, pp 1–8. SKB P-03-03. Svensk Kärnbränslehantering AB.

Pedersen K, Kalmus A, 2003. Site investigation in the Forsmark area. Control of microorganisms content in flushing water used for drilling of KFM02A and KLM04A, pp 1–19. SKB P-03-92, Svensk Kärnbränslehantering AB.

Pedersen K, 2005. Forsmark site investigation. Control of microorganism content in flushing water used for drilling of KFM06A, pp 1–19. SKB P-05-81, Svensk Kärnbränslehantering AB.

Pedersen K, 2005a. Äspö Hard Rock Laboratory. The MICROBE framework. Site descriptions, instrumentation, and characterisation. IPR 05-05, Svensk Kärnbränslehantering AB.

Pedersen K, 2005b. Äspö Hard Rock Laboratory. MICROBE. Analysis of microorganisms and gases in MICROBE groundwater over time during MINICAN drainage of the MICROBE water conducting zone. IPR 05-29, Svensk Kärnbränslehantering AB.

Pedersen K, 2008. Microbiology of Olkiluoto groundwater 2004 – 2006. POSIVA report 2008-02. Posiva OY, Finland

Pitkänen P, Partamies S, Luukonen A, 2004. Hydrochemical interpretation of baseline groundwater conditions at the Olkiluoto site. POSIVA 2003-07, Posiva, Olkiluoto, Finland.

Pitkänen P, Partamies S, 2007. Origin and implications of dissolved gases in groundwater at Olkiluoto. Posiva Report 2007-04. Posiva OY, Finland.

Sherwood Lollar B, Frape S K, Fritz P, Macko S A, Welhan J A, Blomqvist R, Lahemo P W, 1993a. Evidence for bacterially generated hydrocarbon gas in Canadian Shield and Fennoscandian Shield rocks. Geochimica et Cosmochimica Acta 57, 5073–5085.

Sherwood-Lollar B, Frape S K, Weise S M, Fritz P, Macko S A, Welham J A, 1993b. Abiogenic methanogenesis in crystalline rocks. Geochimica et Cosmochemica Acta 57, 5087–5097.

Sherwood Lollar B, Westgate T D, Ward J A, Slater G F, Lacrampe-Couloume G, 2002. Abiogenic formation of gaseous alkanes in the Earth's crust as a minor source of global hydrocarbon reservoirs. Nature 416, 522–524.

Sherwood Lollar B, Lacrampe-Couloume G, Slater G F, Ward J, Moser D P, Gihring T M, Lin L-H, Onstott T C, 2005. Unravelling abiogenic and biogenic sources of methane in the Earth's deep subsurface. Chemical Geology 226. 328–339.

SKB, 2006. Hydrochemical evaluation. Preliminary site description Laxemar subarea – version 1.2. SKB R-06-12, Svensk Kärnbränslehantering AB.

Smellie J, Tullborg E-L, Nilsson A-C, 2008. Explorative analysis and expert judgement of major components and isotopes. SKB R-08-84, Svensk Kärnbränslehantering AB

Staley J.T, Konopka A, 1985. Measurements of in situ activities of nonphotosynthetic microorganisms in aquatic and terrestrial habitats 39:321–346, Annu Rev Microbiol, 39 321–346.

Sternbeck J, Arnér M, Berzell A, 2005. Report no 10054177, AB SVAFO, Sweden.

Stumm W, Morgan J, 1996. Aquatic chemistry, 3rd ed. John Wiley, New York.

Söderberg P, Flodén T, 1991. Pockmark development along a deep crustal structure in the northern Stockholm Archipelago, Baltic Sea. Beitrage Meereskunde 62, 79–102.

Söderberg P, 1993. Seismic stratigraphy, tectonics and gas migration in the Åland Sea, northern Baltic Proper. Stockholm Contributions in Geology, 43(1), 1–67.

Vilks P, Miller H, Doern D, 1991. Natural colloids and suspended particles in the Whiteshell Research area, Manitoba, Canada, and their potential effect on radiocolloid formation. Applied Geochemistry 8, 565–574.

Wacker P, Bergelin A, Nilsson A-C, 2003. Forsmark Site Investigation. Complete hydrochemical characterisation in KFM01A. SKB P-03-94, Svensk Kärnbränslehantering AB.

Wacker P, Bergelin A, Nilsson A-C, 2004a. Forsmark Site Investigation. Hydrochemical characterisation in KFM02A. SKB P-04-70, Svensk Kärnbränslehantering AB.

Wacker P, Bergelin A, Nilsson A-C, 2004b. Forsmark Site Investigation. Complete hydrochemical characterisation in KFM03A. SKB P-04-108, Svensk Kärnbränslehantering AB.

Whiticar M J, 1990. A geochemical perspective of natural gas and atmospheric methane. Organic Geochemistry 16, 531–547.